Submitted to ***Advanced Engineering Materials*** *as* ***REVIEW / PROGRESS REPORT***
Revised version

Recent Progress in Marine Antifouling Technology Based on Graphene and Graphene Oxide Nanocomposite Materials

I. Levchenko[1], A. Kumar[2], A. AL-Jumaili[2,3,4], O. Bazaka[5], E. P. Ivanova[5], C. Riccardi[6], H. E. Roman[6], S. Xu[1], M. V. Jacob[2], O. Baranov[7,8], K. Bazaka[2,9]

[1] Plasma Sources and Application Centre, NIE, Nanyang Technological University, 637616, Singapore
[2] Electronics Materials Lab, College of Science and Engineering, James Cook University, Townsville, QLD 4811, Australia
[3] Medical Physics Department, College of Medical Sciences Techniques, The University of Mashreq, Baghdad, Iraq
[4] Department of Medical Physics, College of Applied Science, University of Fallujah, Iraq
[5] School of Science, RMIT University, PO Box 2476, Melbourne, VIC 3001, Australia
[6] Dipartimento di Fisica "Giuseppe Occhialini", Università degli Studi di Milano-Bicocca, Piazza della Scienza 3, I20126 Milan, Italy
[7] Department of Theoretical Mechanics, Engineering and Robomechanical Systems, National Aerospace University, Kharkiv 61070, Ukraine
[8] Department of Gaseous Electronics, Jožef Stefan Institute, Ljubljana 1000, Slovenia
[9] School of Engineering, The Australian National University, Canberra, ACT 2601, Australia

Sea vessels and artificial sea-based structures like marine oil and gas platforms are severely affected by biofouling, i.e. the formation of thick deposits of living and dead marine organisms that belong to different species and range in size from unicellular bacteria to multicellular seaweed and mussels. This is a significant engineering problem since they essentially alter the geometry of the hull, increasing friction and reducing the speed of vessels, thus increasing the cost and environmental footprint of transportation. Given the scale of global transportation reaches several billion tons per year, the socioeconomic consequences of the reduction in transit speed and increased consumption of fuel continue to drive researchers and engineers to develop strategies by to combat the processes of marine biofouling. Many types of antifouling paints, coatings and materials that have been designed and tested, and in some instances used commercially, suffer from a range of shortcomings, from environmental toxicity to limited efficiency and durability. In this review paper, we present a brief overview of the traditional antifouling materials, and discuss recent achievements in the design of advanced antifouling materials based on such nanomaterials as graphene, nanotubes, nanoparticles, and more complex nanostructures. These materials exhibit excellent antifouling properties and could drive a breakthrough in how we tackle marine biofouling.

Keywords: Environmentally benign materials; Biocidal nanocomposites; Marine biofouling; Antifouling surfaces

Table of Contents

1. Introduction 2
2. Biofouling: A Serious Engineering Challenge for Marine Industry 3
3. How the Films Grow in Water 4
4. Current state-of-the art in the antifouling technology 5
5. Recent Progress in Graphene-Based Antifouling Technologies 10
5.1 Mechanisms of graphene antifouling action: a brief outline 11
5.2 Topography-Based Graphene and RGO Antifouling Technologies 13
5.3 Graphene and RGO with polymer matrixes 17
5.4 Graphene and RGO with metal and metal oxides 24
5.5 Testing graphene-based antifouling materials under the field and simulated natural conditions 28
6. Future Outlook and Challenges 31
Acknowledgements 38
References 38

1. Introduction

Enhancing efficiency of the marine traffic is a very important engineering problem that mostly relies on the advanced materials. Indeed, the marine freight traffic of goods, raw materials and oil amounts to several billion tons per year. In total, about 80% of world cargo transportation is made by sea transport. Not surprisingly, all aspects of sea transportation systems are being continuously improved – from new design of vessels to enhance their hydrodynamics, to greater efficiency of engines, control systems and other important sub-systems. Among these factors, the hydrodynamics of vessels essentially influences the cost of transportation by affecting the fuel consumption of a cargo vessel. However, the sea is a living ecosystem and it actively reacts to the vessel intruding by forming massive deposits of various live and dead organisms on its surface. Organic molecules deposit first, followed by bacteria and larger organisms, such as seaweed and mussels (see a more detailed description of the biofouling formation in the next sub-section); over a relatively short period of time, the cumulative weight and volume of this deposit can become substantial enough to significantly lower the speed of the vessels[1] and lead to premature deterioration of e.g. heat exchangers, pipelines and other important units due to this additional lead, ultimately resulting in the reduction of vessel performance.[2,3,4] Both cost of transportation and fuel consumption unavoidably soar. Many research teams are putting significant effort into finding efficient solutions to combat marine biofouling, yet the issue remains largely unresolved due to the complexities of balancing cost, reliability, efficiency and the impact on the environment.

Various types of antifouling materials and systems were suggested, designed and tested on sea vessels (we provide a brief overview of the traditional materials and technologies in the following sub-section).[5,6] Significant progress has been achieved compared with the first approaches based on metal (copper, lead) plating, yet the sea transportation industry requires much higher efficiency to combat biofouling as the present-day techniques based mainly on biocidal agents do not ensure the desired level of protection.[7,8] Besides, biocidal systems present a significant danger to the marina flora and fauna, in particular in the port areas where the cargo traffic is very dense.[9] Among the most popular biocides was tributyltin, known as TBT, which was used commercially for several decades, demonstrating acceptable efficiency, but finally was banned when it was proven that the use of TBT causes significant decrease in populations of marine organisms.[10,11,12]

Nanotechnology and nanomaterials can be a promising alternative to the biocidal systems that are currently dominating the antifouling materials market.[13,14,15] Indeed, nanotechnological approaches are capable of producing materials and nanoscale metamaterials[16] that demonstrate advanced characteristics making them highly attractive for the use in different applications including, e.g., various sensors,[17,18,19] energy storage,[20,21] energy conversion devices[22 - 25] and many others.[26,27,28] Importantly, many nanotechnology-based antifouling solutions are capable of withstanding aggressive environments typical of e.g. space applications.[29 - 32] Not surprisingly, attempts to use nanomaterials to combat fouling are both numerous and diverse,[33,34,35] utilizing various types of nanostructures for the antifouling materials, e.g. nanorods,[36] nanoparticles,[37] Nanopillars,[38] vertical dendrites,[39] Lotus leaf-like structures[40] and others.

In view of the above said, it can be concluded that the marine transportation industry currently does not possess an efficient, reliable and relatively affordable means to combat biofouling on about 100,000 commercial sea vessels with the gross tonnage over 1 billion tonnes.[41,42,43] In our review, we will first briefly discuss how biofilms and then solid fouling deposits form on the immersed surfaces in seawater; then, we briefly overview the existing biocidal agents and finally, we present examples of the most important recent innovations in the marine antifouling technology based on nanomaterials and nanostructures, including graphene and nanotubes.

2. Biofouling: A Serious Engineering Challenge for Marine Industry

How serious is the fouling problem? In fact, due to the fast growth of fouling settlements in seawater, fouling represents a very serious threat to the vessels and the related industry. **Figures 1a,b** show the images of vessels taken at the time of their planned quinquennial inspection at dry-dock. Examination of these images reveals that the antifouling paint most frequently used as a strategy to reduce organism attachment loses its protective properties with time. Regions where the wall shear stress was high tended to display notably greater levels of fouling, suggesting a positive link between increased wall shear stress and premature deterioration of the antifouling protection, and consequently increased fouling over these areas.[44] Moreover, as it degrades and is leached out into the environment, the protective paint pollutes the port areas.

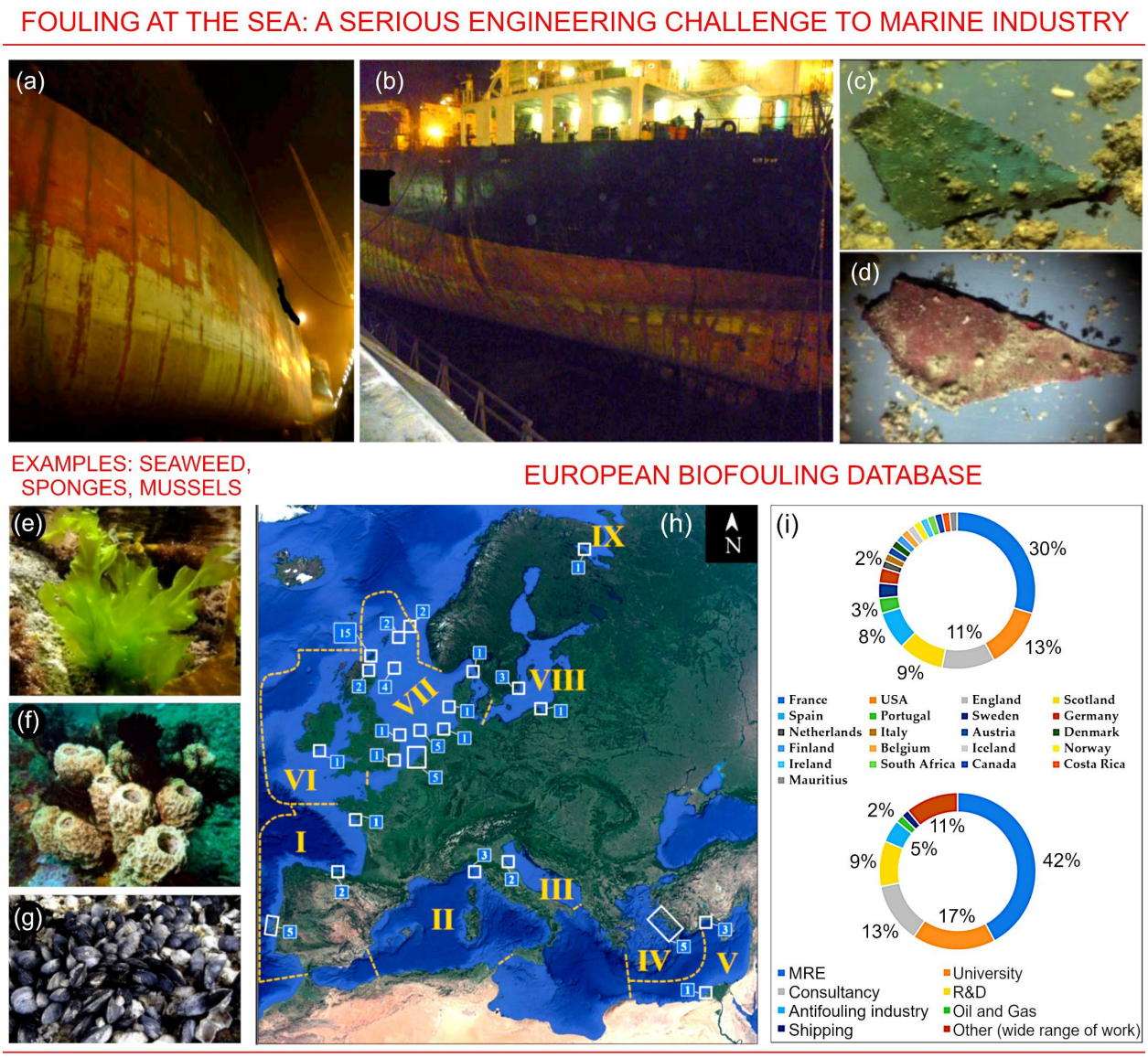

Figure 1. **Marine fouling.** (a,b) Failure of antifouling paints on the surface of a large marine vessel. After 5 years of use, the paint shows signs of notable deterioration that is not uniform across the body of the vessel. Reprinted with permission from Mukherjee *et al.* **2019.**[44] (c,d) Optical visualisation (5x magnification) of antifouling paint particles observed in samples of sediment collected around Colón Port, Panama. Reprinted with permission from Batista-Andrade *et al.* **2018.**[45] (e-g) Several examples of typical fouling organisms – seaweed (e), sponges (f), mussels (g). Reprinted with permission from Chen *et al.* **2021.**[46] (h) The European biofouling database is a large scale initiative designed to capture the variation in biofouling composition and magnitude across geographical sites to inform engineering design and policy. I, South European Atlantic Shelf; II, Western Mediterranean Sea; III, Adriatic Sea; IV, Aegean Sea; V, Levantine Sea; VI, Celtic Seas; VII, North Sea; VIII, Baltic Sea; IX, White Sea. White squares denote the areas and frequency of sampling. (i) Database downloads vary significantly between countries and sectors. Reprinted with permission from Vinagre *et al.* **2020.**[47]

Figures 1c,d depict AF paint particles found in sediment samples acquired near Port of Colón, Panama, an important tourist and commercial centre that routinely experiences a high traffic of commercial and cruise ships and vessels and a large number of vessels undergoing maintenance and repair. Despite of strict bans imposed on many efficient antifouling agents such as tributyltin (TBT) which has been banned since 1998, scientists remain deeply concerned about their impact, given the large amount of potentially dangerous antifouling agents already accumulated in water, sediments and living ecosystems.

Fouling starts rapidly when the pain is lost. **Figures 1e-g** illustrate several examples of typical fouling organisms – seaweed (e), sponges (f), mussels (g). The dominant species and their relative abundance is dependent on the ecosystem, which presents an extra degree of complexity for the design of broad spectrum antifouling strategies. **Figures 1h,i** show the sampling map for the European biofouling database, as well as the rate with which this information is accessed by different countries and maritime industry sectors to inform their decision and policy making. The fouling data is analysed with respect to immersion depth (up to 90 m) and time (short term of 10 days to long term of ~40 years). It should be noted that entries from the North Sea Ecoregion are over-represented when compared to Celtic Sea and White Sea Ecoregions.[47]

Why new antifouling materials are needed? Apart from unsatisfactory efficiency if the currently used antifouling materials, they represent a serious threat to the global ecosystem. **Figure 2** shows some examples of the wide geography of current efforts on mapping the antifouling agents taking from the most recent publications; the reader can also refer to numerous recent publications to obtain more information about recent results on mapping the residual antifouling agents worldwide. The sites are marked with dots on the maps, and the maps show several tens of sites for each sampling location. Apparently, global collection of antifouling data and measurement of paint-caused pollution means significant costs to the global economy. Thus, fouling represents a serious threat to the marine industry, and application of nanomaterials-based antifouling platforms could be a way to the solution of this problem.

3. How the Films Grow in Water

When a surface is immersed in a water body, the process of fouling proceed in several stages, as shown in **Figure 3**. As a rule, fouling starts from the adsorption of organic molecules, the bacteria attach to the initial level of sediments, then the microscopic organisms precipitate and attach to the surface under action of various physical and chemical processes.[48,49] A steady continuous biofilm is formed.[50,51] In turn, this biofilm provides nutrition for larger organisms, and unicellular eukaryotic organisms such as microalgae and diatoms attach and form a thicker layer.[52,53] Later, attachment of larger multicellular organisms starts; this process is called macrofouling. Finally, invertebrates such as e.g. mollusks attach and form sometimes gigantic build-ups capable of causing a significant drop in the ship velocity and possible collapse of the structure due to a change in geometry and weight of the structure.

Biofouling is affected by various environmental conditions including temperature, availability of nutrient and salinity of water first of all, and then other factors.[54] Besides, water salinity influences the composition of biofilms. Temperature directly affects the rate of fouling, with the latter being higher in warm water.[55] Another important factor is the material and texture of the surface and interestingly, while some organisms prefer hydrophilic surfaces, other prefer hydrophobic surfaces and hence, hydrophobicity or hydrophilicity (i.e. the level of surface energy) cannot be used as a critical factor to prevent marine fouling.[56,57] Surface topology, i.e. roughness, regularity, shapes of surface hillock etc. also influences the fouling dynamics.[58] While the large number of factors influencing the fouling makes for a very complex picture to deconvolute, this also provides many opportunities for controlling and preventing the fouling via surface topology, energy, chemistry, and synergistic effects.[59] Below we discuss various aspects of such novel approaches.

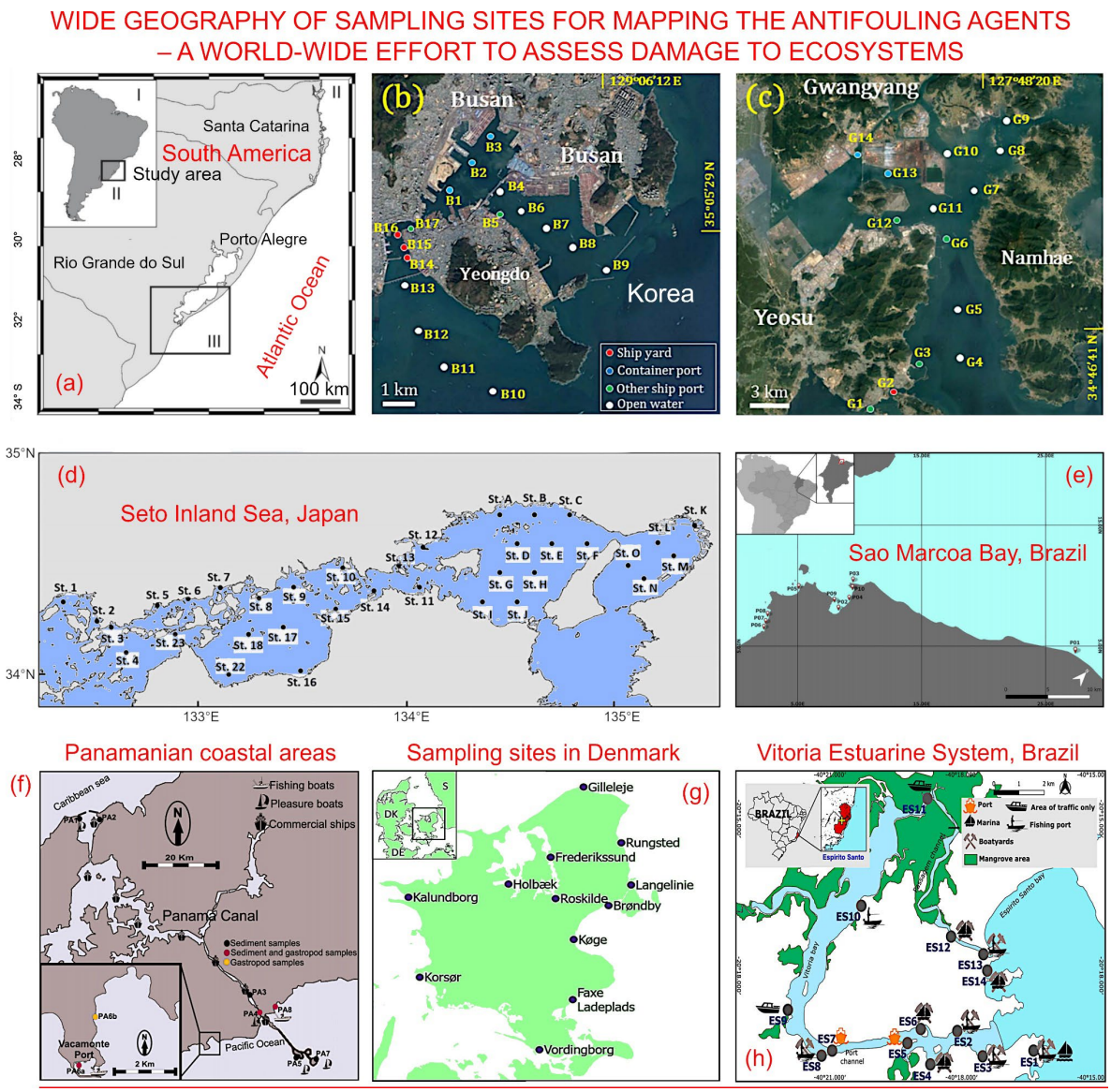

Figure 2. Threat to the global ecosystem: The geography of sampling sites for the mapping of levels of residual antifouling agents in ecosystems. (a) Seawater samples from Cassino Beach, Rio Grande, Rio Grande do Sul, Brazil. Reprinted with permission from *Agostini et al.* **2021.**[60] (b, c) Map showing sampling sites in Korea, near Busan and Gwanguang. Reprinted with permission from *Lam et al.* **2017.**[10] (d) Map showing the sample stations (black circles) in the central and eastern parts of the seto Inland Sea, Japan. Reprinted with permission from *Onduka et al.* **2020.**[61] (e) Sampling sites along São Marcos Bay, Brazil. Reprinted with permission from *Viana et al.* **2020.**[62] (f) Sampling sites along the Panamanian coastal areas. Reprinted with permission from Batista-Andrade *et al.* **2018.**[45] (g) Location of sampling sites in Denmark. The right-hand side shows the specific sampling sites in Roskilde and Brøndby (red circles). Reprinted with permission from *Koning et al.* **2020.**[63] (h) Sampling sites along the Vitoria Estuarine System, Brazil. Reprinted with permission from *Abreu et al.* **2021.**[64]

4. Current state-of-the art in the antifouling technology

The history of antifouling technologies started shortly after the first vessels appeared in seas.[65] In modern times, for several decades, tributyltin (TBT) was considered as a state-of-the-art, yet ultimately it was banned in 2008 due to its toxicity. To replace it, various biocide agents were developed[66,67,68] such as DCOIT (Sea Nine 211, Dichlorooctylisothiazolinone),[69] Diuron (1,1-dimethyl, 3-(3',4'-dichlorophenyl) urea), Irgarol 1051 ((2-methythiol-4-tert-butylamino-6-cyclopropylamino-s-triazine),[70] and metal oxide-based materials.[71] However, they still represent a danger to sea ecosystems.[72] **Table 1** lists the commonly used antifouling biocides along with their action mechanism, environmental consequences for their use and their estimated half-life in seawater (the latter being a function of broad range of environmental conditions). It should be mentioned that the antifouling coatings constitute a huge sector of maritime economy.[73]

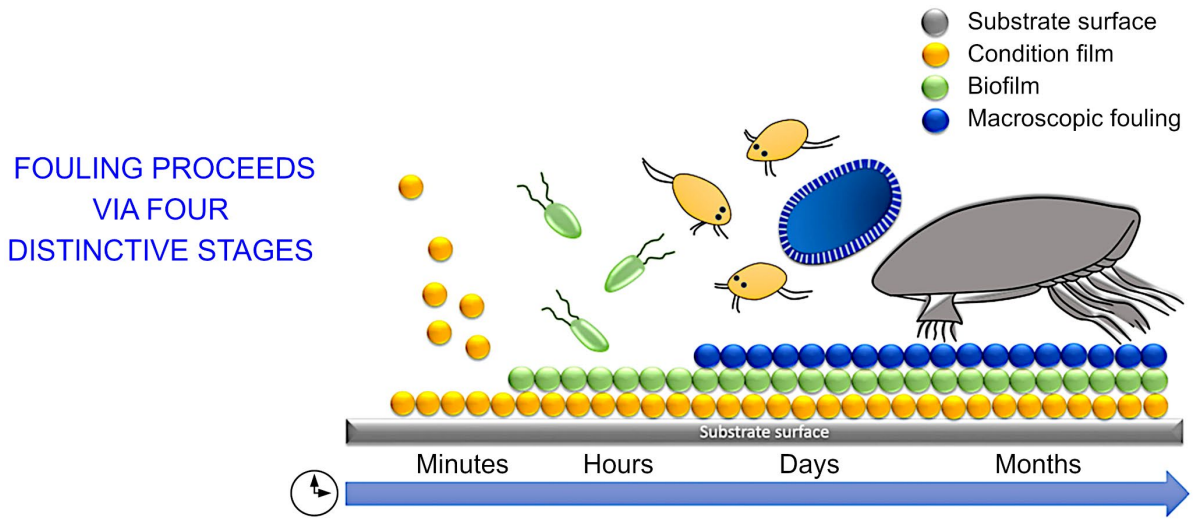

Figure 3. The process of marine fouling can be broken down into four distinct stages, starting from the formation of a prime film, then biofilm is formed, followed with the diatom and protozoan attachment and growth, and finally invertebrates and other macro-organisms. It should be noted that this break down into stages is an over-simplification of the highly dynamic and complex real life process, and these stages may take place concurrently or overlap. Reprinted with permission from Tian *et al.* **2021.**[74]

Table 1. Commonly used biocides and their action mechanisms. Data from [52,75,76,77].

Biocide	$T_{1/2\ seawater}$ (days)	Action mechanism	Consequences
Irgarol	100 – 250	Inhibitor of PS II electron transport	Fatal effect on marine ecosystem
Diuron	31.4 – 365	Inhibitor of PS II electron transport	Toxic to algae and bacteria
Chlorothalonil	1.8 – 8	Mitochondrial electron transport inhibitor	Toxic effect on fish
Dichlofluanid	0.12 - 0.75	Inhibitor of PS II electron transport	Toxic effect (embryo toxicity)
Zn pyrithione	< 1	Multi-site inhibitor	Toxic to aquatic flora and fauna
Cu pyrithione	12.9 – 96	Multi-site inhibitor	High toxicity to marine organisms
DCOIT (Sea nine)	0.004 – 3	Inhibitor of electron transport	High toxicity to marine organisms
Tralopyril	0.67	Mitochondrial electron transport inhibitor	Toxicity to marine invertebrates
Capsaicin	13	Nervous system and metabolic disruptor	Adverse effect on non-target marine organisms
Nonivamide	8.8	Nervous system and metabolic disruptor	Toxic effect on algae

Below we briefly overview several most important biocide systems that are widely used but need replacement with more efficient techniques.[78] The classification below is based on the mechanism of biocide release from the polymer matrix, the latter commonly referred to as the binder. In the next part of the paper, we overview the novel nanomaterial-based antifouling systems.

Self-polishing copolymer coatings use the effect of controlled seawater penetration into the coating to trigger biocide release.[79] The hydrophobic matrix prevents water from penetrating into the film, restricting it to the pores created by soluble biocidal particles. As the copolymer matrix is easily hydrolyzable in seawater, controlled and slow hydrolysis of the coating takes place, confined to a few nanometer thick layers from the surface. In time, there is an increase in leached areas with an increase in dissolution of biocides, making the copolymer matrix brittle and easily erodible by seawater.

The coatings based on insoluble paints use binding agents which contain biocide agents. High level of biocide incorporation closely packs active molecules, making them come in contact with each other and resulting in their gradual release (**Figure 4a**). Leaching of biocides from such coatings leads to the formation of a honeycomb structure, its surface becomes rougher and susceptible to retaining of more of

seawater pollutants, accumulation of which prevents further release of biocides. Apparently, the service life of such systems is limited by the amount of biocide in the surficial layer of the paint. To overcome this problem, soluble coatings were proposed where binders dissolve and release more biocides (**Figure 4b**). In this type of a coating, the leaching layer is thin, and biocides are directly exposed to water; the combination of these two factors increase a lifespan of the outer layer. However, these coatings have poor mechanical strength and limited biocide loading capacity. The binder in the controlled depletion polymer coating is reinforced with organic rosins which control the hydration and dissolution of the soluble binder in the slower manner than rosin-based derivatives.[73]

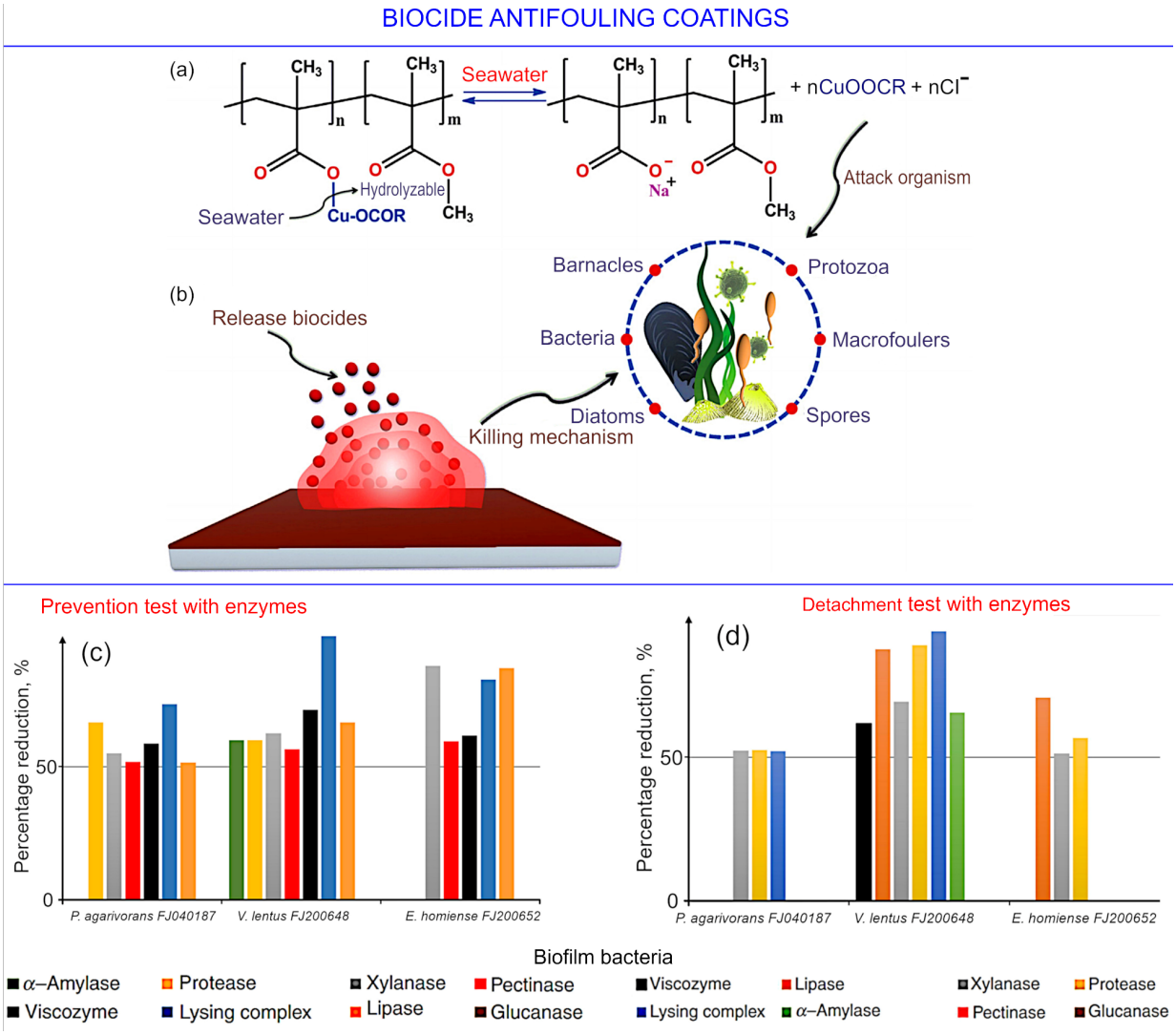

Figure 4. **Established technologies for marine antifouling.** (a) Main reaction of the general chemical structure of the hydrolyzable polymethacrylic acid copolymer with seawater. (b) Killing mechanism of the biocide anti-fouling coating prevents bioadhesion through its toxic effects. The matrix is decomposed by the hydrolysis of the pendant groups of the copolymer chain, thus a part of the fouling organisms are released along with the matrix.[80] Reprinted with permission from Han *et al.,* **2021.**[81] (c) Efficacy when enzymes used as part of a pre-vention and (d) as a detachment strategy. The enzymes analyzed in this investigation have potential as environ-mentally friendly antifouling agents for marine antifouling. Reprinted with permission from Aykin *et al.,* **2019.**[82]

Removal of the leached section of the coating exposes a new fresh area of coating for further releases of biocidal molecules, a process termed self-polishing.[50] Self-polishing coatings have a polishing rate of 5-20 μm per year which has extended the dry docking intervals for vessels for up to 5 years.[83] Besides, the enzyme-based coatings are being actively investigated as promising antifouling material.[84] A direct comparison of the approaches based on organism detachment and attachment prevention has been made and the results indicate that lysing complex enzyme were the most efficient for the prevention of

adhesion and for enhancing the detachment.[82] The results of this comparison are shown in **Figure 4cd**. Apparently, the mixtures of enzymes analyzed in this investigation could be used as efficient antifouling agents of the antifouling coatings. On the other hand, while considered more environmentally benign, the stability and self-degradation of enzymes remain a challenge.[85] The catalytic activity and lifespan of enzymes are known to be affected by variations in seawater temperature (-2 to 30 °C), quantity and distribution of enzymes in coatings, as well as the choice of coating matrices.

Another large group of antifouling materials are the non-toxic coatings capable of releasing the foulant. They also feature the nonstick properties,[86,87] and the surface wettability is considered the most important factor in determining coating efficacy. Importantly, substrate having a low value of elastic modulus shows minimum adhesion.[88,89] The critical force required to remove the fouling showed a positive relationship with the square root of surface energy, Y_c, and elastic modulus, E, as P $\approx\sqrt{Y_c E}$.

In the late 1970s, UV resistant, easy to clean polytetrafluoroethylene (PTFE) filled fluorinated polyurethane coatings were developed,[90] but the damage from barnacle shells would result in the roughened surface that enabled strong adherence of barnacles and prevented their easy removal.[91] These limitations of fluoropolymers have driven current research towards elastomeric silicon-based coatings. Poly(methylphenylsiloxane) was combined with cured silicone rubber to enhance its AF. These coatings feature low surface energy, elastic modulus and glass transition temperature, T_g = -127 ºC, which makes them flexible and allows the polymer to adopt the lowest surface energy configuration.[92,93] Multiwall and single wall carbon nanotubes-modified PDMS coatings have shown an increased contact angle, decreased roughness and surface energy with improved self-cleaning properties. Photo-reactive silicone functionalized with spherical single crystal TiO_2 particles showed superior FR properties compared to tailored nanocomposites.[94,95] Although hybrid silicone-based FR coatings dominate the present market, the fouling release property of PDMS is not effective at a low sailing speed and during idle periods, and have limited efficacy against colonization by diatoms and bacteria. Moreover, they have poor mechanical properties because of low elastic modulus and are thus quite susceptible to damage that can increase their surface roughness. Also, the biodegradability behavior of PDMS is yet to be thoroughly studied.

Non-fouling coatings influence the protein adhesion and adsorption on a surface.[96] The hydration layer and the steric repulsion are two main theories which explain the anti-fouling behaviour of these coatings. There is an unfavourable entropy change when there is protein adsorption on the substrate due to compression of a free end of polymer chains.[97] Thus, there is an entropically driven repulsion for any non-specific protein absorption.

The poly(ethylene glycol) chain length and grafting density have the significant effect on their protein repellency. Physical and chemical adsorption, covalent attachment and block or graft polymerization are used for immobilization of poly(ethylene glycol) chains on surfaces, with the coating properties depending strongly on the nature of the substrate and the chosen grafting process.[98] **Figure 5a-c** illustrates the poly (ethylene glycol)-utilizing coating.[99] Lower hydration potential of thinner films and entanglement and crowding in thicker films seems to be a plausible explanation for this behavior. The self-assembled monolayer (SAM) of oligo-(ethylene glycol) and PEG was found to inhibit spore settlement, while PEG allowed settlement but with reduced adhesion strength which can be detached by applying minor hydrodynamic force. Despite good protein repellency, PEG undergoes autoxidation and enzymatic cleaving in presence of oxygen and transition of metal ions which are abundant in seawater. Mechanical robustness of PEG-based coatings is another major limitation. To overcome stability challenge of poly(ethylene glycol)-based coatings, zwitterionic polymers were proposed. The charges can be on the same monomer (*e.g.* polybetaines and phosphorylcholines) or on different monomers (*e.g.* polysulfobetaine methacrylate).[100]

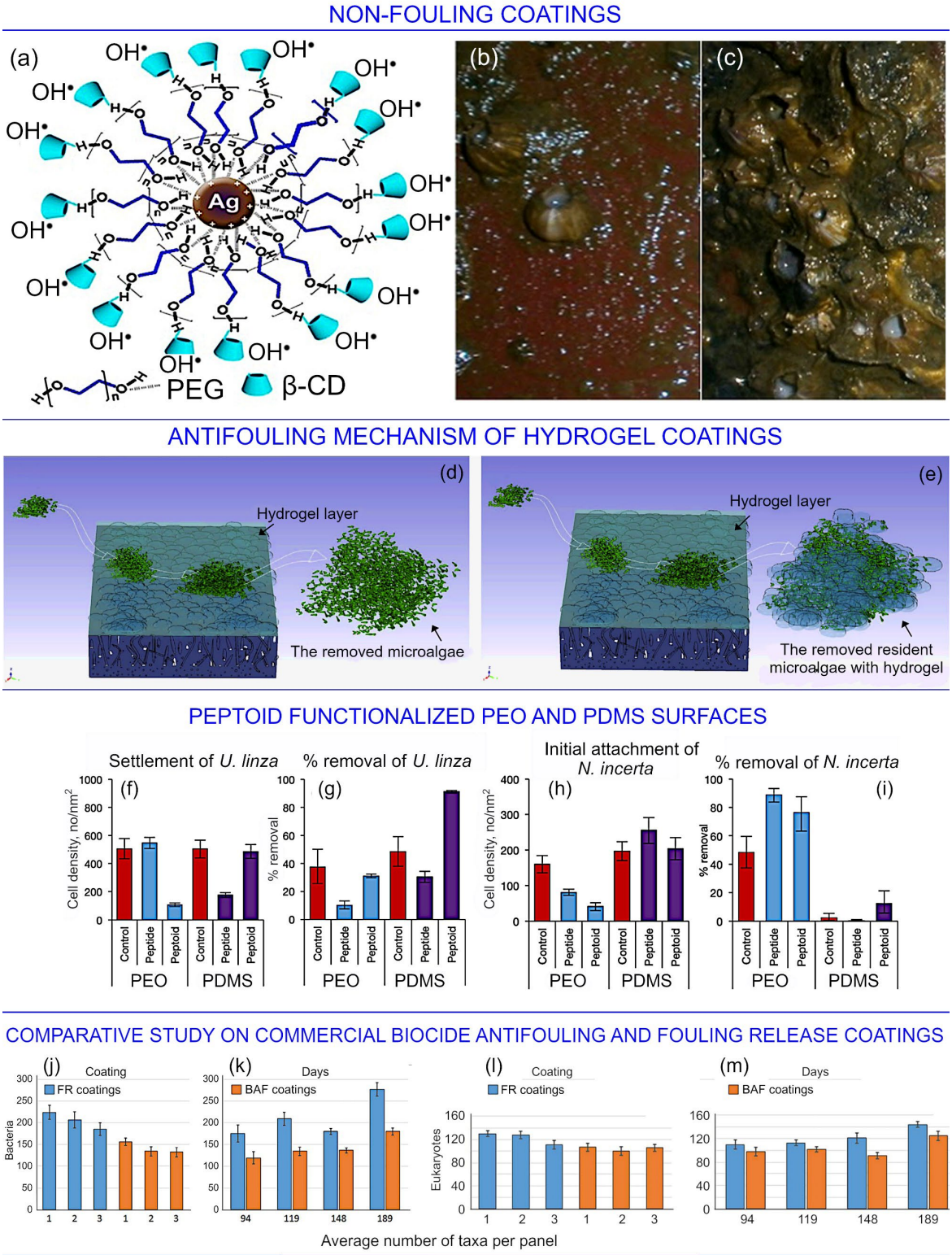

Figure 5. **Established technologies for marine antifouling.** (a) Proposed model of Ag loaded biopolymer complex. (b,c) Photograph of the coating panels (b) after 12 months and (c) Control panel without biocide. Reprinted with permission from Punitha *et al.* **2017.**[101] **(d,e)** Schematic illustration of the underwater self-cleaning mechanism of the SHRHS: (d) It provides a smooth and highly slippery surface. The trapped water is retained by the hydrogel surface, leading to attachment difficulty for the organism. It also provides a self-regeneration character, where the resident organisms can be carried off with hydrogel peeling. Reprinted with permission.[102] Peptoid functionalized PEO and PDMS surfaces. (a,b) Settlement and percentage removal of *Ulva linza*, and (c,d) initial attachment and percentage removal of *Nitkora incerta* on peptide and peptoid functionalized polyethylene oxide (PEO) and polydimethylsiloxane (PDMS) surfaces. Adapted with permission from Patterson et al. 2017.[104] (j-m) Comparative study on the antifouling efficiency of the commercial biocide antifouling (BAF) and fouling release (FR) coatings. (a-d) Average number of fouling organisms on six different coatings with respect to (a, b) coating types and (c,d) immersion period. The difference in adherence of marine bacteria and eukaryotes on BAF and FR was observed, and an understanding of the observed differences will influence future developments of novel antifouling technologies. Reprinted with permission from Winfield *et al.* **2018**.[103]

Figure 5d,e shows the antifouling mechanism of hydrogel coatings, where the hydration layer interrupts the initial adhesion of proteins, and peeling off the top layer along with settled organisms imparts self-regenerating properties to this coatings. Xue *et al.* fabricated slippery hydrogel-released hydrous surface (SHRHS) by blending sodium polyacrylate (PAAS) powder into a silicone resin. The coating showed lower attachment of microalgae in comparison with the silicone surface due to the formation of a strong hydration layer and slow hydrolysis that allows for periodic self-regeneration. The short-term stability due to poor mechanical properties and difficulty in using the coating over large marine structures have limited further advancements in hydrogel-based coatings.

Another approach involves the use of peptoids (**Figure 5f-i**). Patterson investigated the effect of a position, configuration and a number of arginine residues in arginine-rich oligopeptide SAM on their interaction with *Ulva* spores, with the former found to influence the settlement of spores.[104]

Winfield *et al*. made a comparative study on the antifouling efficiency of three commercial biocide antifouling and fouling release coatings. A comparative study of the antifouling efficiency of fouling release coatings (Intersleek 700, Intersleek 900, and Intersleek 1100) and biocide antifouling coatings (Intersmooth 7460, Intersmooth 7465, and Intercept 8000) is shown in **Figure 5j-m.**[103] The difference in adherence of marine bacteria and eukaryotes on these coatings was observed, and an understanding of the observed differences will influence future developments of novel antifouling technologies.

The action of the above overviewed antifouling materials is mostly based on specific chemicals killing some classes of marine organisms, or physico-chemical properties of the surface, such as its morphology, repelling the organisms. Despite many years of extensive effort, the performance of antifouling systems still requires significant improvement. Below we overview the recent achievements in the novel approaches to marine antifouling, focusing on platforms based on various nanoscale materials.

5. Recent Progress in Graphene-Based Antifouling Technologies

Various other antimicrobial applications are shown in **Figure 6**.[105] Along with other antimicrobial applications, graphene and graphene oxide (GO) proved to be very efficient agents against marine fouling, and very important is the fact that graphene and GO feature *non-chemical* action, thus not causing poisoning of the ecosystem.

- ✓ *Flakes of graphene and GO are essentially two-dimensional structure that feature very sharp edges and can create complex surface topographies, when mixed with other materials to form the antifouling coatings and paints.*

On the other hand, graphene and GO are among the strongest materials ever known, this ensuring endurance and long life of the antifouling coatings and paints made with graphene and GO. Let us first examine how complex surface topographies combat the fouling, and then examine several recent examples where graphene and RGO were used as non-chemical, non-toxic but still very efficient antifouling argent.

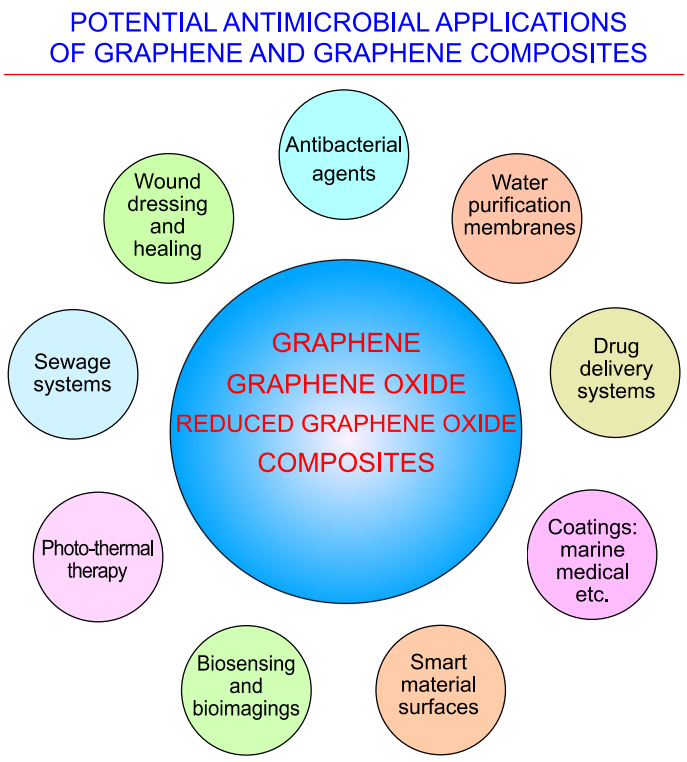

Figure 6. Potential antimicrobial applications of graphene, graphene oxide, reduced graphene oxide and graphene-based composites. Adapted from Staneva *et al.,* **2021**[105] under terms and conditions of CC BY license.

5.1 Mechanisms of graphene antifouling action: A brief outline

Here we start from a brief outline of the several mechanisms of graphene action and interaction with living cells, to better understand the antifouling action of various graphene-based antifouling nanocomposites. It should be noted that graphene interaction with living cells features quite a large number of physical and chemical processes, and the complete understanding of this complex phenomena still requires further research efforts. In general, several types of mechanisms are considered, yet the implementations of these mechanisms depend on the specific architectures, materials, configurations and many other factors. Importantly, these mechanisms could be synergistically combined, as we show below in some of the examples.

Specifically, the four main types of mechanisms can be formulated, namely:[106]

1. Membrane stress. Graphene features very high aspect ratio and very high mechanical strength due to the C-C sp^2 bonds; this results in very sharp edges damaging cell membranes;
2. Wrapping effect. In its particle form, graphene wraps the cells and thus isolate them from the ambient, causing their death;
3. Oxidative stress. Graphene produces reactive oxygen species (ROS) damaging the cells;
4. Electron transfer. Graphene is an excellent electron acceptor and it transfers electrons from cell membranes, impairing the cell activity.

When it comes to nanomaterials and composites built using graphene and its derivatives, the bactericidal and antifouling activity often stems from both its unique physical and chemical characteristics (**Figure 7a**). Mechanical aspects of this activity are related to the ability of graphene sheets to impact damage to the membrane upon contact with the cell by cutting the membrane with its sharp reactive edge or by stretching the membrane until the integrity is lost under the weight of the cell.[109] Where graphene sheets are not immobilized on the surface, there is a possibility of wrapping of the sheet around the cell, leading to the entrapment and death of the latter. From the chemical standpoint, the reactive edges and lattice defects enable graphene to generate reactive oxygen species (ROS). These species result in oxidative stress and damage of cell DNA and proteins, and interference with processes that are critical to cell survival. The relative contribution of these factors to overall toxicity of graphene to cells is determined by such properties of graphene as the size and composition of its flakes, presence of defects and functionalization. In addition to graphene-specific factors, properties of the coating within which graphene is contained also play an important role.

Examples of such factors include the concentration of graphene particles, their aggregation and dispersion, orientation and alignment in space (*e.g.* vertical alignment maximises cell exposure to reactive edges, patterns controls surface area available for attachment, etc.). **Figure 7b** illustrates another process, namely the mass loss due to the liquid release in the small unilamellar vesicle and removal of the lipid fragments in the rat basophilic leukemia (RBL–2H3) cells, thus causing their apoptosis.[109] **Figure 7c** describes the interaction of phase zinc phthalocyanine ZnPc–GO nanocomposites with *Escherichia coli*. Graphene oxide flakes in potato-chip-like α-phase zinc phthalocyanine ZnPc–GO nanocomposite demonstrate strong π– π intermolecular interactions, which not only allows them to form stacks between sheets, but also ensure efficient removal and transfer of electrons away from the surface of the cells. This is well illustrated by an example of electronegatively surface charged *Escherichia coli* bacterial cells that adhere strongly to the electron-withdrawing nanorod-like β-phase ZnPc–GO (ZnPc(B)–GO). The synergistic effects between oxide support layers and graphene are illustrated in **Figure 7d**. The synergistic effects of the graphene layer and support layer allowed to reach good permeability and good antifouling properties for the membrane.

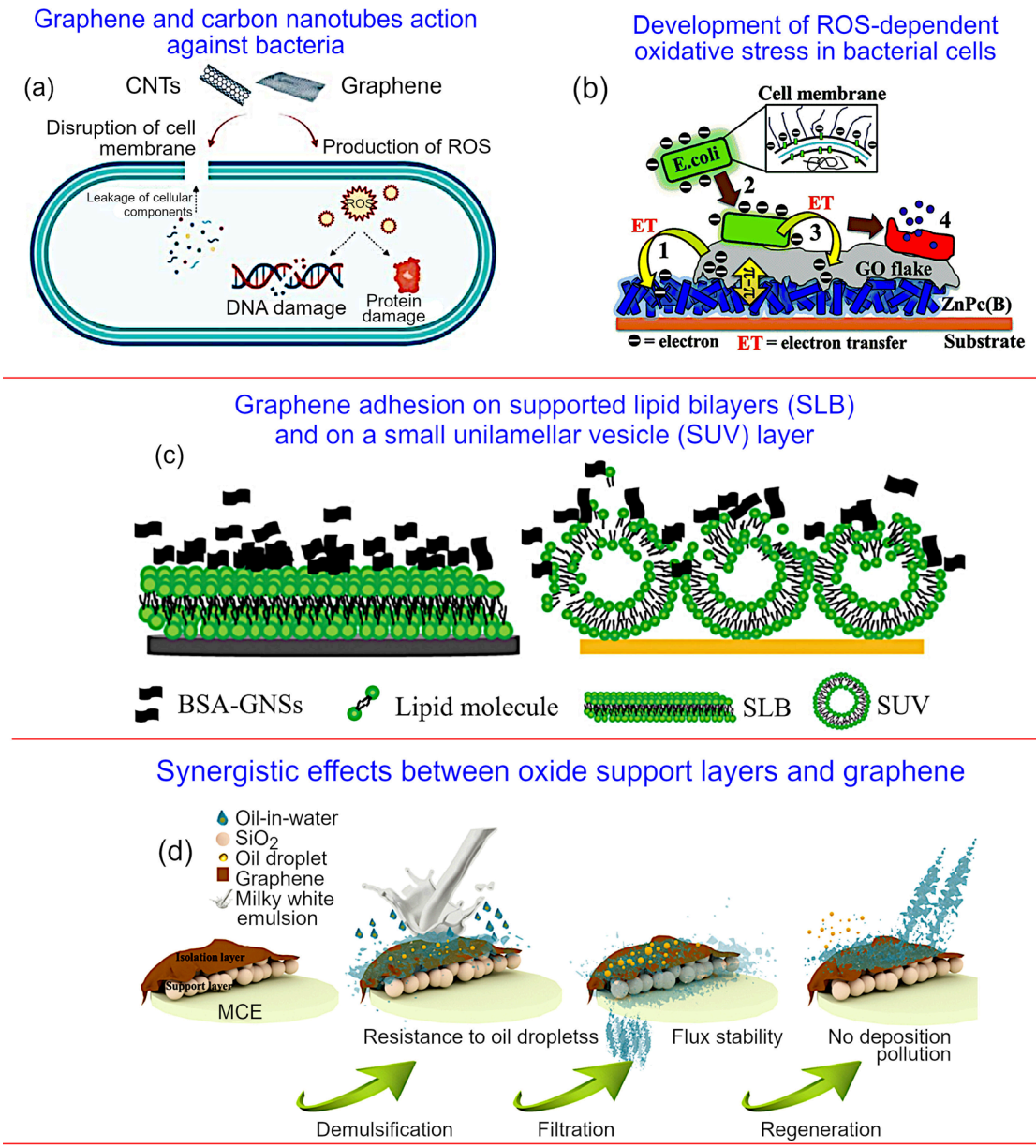

Figure 7. How graphene-based nanocomposites combat the fouling? (a) Schematics of graphene and carbon nanotubes action against bacteria. Quite different effects could have place, such as disruption of cell membranes, production of ROS, DNA and protein damage and others. Reprinted from F. Sousa-Cardoso *et al.* **2022**[107] under terms and conditions of CC BY license. (b) Schematic diagram illustrating the proposed mechanism for the interaction between the *Escherichia coli* cells and graphene oxide incorporated zinc phthalocyanine (ZnPc–GO). α-phase nanocomposites demonstrate strong π– π interactions and an efficient electron transfer. Reprinted with permission from N. Das *et al*. **2021**.[108] (c) Schematics of the graphene nanosheets adhesion on supported lipid bilayers (SLB) and on a small unilamellar vesicle (SUV) layer (with disrupted small unilamellar vesicles). Reprinted with permission from L. Liu *et al*. **2020**.[109] (d) Synergistic effects between oxide support layers and graphene. Reprinted with permission from L. Feng *et al.* **2020**.[110]

Figure 8 shows two more very important examples of biocidal activity of graphene – via visible light radiation and electromagnetic radiation which are capable of intensifying the electron transfer between the cells and the surface of the material.

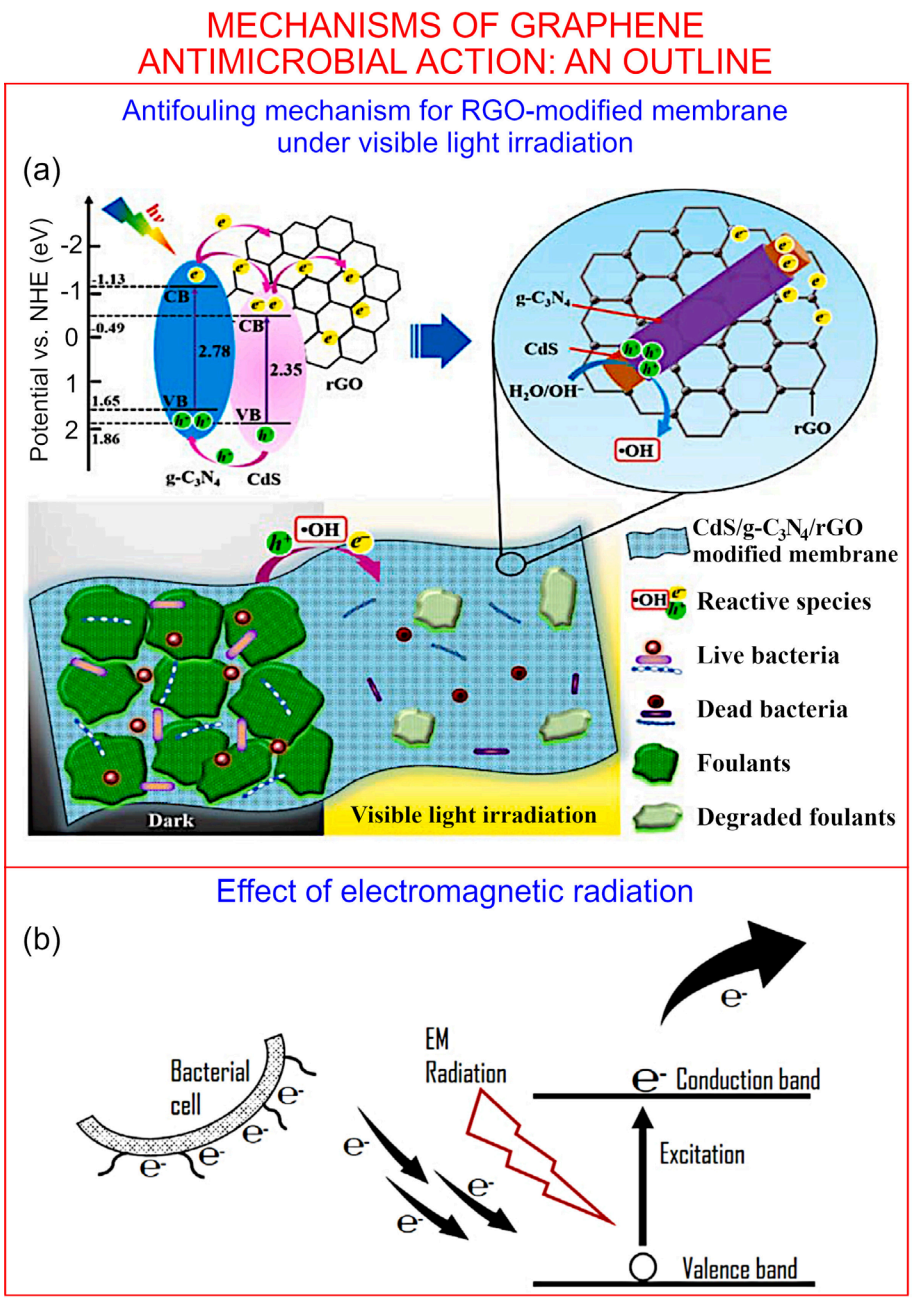

Figure 8. How do graphene-based nanocomposites combat fouling? (a) Mechanisms behind biocidal and fouling-retarding activity of reduced graphene-modified membrane under aquatic conditions when irradiated with visible light. Reprinted with permission from L. Ni *et al*. **2020**.[111] (b) Enhancement of biocidal activity of graphene-based nanomaterials by means of electromagnetic radiation, with the proposed mechanism of action. Reprinted with permission from A. Radhi *et al*. **2021**.[112]

5.2 Topography-Based Graphene and RGO Antifouling Technologies

Indeed, topography of the water-immersed surfaces significantly influences the hydrophobicity and growth of biofouling,[113,114] with shark skin and lotus leaves known to resist fouling because of their distinct micro/nano topography. **Figure 9a,b** illustrates the attachment point theory introduced by Scardinio *et al.*, assuming that the number of attachment points where marine organisms can attach to the surface directly influences the process of biofouling.[115,116] Barnacle settlement was reduced by almost 100% on textured PVC as compared to smooth PVC, with cyprid settlement shown to correlate with the aspect ratio of the surface features. Surface topography similar to the shark skin, with imbricate boundary structure and V-grove riblets, demonstrated to be most effective with respect to antifouling behavior, as shown in **Figure 9c**. The raised structure of rose petals can provide refuge to foulants against hydrodynamic shear, and depressed pattern of taro leaf can increase the number of adhesion points promoting string attachment. The shape of boundary structure had a more pronounced effect on antifouling performance than surface hydrophobicity. Topographical features having a single length scale are not likely to display antifouling activity as organisms creating biofouling come in varied sizes and shapes.

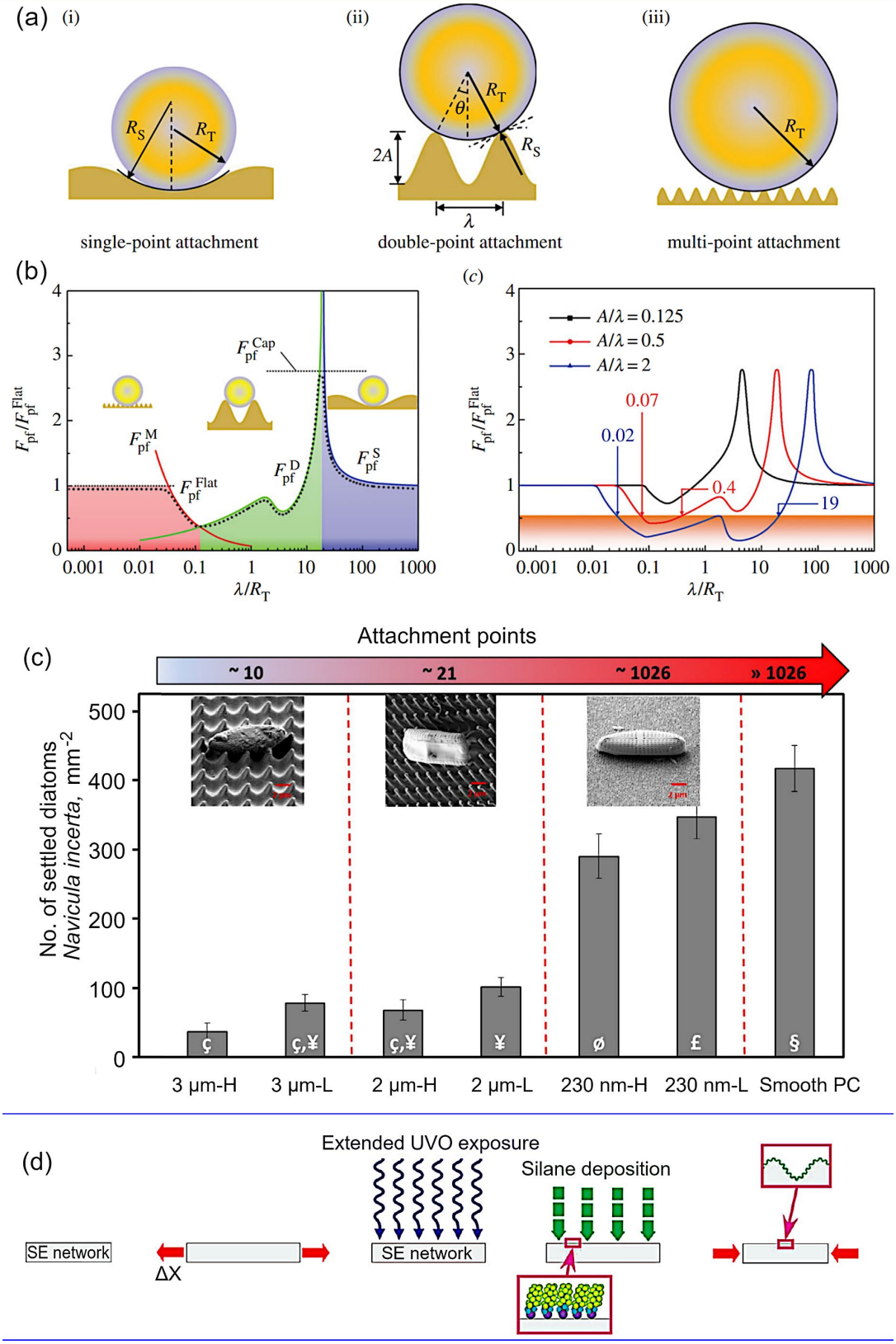

Figure 9. How nanostructured surface combats the fouling? (a) Schematic of the three possible configurations of an elastic cylinder in an adhesive contact with a wavy substrate. (b) Variation of the normalized pull-off force with l/R_T for A/lambda = 0.5. (c) Effect of A/lambda on pull-off force. Reprinted with permission from Fu *et al.* **2018.**[115] (c) The density of settled cells of *N. incerta* on different tapered microstructures made of polycarbonate (PC). Smooth PC is included as control. Structures indicated with an H are higher than the corresponding l structures. Reprinted with permission from Xiao *et al.* **2018**.[116] (d) Schematic representation of the process of fabrication of surfaces with uniaxial hierarchically wrinkled surface topologies (uHWST). Reprinted with permission from Efimenko *et al.*[117]

Efimenko *et al.* fabricated uniaxial and biaxial hierarchically wrinkled surface topography (HWST), with wrinkles varying from tens of nanometer to the fraction of millimeter arranged in the nested pattern, which remained free of fouling for 18 months during the field test in seawater (**Figure 9d**).[117] Topography is also capable of influencing the wettability, imparting the antifouling property similar to that of hydrophobic fouling release coating and hydrophilic non-fouling coating. Thus, a fine balance between roughness, attachment points and size range of a microtexture is essential for fabrication of surface topography for superior antifouling performance.[118,119,120]

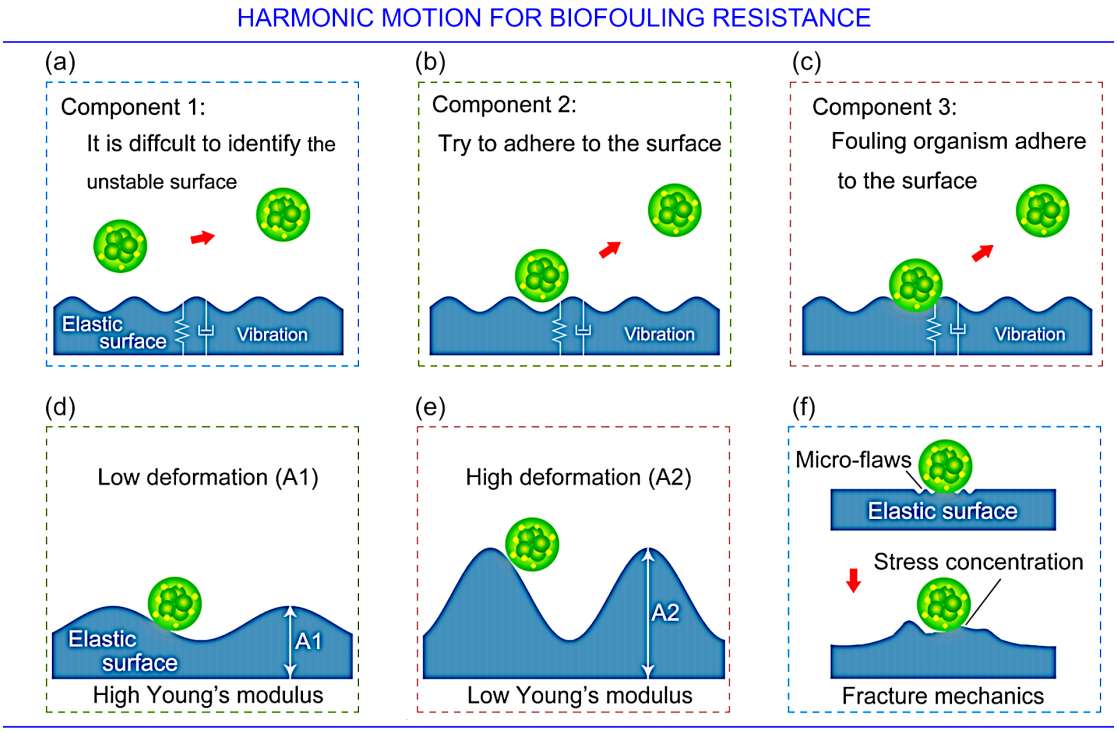

Figure 10. **Graphene oxide – silicone rubber composite membranes for the combined antifouling effect**. (a-c) Effect of the "harmonic shift" on antifouling activity. (d) **Both high elasticity** and Young's modulus. (e) Low Young's modulus and high elasticity. (f) A schematic of the action of fracture mechanics with respect to antifouling. Reprinted from Jin *et al.* **2019**[88] under the terms and conditions of CC BY license.

In the recent study by Jin *et al*. the graphene oxide/silicone rubber composite membranes were used to produce a combined antifouling effect.[88] Interestingly, the authors discovered the influence of the coating colour, but only under non-static conditions. After considering the dolphin's skin as a starting point, the authors fabricated and tested the antifouling performance of the membranes produced on a base of graphene oxide and silicone rubber, which exhibited tuneable physical and mechanical characteristics such as free energy and elastic modulus, which are necessary to hinder biofouling. Diatom attachment characterization carried out under static conditions showed that the colour pattern is not a factor of influence, unlike the synergetic conjunction of the effects caused by the colours and elastic modulus, which enhances greatly the antifouling behaviour. Moreover, the results are explained by use of a theoretical assumption about the "harmonic motion effect" developed by the authors. Based on the diatom attachment research, the content of 0.36 wt. % was found to be optimal for graphene oxide with respect to the antifouling effect. In addition, it was concluded about the interchangeability of graphene and graphene oxide to improve the antifouling behaviour of silicone rubber. Various behaviours of graphene oxide/silicone rubber composite membranes are illustrated in **Figure 10**.

One more example of a bio-inspired graphene-based antifouling system was the composite made of graphene-silicone elastomers featured with a tentacle structure (TS-GSE), which was suggested after considering the antifouling characteristics of corals. This time, three factors, namely high electronegativity, low surface energy, and optimal elastic modulus, were combined to achieve the goal. The surface layer of modified graphene-silicone elastomers is known as the material that removes bacteria by a physical effect. Outcomes of the modelling revealed that the elasticity of the material is characterized by an effect of a harmonic shift at the frequency of 10 Hz exhibited as the deformation under condition of the fluid flow. This shift urges the elastic surface to be unstable, thus removing the foulants. Both static and dynamic conditions were applied to verify the effect on the bacteria attachment with respect to the antiadhesion behaviour of modified graphene-silicone elastomers, which exhibited high antiadhesion response for Gram-positive and Gram-negative bacteria. **Figure 11** illustrates the difference in processes in non-bactericidal and bactericidal antifouling films of graphene-silicone elastomers modified with tentacle structures.

A mechanism describing the physical nature of bacterial removal and the creation of a bacteria-free layer on the tentacle-modified graphene-silicone elastomers composite material is shown **Figure 11a**. For comparison, a coating that combines the physical bacterial repulsion with a chemical action of biocide released from the surface was also exposed to bacteria under the same conditions (**Figure 11b**). While promising in principle, the presence of chemical agents resulted in cell death. When components of cytoplasm leaked from dead bacteria on the surface, the physical antifouling performance of the layer was compromised, suggesting a limitation that needs to be addressed. It was suggested that the attachment of organic molecules released from dying cells led to the formation of a so-called 'conditioning film', allowing for subsequent attachment of cells and eventual biofilm formation. As such, the non-biocidal tentacle-modified graphene-silicone elastomers composite films revealed prolonged antiadhesion effect, while the bactericidal coatings of quaternary ammonium compounds do not fit the antifouling requirements.

Graphene composites can be also used for the fabrication of elastic graphene – silicone rubber composite membranes with antifouling properties (**Figures 11c-g**). These 2D structures possess both the low values of surface energy and tunable elastic modulus to be used as an antifouling material. The membranes exhibited much better antifouling effect than the rigid sheets made of polystyrene, when subjecting them to hydrodynamic tests. At the same time, the use of laser-displacement sensor allowed the research to reveal the micron-size deformations on the surface, and the assumption about their important role was verified by implementing a mechanical model. **Figure 11c** illustrates the setup and methodic of the displacement measurement, and **Figure 11d** shows the optical photographs of pristine samples before and after the tests on bacteria attachment in the flowing water. The results of the research confirm this unstable surface as suitable to create the antifouling effect. From the study of the bacterial attachment, a new membrane-shaped material was developed by introducing just 0.36 wt % graphene into the matrix to fit the antifouling demands. The results of the experiments are illustrated in **Figure 11e-g**. **Figure 11e** illustrates the characterization on the spread sample, when the graphene-silicone rubber composite sample with 0.36 wt % is settled with low concentration of bacteria, while pristine silicone rubber membrane without the graphene content reveal the highest population of the bacteria. Similar results were obtained for the optical density measurements (**Figure 11f**) and the pull-off force (**Figure 11g**).

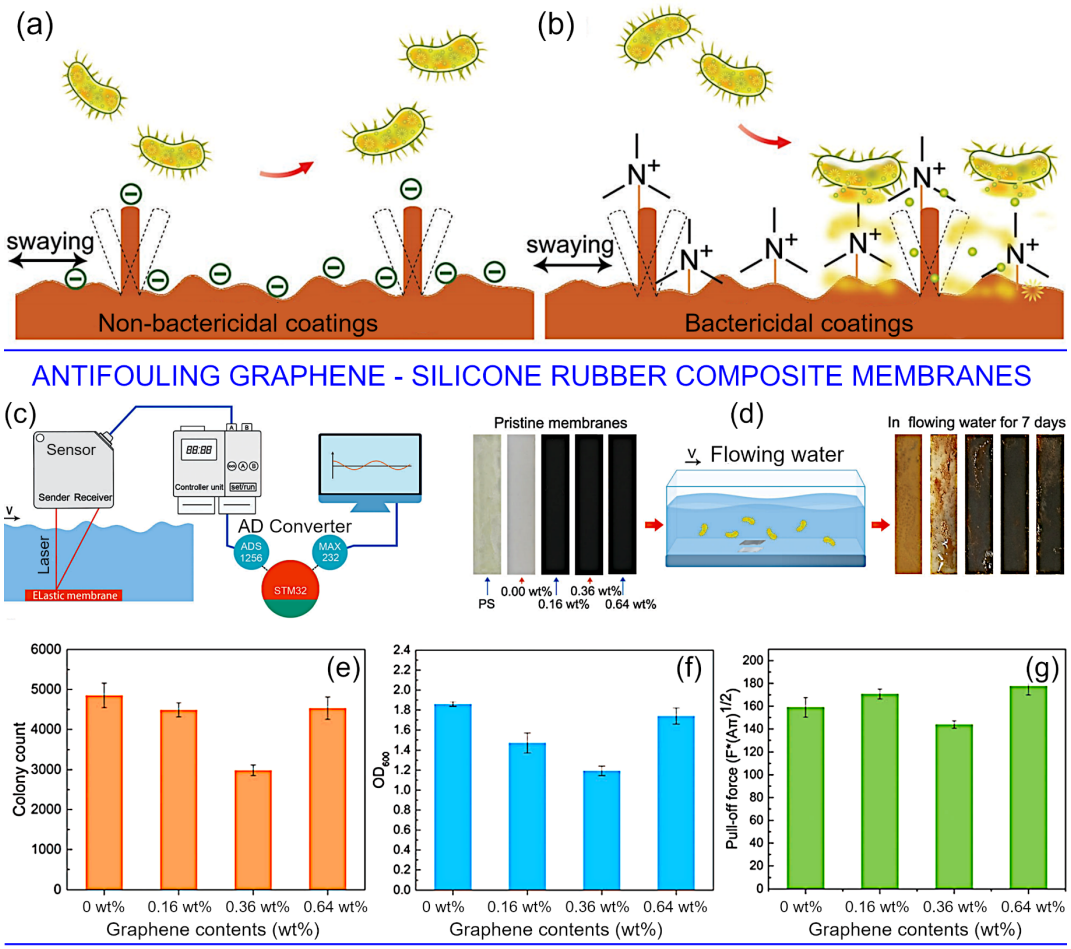

Figure 11. **Antifouling films of graphene-silicone elastomers modified with tentacle structures**. Schematic of the effect caused by the non-bactericidal (a) and bactericidal coatings (b). The non-bactericidal film of tentacle-modified graphene-silicone elastomers composite material can remove bacteria through a physical mechanism. Reprinted with **permission.**[121] **Antifouling elastic graphene – silicone rubber composite membranes**. (c) Illustration of the setup and methodic used for the laser-displacement measurement; (d) Optical photographs of pristine samples before and after the tests on the attachment of bacteria in the flowing water; Histograms that show the effect of the graphene contents on colony counts (e), OD_{600} results after 7 days for four samples (f), pull-off force of the membranes calculated by engaging the "Griffith's theory of rupture" (g). Reprinted with **permission.**[122]

5.3 Graphene and RGO with polymer matrixes

Combination of graphene and graphene oxide flakes with polymer matrixes allows designing very efficient marine antifouling coatings. In the recently published study, two innovative marine fouling release surfaces have been described. These two new types of superhydrophobic polydimethylsiloxane (PDMS) nanocomposite material were loaded with graphene oxide/boehmite nanorods (GO-γ-AlOOH) and reduced graphene oxide (RGO) nanofillers (**Figure 12a**). The antifouling and self-cleaning capabilities of these materials were altered by controlling the design and distribution of the nanofillers in the PDMS matrix. The γ-AlOOH nanorods possessed a single crystallinity and were around 200 nm long with mean diameter of about 10–20 nm. The reduces graphene oxide was made using a hydrothermal process, while the GO-γ-AlOOH nanocomposite coatings as fouling-release materials were fabricated using a chemical deposition process.

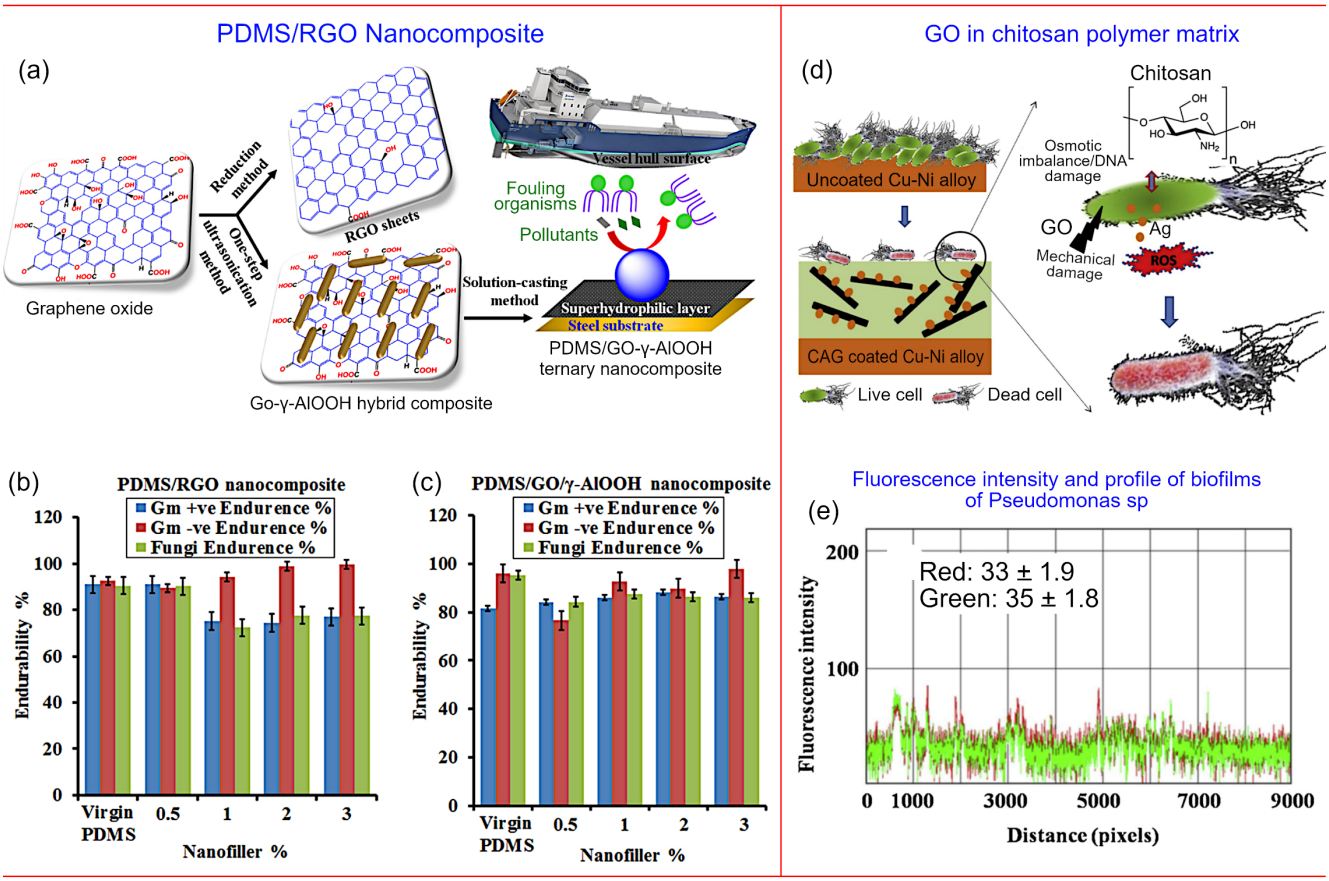

Figure 12. **Graphene and RGO with polymer matrixes**. (a) Fabrication of fouling release and superhydrophobic coatings on ship hulls using reduced GO and GO-γ-AlOOH from GO are prepared, using reduction technique and single-step ultrasonication processes respectively. (b) Percentages of microbial strains that were able to survive after being exposed to samples coated with RGO/PDMS material against gramme-negative, gramme-positive, and fungal strains, respectively while (c) Percentages of microbial strains that were able to survive after coming into contact with materials coated with PDMS/GO-c-AlOOH material against gramme-negative, gramme-postive, and fungal strains, respectively. Reprinted with permission from Selim *et al.* **2022.**[123] (d) An illustration of the theory behind how ternary composite coated Cu-Ni samples exhibit antibacterial activity (e) *Pseudomonas* sp. biofilms' fluorescence intensity and line profile on a sample containing 0.025 weight percent of graphene oxide and 0.5 g/L of chitosan. Reprinted with permission from Jena *et al.* **2020.**[124]

Chosen microorganisms were used in laboratory tests for 30 days to gauge the coatings antifouling effectiveness. In comparison to siloxane/RGO coatings, siloxane/GO-γ-AlOOH nanorod coatings demonstrated stronger antibacterial activity against several strains of bacteria. The least biodegradability percentage (1.6%) was found in the siloxane/GO-γ-AlOOH nanorod coatings (3 wt%), and the gramme-negative and gramme-positive microbial tolerance percentages were 97.94% and 86.42%, respectively.To corroborate the coatings' antifouling performance for forty-five days in a equatorial region, a field test in natural saltwater was carried out. The uniformity of the GO-γ-AlOOH (3 wt%) distribution was the most significant superhydrophobic nanostructured antifouling coating (**Figure 12b,c**).

Figure 12d shows the hypothesised mechanism for the antibacterial activity provided by Cu-Ni samples covered with ternary composites. Utilizing a low-cost, industrially scalable electrophoretic deposition (EPD) technique, a novel ternary composite coating made of graphene oxide, chitosan, and silver on Cu-Ni Alloy exhibits significantly improved anticorrosive and antibacterial capabilities. The amide bond between the chitosan and GO made the favorable mechanical interlinking resulting in crack free sturdy film. Based on the microbiological assesement, the ternary composite exhibits strong antibacterial action, which has prospective uses in the maritime environment (**Figure 12e**).

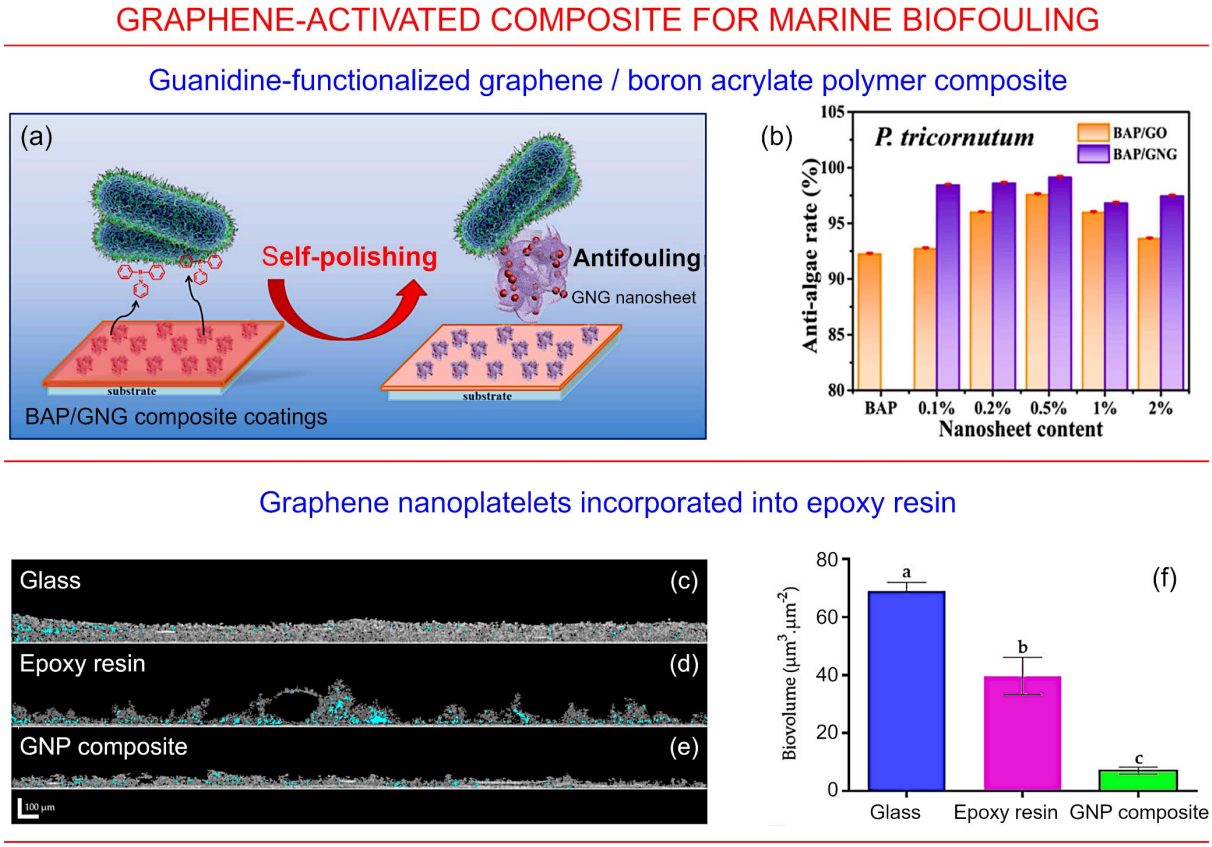

Figure 13. Graphene and RGO with polymer matrixes. (a) A schematic illustrating the self-polishing boron acrylate polymer/guanidine-functionalized graphene composites' potential antifouling mechanism (b) Anti-algae activity of the novel antifouling coatings as a function of nanosheet content against *P. tricornutum*. Reprinted with permission from Zhang *et al.* **2021.**[125] (c-e) Representative two dimesonal transverse optical coherence tomography pictures of biofilms produced by Lusitaniella coriacea LEGE 07157 on (c) glass, (d) epoxy resin, and (e) GNP composite after exposure of 49 days. Blue is used to denote the biofilm architecture void areas (scale bar = 100 µm). (f) Cyanobacterial biofilm volume data were derived from confocal files. The means and ± SD are displayed. Reprinted with permission from Romeu *et al.* **2022.**[126]

Zhang *et al*. recently published a variety of antifouling hybrid coatings. These coatings were based on guanidine-modified graphene (GNG) and boron acrylate polymer (BAP) having self-polishing properties (**Figure 13a**).[125] Compared to graphene oxide, GNG exhibited more surface wrinkling and was distributed more evenly inside and outside of BAP, leading to tighter binding of inorganic and organic chemicals at the interface. The hybrid coatings made of BAP and GNG performed exceptionally well against algae adhesion. In particular, suppression rate of *Phaeodactylum tricornutum* reached 99.2% (**Figure 13b**). Also high bactericidal rates of up to 95 % and 94.2%, were found against *Staphylococcus aureus* and *Escherichia coli,* respectively. This performance is attributed to the self-polishing nature of

BPA, revealing the guanidine-modified graphene on the exterior. In one respect, the produced guanidine-modified graphene served as a filler and enhanced the antifouling performance by modifying the coating's hydrolysis rate. In other respect, the polymer matrix hydrolysis and baring of guanidine-modified graphene improved the antifouling efficiency. BAP/GNG exhibits promise as an antifouling coating with potential uses in marine antifouling.

An interesting comparative study of the pristine graphene nanoplatelet (GNP) containing coating was recently reported by Romeu et al.[126] Compared to the untreated surfaces (glass & epoxy resin), the biofilms formed on the GNP composite had decreased wet weight, thickness, biovolume, and surface coverage during the maturation stage. Additionally, the GNP composite promoted the growth of a denser biofilm and deferred the formation of cyanobacterial biofilm. (**Figure 13c-e**). The monitoring of cyanobacterial biofilm activity over time carried out in this study is especially pertinent because the graphene coating should function as a lasting antifouling material for use in marine environments. (**Figure 13f**). Future research will analyse these GNP-based composites through in vitro testing to evaluate their effectiveness against diverse-genus biofilms, and in-situ to evaluate their impact on the development of biofilms by other microfoulers or to gauge the potential adverse effects of severe marine conditions on these nanostructured coatings. Future tests ought to pay attention to tribological standards like the temperature, wear, friction coefficient, and appropriate durability for the application, as well as surface analysis for extended-period assays.

Figure 14a demonstrates the self-polishing antifouling and anticorrosion a processes of antifouling paint based on composite of graphene oxide and acrylate changed by propenoic acid. Propenoic acid that contains carboxyl group was used to functionalized graphene oxide. In situ radical polymerization was used to create an propenoic acid transformed graphene oxide/acrylate material Because of the molecular bonding among acrylic resin and AGO, the compatibility and distribution of the acrylic acid-transformed graphene oxide in materials can be enhanced. These composite materials have both hydrolysis and corrosion resistant characteristics. These materials are lighter and more environmentally benign when compared to the commonly used zinc-laden corrosion resistant coatings. This material, unlike zinc powder, does not react with seawater when used in an underwater setting to reduce the efficacy of the coating. In the meantime, this material exhibits self-cleaning antifouling properties in marine environment. Moreover, it was discovered that AGO's synergistic processes enhanced the effectiveness of the corrosion resistance and self-cleaning antifouling properties of the material.

The pristine graphene nanoplatelets/polydimethylsiloxane (PDMS) with 5 wt% of graphene nanoplatelets also demonstrate very good antifouling activity (**Figure 14b,c**).[128] Over for 42 days, this novel material was evaluated for its ability to reduce biofilms in controlled hydrodynamic circumstances resembling marine environment. When subjected to the material with 5 wt% of graphene nanoplatelets for 24 h, *C. marina* produced endogenous reactive oxygen species (ROS), increased metabolic action, and membrane deterioration, as revealed by flow cytometry. Besides, in comparison to PDMS, *C. marina* biofilms produced on this composite reliably displayed reduced cell count and thickness (down to 43% reductions). When contrasted with PDMS, full-grown biofilms formed on graphene-based materials had reduced voids (34% reduction) and less biovolume (25% reduction), according to the biofilm morphology study. This material demonstrated promising potential as a marine antifouling coating by preventing the growth of the C. marina biofilm.

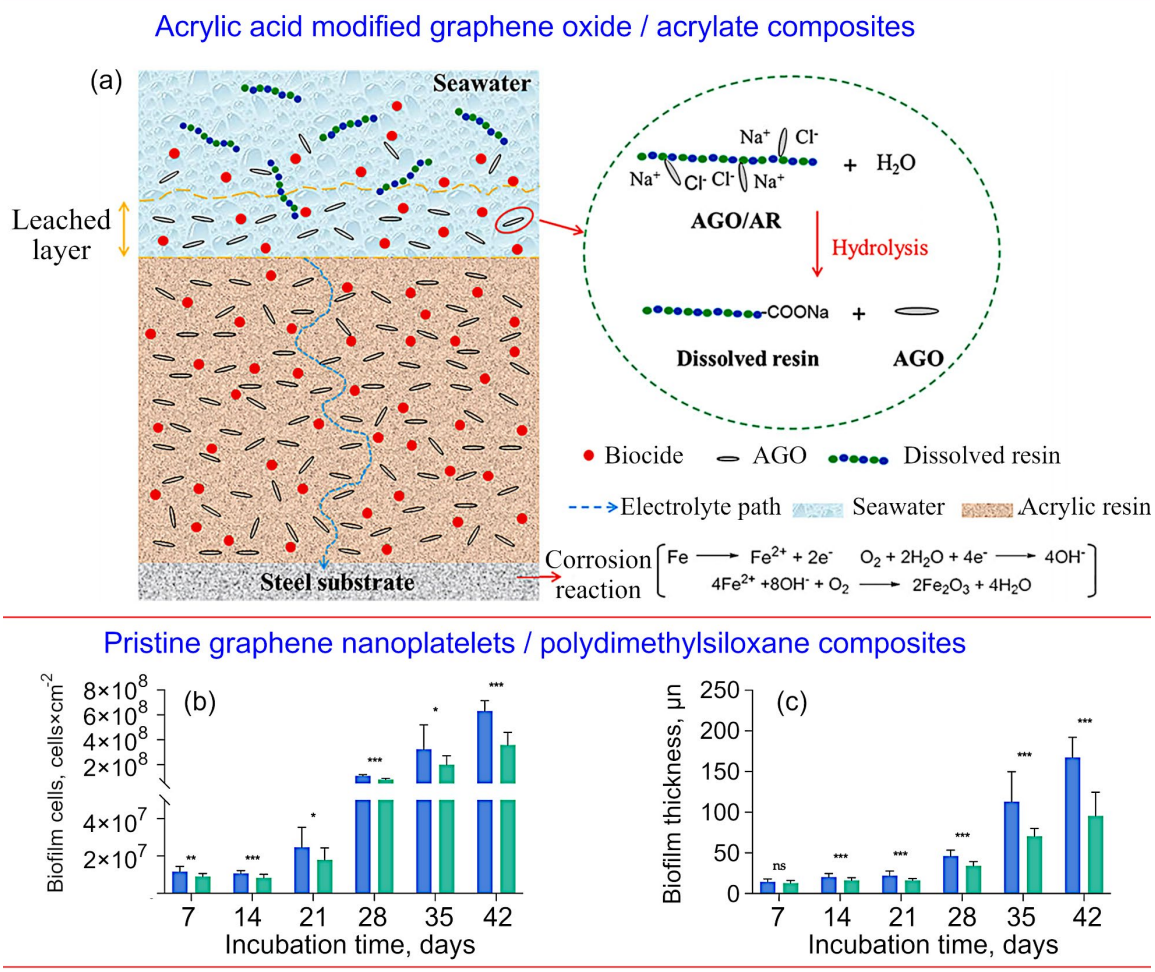

Figure 14. (a) Implemented mechanisms for anticorrosion and self-polishing antifouling of acrylic acid modified graphene oxide/acrylate composites-based paint. Reprinted with permission from Li *et al.* **2022.**[127] Quantitative estimation of the amount of *C. marina* biofilm deposited on polydimethylsiloxane (■) and in a sample containing 5 wt% of graphene nanoplatelets (■), for a total period of 42 days. The plot reports: (b) the density of biofilm cells [cells/cm^2], and (c) the measured biofilm thickness [µm]. For convenience, the results report (mean value ± SD). The statistical significance is represented by the p-values: (Non-Significant: $p \geq 0.05$; (*) $p \leq 0.05$; (**) $p \leq 0.01$; (***) $p \leq 0.001$). Reprinted from Sousa-Cardoso *et al.* **2022**[128] under terms and conditions of CC BY license.

The polyaniline/p-phenylenediamine-functionalized multifunctional graphene oxide coatings were also recently reported. They show excellent macroscopic antifouling properties in the experiments performed at typical marine conditions.[129,130] Scheme of synthesis process for the epoxy coatings reinforced with polyaniline (PANI)/p-phenylenediamine-functionalized graphene oxide (PGO) and the PANI–PGO nanocomposites is illustrated in **Figure 15a**. Selected PANI-PGO composites of different mass ratios were employed, while the sample with 1:1 mass ratio is shown in the figure. In order to deal with PANI-PGO at 0°C, a polymerization method was utilized with the assistance of ultrasound techniques. The coatings consisting of films of Epoxy/PANI–PGO (x), for x = (0.05–0.40) g, were brushed onto standard carbon-steel substrates. **Figures 15b,c** illustrate the capability of the PANI–PGO nano-composite coatings for their use in developing high quality epoxy paints against corrosive environments.

Epoxy-matrix polyaniline/p-phenylenediamine-functionalized graphene oxide

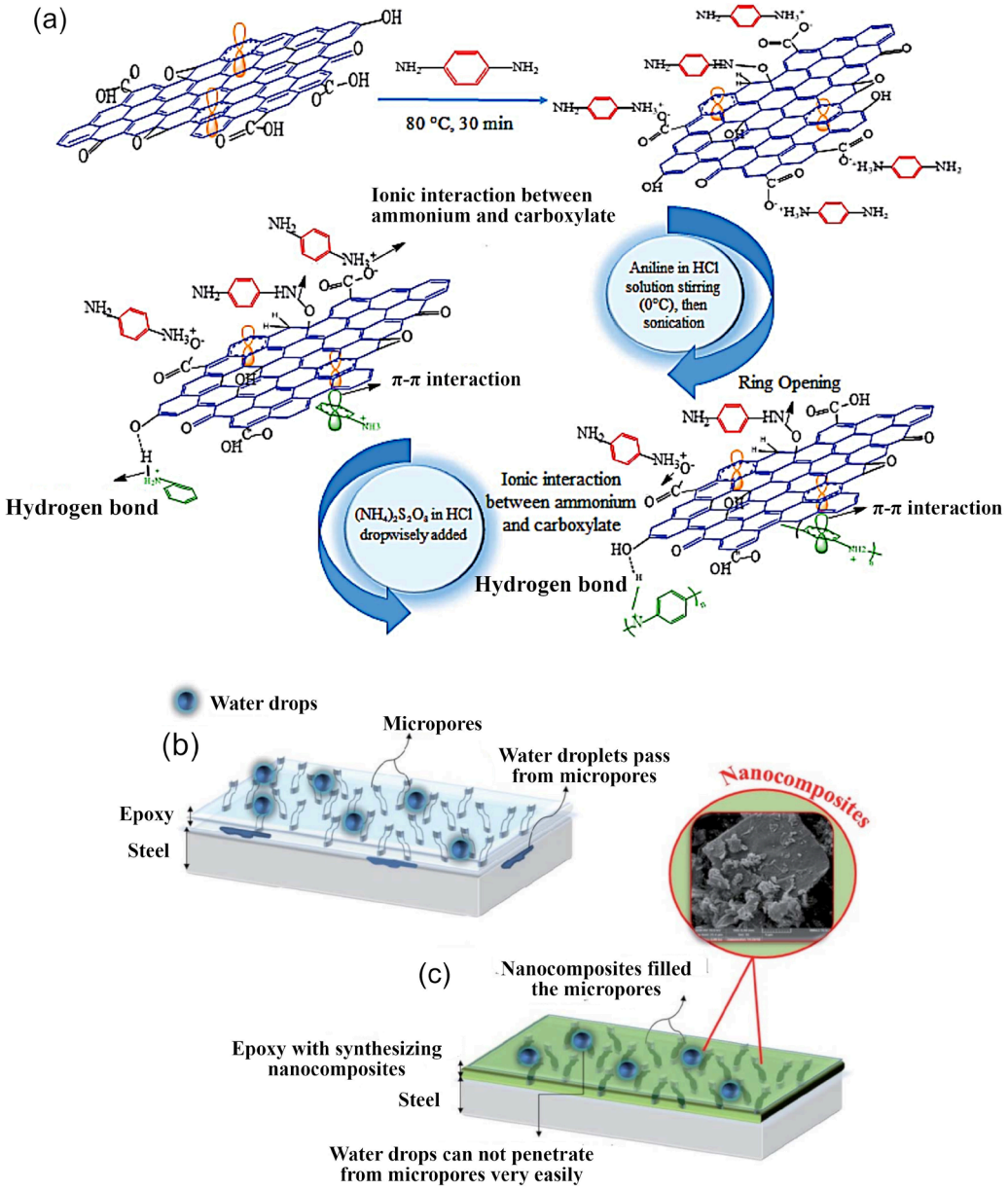

Figure 15. (a) Scheme of synthesis process for the epoxy coatings reinforced with polyaniline (PANI)/p -phenylenediamine-functionalized graphene oxide (PGO). (b,c) Performance of an Epoxy/PANI-PGO coating in the presence of a corrosive electrolyte as a function of time: (b) A pure epoxy film is colorless and features a high density of holes on its surface allowing water molecules to pass through. (c) When the epoxy film contains additional PANI-PGO nanoparticles, the pores reduce their size considerably thus limiting the passage of water. (d) Optical visualization of macroscopic fouling on the surfaces of E/PANI–PGO coatings prior to and subsequent to three month-long exposure to an aquarium environment. Reprinted from Fazli-Shokouhi *et al.* **2021**[130] under terms and conditions of CC NC license.

Figure 16a illustrates the technological process for the preparation of graphene oxide-nano-SiO_2/polydimethylsiloxane composite coating. A simple technique based on anodic electrophoretic deposition, augmented with dip coating, on carbon steel was used to produce these highly corrosion resistant and anti-biofouling composites, also characterized by a long durability. The coated samples showed a reduced density of bacterial cell and biofilm formation as demonstrated by the authors, based on epifluorescence together with confocal laser scanning microscopy. The authors conclude that the toxic effect of GO and the poor bio-adhesion on the PDMS surface, the latter induced by the enhanced surface stiffness produced by the Si–O–Si network, can explain the observed excellent antibacterial activity and anti-biofouling properties of the new composite coating. One can expect that GSP coatings on a CS surface can find very promising applications in real marine environments since they can provide significant and lasting protection against corrosion in 3.5 wt% NaCl solutions, together with their remarkable antibiofouling properties.

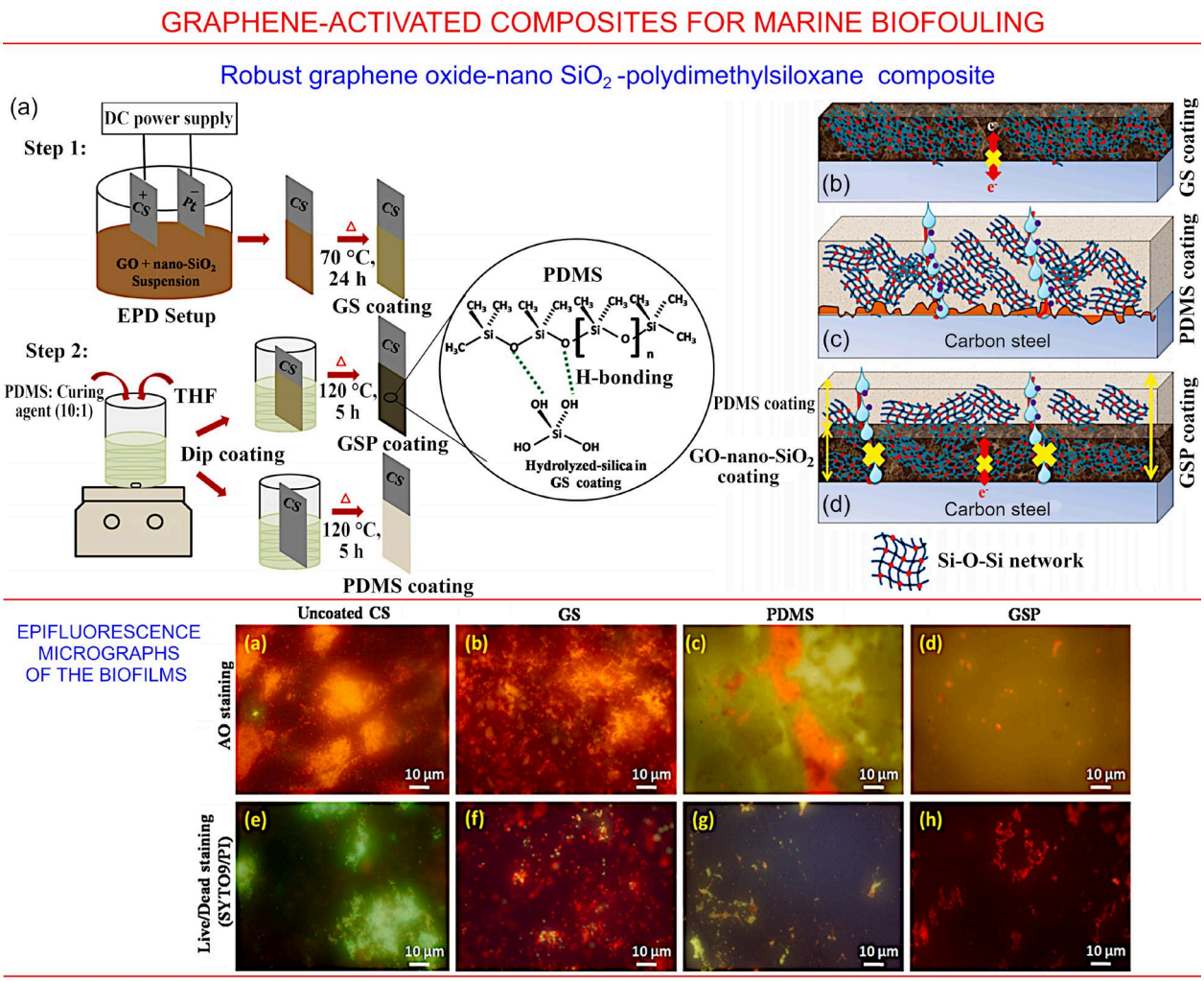

Figure 16. **Upper panel**: (a) Scheme of the technological process for the preparation of graphene oxide-nano-SiO_2 / polydimethylsiloxane composite coating. (b-c) Schematic illustration of the possible mechanism suggested for surface protection against corrosion, in the cases: (b) GS coating, (c) polydimethylsiloxane, (d) GO-nano-SiO_2/PDMS coating. **Bottom panel**: Epifluorescent microscopy shows the formation of *Pseudomonas* sp. biofilms (AO stained) on the surfaces of (a) uncoated CS, (b) GS, (c) PDMS, (d) GSP coated samples after 6 h of incubation. Reprinted with permission from Jena *et al.* **2021.**[131]

Figures 16b-d illustrates the suggested mechanism of surface protection in the three cases considered: GS, PDMS and GSP coatings of carbon steel surfaces. The former exhibited much better resistance to corrosion and lower galvanic current than in the case of GSP. The PDMS displayed high corrosion resistance only at the initial immersion period, then showing a decreased resistance, followed by a gradually increased one at later times. This complex variation of corrosion resistance in time can be attributed

to percolation effects that the electrolyte undergoes via the micro-pores present in the coating. GSP coating displayed a similar trend in the impedance behavior, its value was however higher than in the case of PDMS coating, suggesting a better protection performance against corrosion. The bottom panel of **Figure 16** illustrates the formation of *Pseudomonas sp.* Biofilms.

We should stress here that the corrosion in marine environment is one of the key processes related to biofouling. Indeed, many antifouling materials feature low-porosity, smooth surfaces (including self-polishing materials) that significantly inhibit attachment of fouling organisms onto the surface and prohibit the supply of water and nutritional substances to them. Corrosion creates highly porous surface that catalyses and significantly promotes the following fouling. Not surprisingly, many publications (including several those discussed in our review) consider the materials that feature both antifouling and anti-corrosive properties in the context of ***biocorrosion***. For example, S. Fazli-Shokouhi *et al.*, describe the material with dual anti-corrosion and anti-fouling performance, the corrosion- and fouling-mitigating characteristics of commercially-available epoxy coatings were significantly enhanced through functionalization with graphene oxide composites.[130] Z. Liu with coauthors proposed the dual-functional coatings for corrosion resistance and antifouling applications.[132] A. Balakrishnan with coauthors have described the coatings with improved anti-corrosion and anti-biofouling properties.[169] Y. Li with coauthors proposed the synergistic mechanisms of anticorrosion and antifouling properties.[127] Also, various aspects of the interrelation of corrosion and biofouling have also been considered in the classical publications. For instance, mild steel and other metals and alloys that are readily susceptible to corrosion have also been shown to be subject to fouling due to their reactivity with oxygen, and in return the attachment of the foulant initiates and promotes crevice corrosion at the point of attachment. Of carious strategies to mitigate these two processes, polymer coatings are frequently used to limit both processes.[133] As an example of very recent graphene-based approach to the corrosion prevention, we describe here the graphene oxide-nano-SiO_2/polydimethylsiloxane composite coating.

5.4 Graphene and RGO with metal and metal oxides

Graphene and RGO-based marine antifouling coatings could be also activated with various metals and metal oxides. This direction is also fast developing, and several important results were recently reported. The question arises of how can one prevent a significant grow of a biofilm on sensors immersed in seawater (e.g. sensors for monitoring seabed, fish farming and many others). To this end, a series of nanocomposites of graphene oxide containing silver nanoparticles (GOA) have been developed and used as coatings of standard sensor materials such as polypropylene. Antifouling tests performed using *Halomonas Pacifica* (*H. Pacifica*) and different mixtures of commonly spread marine algae have proved the suitability of GOA as very useful coatings. Indeed, the good antifouling properties of GOA-based composites have been related to the high dispersibility of Ag nanoparticles. These observations might help the development of antifouling materials for sensors in more general cases, as they show 83% biofilm inhibition against *H. Pacifica* and 56% against the used algae mixtures. **Figure 17a** illustrates the technological process used to prepare this composite, and **Figure 17b** shows the assessment of antifouling activity, with the graphene composites demonstrating significant fouling protection.

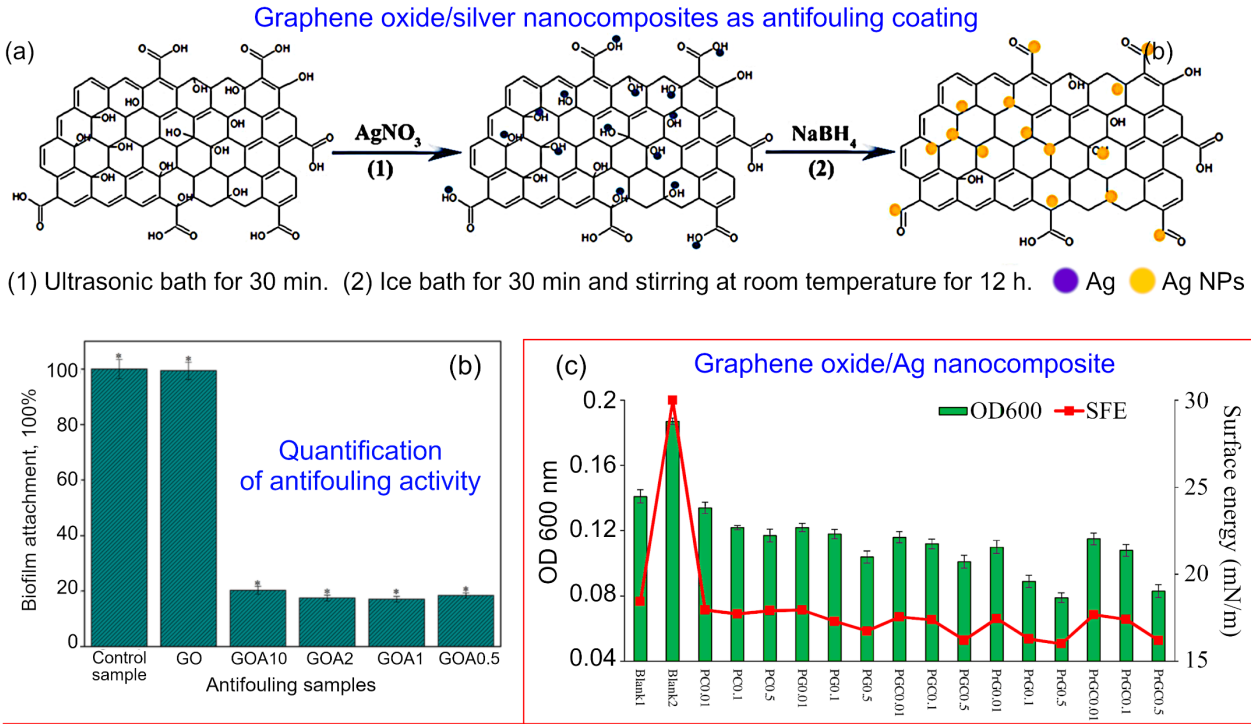

Figure 17. (a,b) **Graphene oxide/silver nanocomposites as antifouling coatings**. (a) Simplified representation of the fabrication of graphene oxide (GO)/silver nanoparticles (Ag NPs) nanocomposites (GOA). (b) Biofilm attachment (in %) to quantify the resulting antifouling activity in the cases: Control sample, GO and GOA nanocomposites. The bars report, mean value ± SD, for the three cases. The statistical significance is assumed for p-values: $P < 0.05$ (Student's *t*-test). Reprinted from Zhang *et al.* **2021**[134] under terms and conditions of CC BY license. (c) **Graphene oxide/Ag nanocomposite.** The optical density due to bacteria and the surface energy (Nm/m) for the coating surfaces in 4 days of immersion in natural sea water (see the list of sample marking in the original publication). Reprinted with permission from Soleimani *et al.* **2021**.[135]

Figure 17c presents the results of foiling tests for another reduced graphenes oxide/silver nanocomposite. The nano-fillers, graphenes oxide/Ag nanocomposites, bare GO and multi-wall carbon nanotubes (MWCNTs), were separately introduced into PDMS-based coatings having, respectively 0.01, 0.1, and 0.5%wt. The different sample surfaces were characterized by measuring pseudo-barnacle adhesion strength and water static contact angles, while the field immersion was evaluated in natural seawater. Among the three samples, the 0.5 wt% of graphenes oxide/Ag nanocomposites displayed the best results. A synergistic effect between *A. Marina* and silver in the structure of graphene-based nanocomposites allowed for outstanding results of antifouling efficiency for PDMS-based coatings.

The micron-scaled graphene flakes were used as supporting and framing material for clusters of Ag nanoparticles, to produce the material combining anti-microbial and SERS (surface-enhanced Raman spectroscopy) properties. In **Figure 18a,** the processes of few graphene (FLG) flakes synthesis and of hydrothermal reduction of graphene-Ag nano-composite are illustrated. The authors novel design consisted of a 2-step synthesis method of GAg nanocomposites by introducing a bypass to avoid the formation of graphene oxide. As a result, it produces Ag nanoparticles located on graphene sheets via a soft hydrothermal reduction process. It was found that GAg inhibited Halomonas pacifica, responsible for a microbe type of biofilm, with just a 1.3 wt.% loading of Ag. While all GAg samples produced significant biofilm inhibitions, the Ag loading (i.e. 4.9 wt.% Ag) was able to result in 99.6% of biofilm inhibition. Furthermore, marine microalgae such as *Dunaliella tertiolecta* and *Isochrysis sp.* could not proliferate in the presence of GAg, which inhibited the associated organisms growth by more than 80% after 96 h. The remarkable marine antifouling properties of GAg were a result of the synergy between biocidal AgNPs, firmly located on the robust graphene sheets, and the intrinsic flexibility of the latter, allowing for maximizing the active surface area in contact with specific target organisms. **Figure 18b** shoes the results of the antifouling tests.

Graphene oxide/silver nanocomposites as antifouling coating

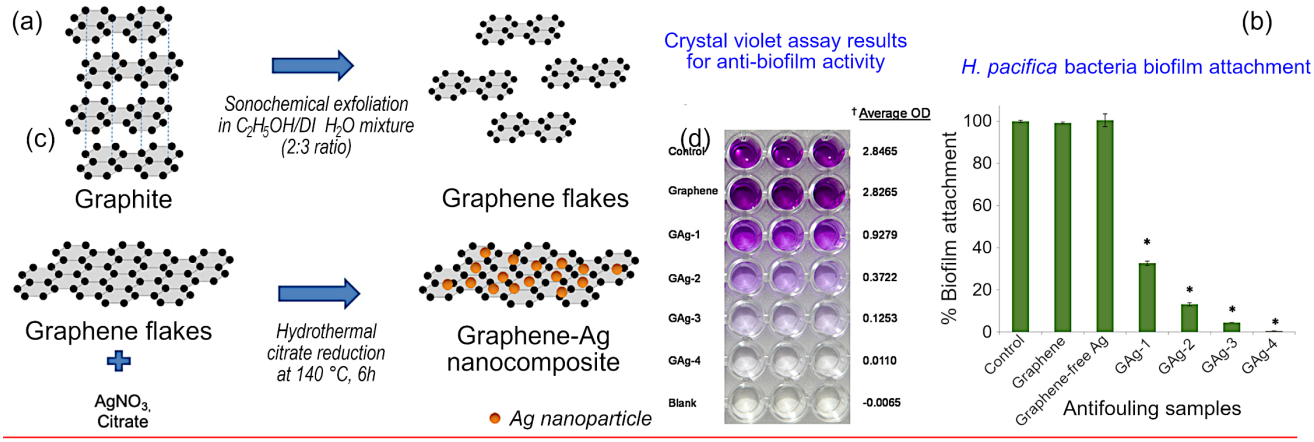

Figure 18. (a) Illustration of the synthesis process (not to scale) in the cases of: few-layer graphene (FLG) flakes, and graphene-Ag nanocomposite formation induced by a hydrothermal reduction process. (b) Attachment of H. Pacifica bacteria biofilm after crystal violet analysis aimed at determining the anti-biofilm activity of different materials, for GAg at 0.1 mg/ml († indicates the average OD measured at 570 nm). The bars indicate the value, mean ± S.D., for each of the three experiments performed independently. The '*' refers to the statistical significance of the data corresponding to the p-value: $P < 0.05$ (Student's t-test). Reprinted with permission from Yee *et al.*[136] Copyright Elsevier.

While silver oxide-graphene composites are indeed quite efficient for the marine antifouling coatings and paints, other metal oxides such as Zn and Cu are also under investigation.[137,138] **Figure 19** illustrates the process of fabrication of the polydimethysiloxane/ZnO–graphene oxide antifouling coating and its antifouling properties. The ZnO–graphene oxide (ZnO–GO) nanocomposites were synthesized by employing a facile one-pot reaction. In order to produce PDMS/ZnO–GO nanocomposites (PZGO), a simple solution mixing method was used to add suitable quantities of ZnO–GO to the polydimet-hylsiloxane-PDMS matrix. The final coating was produced by spinning of PZGO/tetrahydrofuran suspension. The antifouling tests were performed using two marine microorganisms: the cyanobacterium Synechococcus sp. (Strain PCC 7002) and the diatom Phaeodactylum tricornutum. The sample with mass ratio of ZnO–GO to PDMS of 0.2 wt % (PZGO 0.2) showed remarkably good antifouling properties for the composite containing 8.5% of Synechococcus sp. biofilm coverage, while PZGO 0.1 (mass ratio of ZnO–GO to PDMS: 0.1 wt%) showed only 2.4% P. tricornutum biofilm coverage. The antifouling properties of synthesized PZGO nanocomposites can be attributed to their high Ra and hydrophobicity, which were obtained due to the good dispersion of ZnO–GO in the PDMS matrix. This study further suggests that PZGO nanocomposites have a promising potential use in building future sensor's antifouling coating, in particular due to their improved durability.

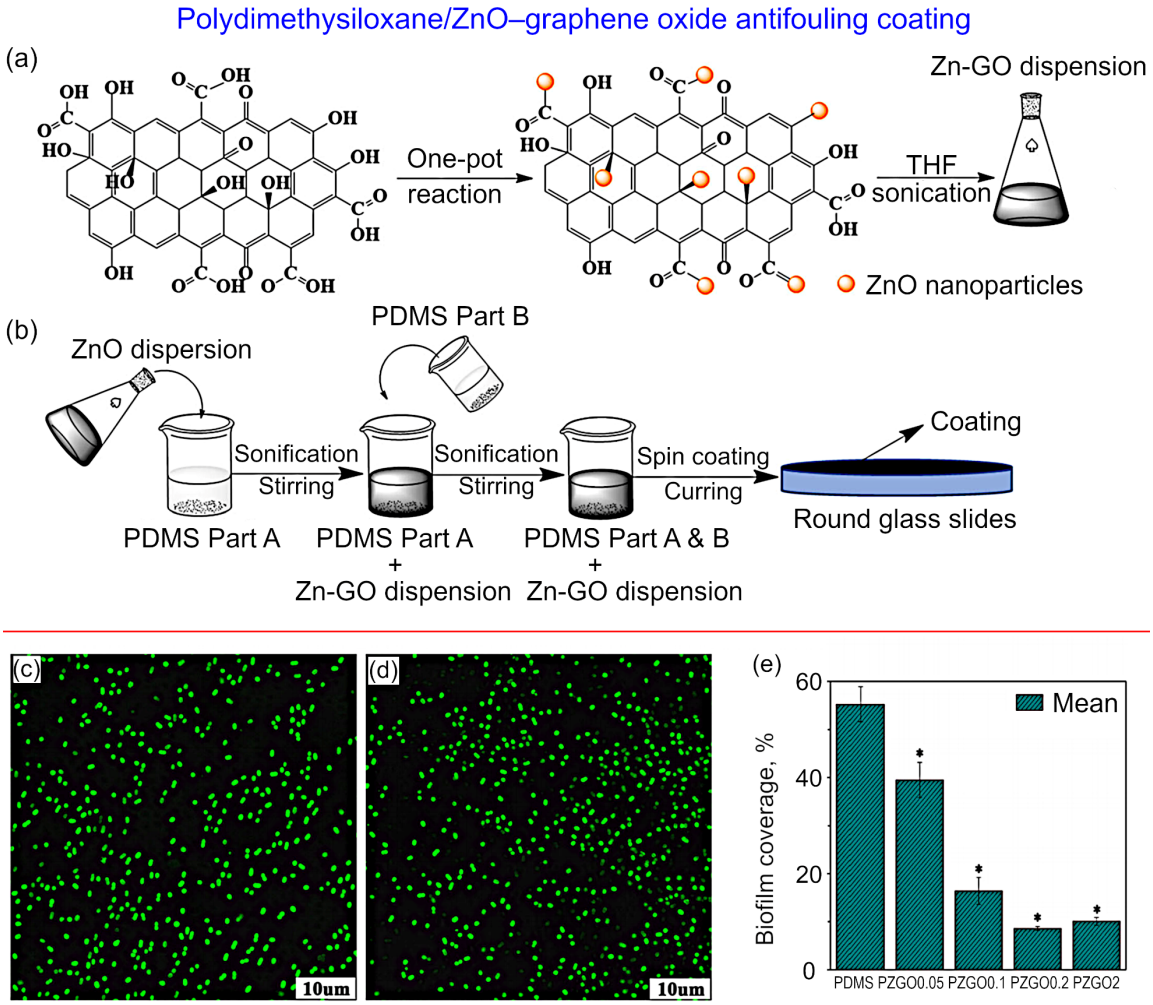

Figure 19. **Polydimethysiloxane/ZnO–Graphene oxide antifouling coating**. Upper panel: (a) One-pot method for the preparation of ZnO–graphene oxide nanocomposites. (b) PDMS/ZnO–graphene oxide nanocomposite preparation followed by spin coating of the surface. **Lower panel**: Images produced by confocal laser scanning microscopy to show the adhesion of *Synechoccocus sp 7002* on: (c) PZGO0.2 sample (composite with ZnO–graphene oxide mass ratio to PDMS of 0.2 wt %), (d) PZGO2 sample (composite with ZnO–graphene oxide mass ratio to PDMS of 2 wt %). (e) Biofilm coverage (in % adhesion ratio) of *Synechoccocus sp 7002*. The error bars are displayed as ± SD (n = 5), for statistically significant p-values: *P < 0.05. The slight increase of biofilm coverage for samples with more than 0.2 wt% of ZnO/graphene oxide is due to significant aggregation of ZnO-graphene oxide. Reprinted from Zhang *et al.* **2022**[137] under terms and conditions of CC BY license.

In addition to shipping industry, fouling is a significant issue in water decontamination/purification, and similarly there is a strong demand for materials with antifouling properties. This is because organisms that exist in water have a tendency to settle on the surfaces of the systems used for purification, including in pipes and on membranes, thereby creating conditions for reduced flow and bio-corrosion, generating risks for human health due to biocontamination as well as release of potentially harmful agents from antifouling surfaces, and increase the cost of using water purification technologies, especially by developing economies or rural and remote communities. A novel strategy for creation of coatings that do not release biocides relies on the implementation of polydimethylsiloxane and polyurethane-based matrices to fabricate ceramic filters for the purpose. According to the experiments on the antimicrobial activity and biocide release, the population of methicillin-resistant *Staphylococcus aureusbacteria* on the filters covered by the polyurethane-based material with the addition of grafted Econea biocide was decreased to 66 %, and no biocide release was observed after being exposed to water for 45 days. The surfaces of a polyurethane-based composite also revealed the enhanced suppression with respect to the

growth of *Enterococcus faecalis* biofilms at flow conditions, in comparison with the pure polyurethane-based composite. Thus, the water filters with the coatings can be considered as a suitable substitution to decrease the biofouling contamination of water, thus reducing the environmental risks.[139]

5.5 Testing graphene-based antifouling materials under the field and simulated natural conditions

Graphene and RGO-based marine antifouling coatings are complex material systems that often rely on a combination of several distinct but synergistic physical and chemical effects to mitigate the attachment and propagation of marine fouling organisms. Due to the complexity and potential interdependency of some of these mechanisms, coupled with a complex and dynamic nature of the systems in which the coatings operate, prediction of long-term antifouling efficiency of the newly developed materials is a challenge, and deeper understanding of the mechanisms as well as cheap, reliable methods for comprehensive predictive modelling of their antifouling efficiency are of critical importance for the rapid development of new antifouling materials. At present, the direct tests of the novel antifouling materials are currently considered as a very important stage of the implementation of such materials. Here we briefly overview several typical examples of testing graphene-based antifouling materials under the field and simulated natural conditions, *i.e.* directly under sea conditions and in sea water.

Figure 20a shows the results of a 45 day field test of polydimethylsiloxane/reduced graphene oxide and polydimethylsiloxane/graphene oxide/boehmite nanorod nanocomposites. A field trial carried out in seawater was developed on a base of screening process to achieve visual estimations of the efficacy of the coating. The panels used in the test were cleaned and de-rusted prior to coating them with a first epoxy primer and epoxy-silicone tie layer. The obtained original polydimethylsiloxane nanocomposites were achieved by utilizing a pigment of ferric oxide and surfactant. The polydimethylsiloxane-based upper layer formulas were printed on both surfaces and dried for 24 h at ambient air temperature; the thickness was 150 μm. The treated panels were put into the seawater with the salinity of 37%, pH of 7.6–8.3 kept at the temperature of 23–28 °C.[123] The results of these direct field tests were used to prove the efficiency of these novel materials.

The results of the long-term (about a year) *in situ* marine fouling tests in a sheltered bay connected to the south China sea are shown in **Figure 20b**. The graphene@cuprous oxide (rGO@Cu_2O) material was developed and mixed with graphene oxide, copper (II) sulfate, sodium hydroxide and L-ascorbic acid by use of an in-situ treatment process. The thin layer with a thickness of ~400 μm was painted on the panels by use of a brush. Three panels were engaged for every coating; then the panels were arranged in seawater at the depths of 0.2 to 2.0 m from a raft in a bay at Xiamen, China, where only a slow water motion was observed. After the experiment, the panels were extracted from the seawater, washed, and went for studies. The authors focused on barnacles attached on the panels to estimate the extent of marine biofouling, as barnacles are considered to be the main macro-fouler that can significantly change the drag profile of the surface.

Figures 20c,d illustrate the trial of bio-inspired graphene-silicone elastomers of various structures in simulated marine environment. Very interesting experiments on antifouling tests *in dynamic conditions* were recently reported by Bing *at al.*[121] The experiments to understand the antifouling properties were performed by studying the formation of biofilms by *P. pantotrophus* and *B. subtilis.* The authors proposed a custom tool to simulate the marine conditions. The coatings were located at the lower part of the studied region in the tool, and the speed of flow was sustained at 0.2-0.5 ms^{-1}. **Figure 20c** illustrates the development of biofilm for *P. pantotrophus* and *B. subtilis*, respectively. **Figure 20d** illustrates the production of bubbles of gas on the surface of the antibiofouling thin films. These experiments conducted under *dynamic conditions* confirmed the efficiency of this novel approach.

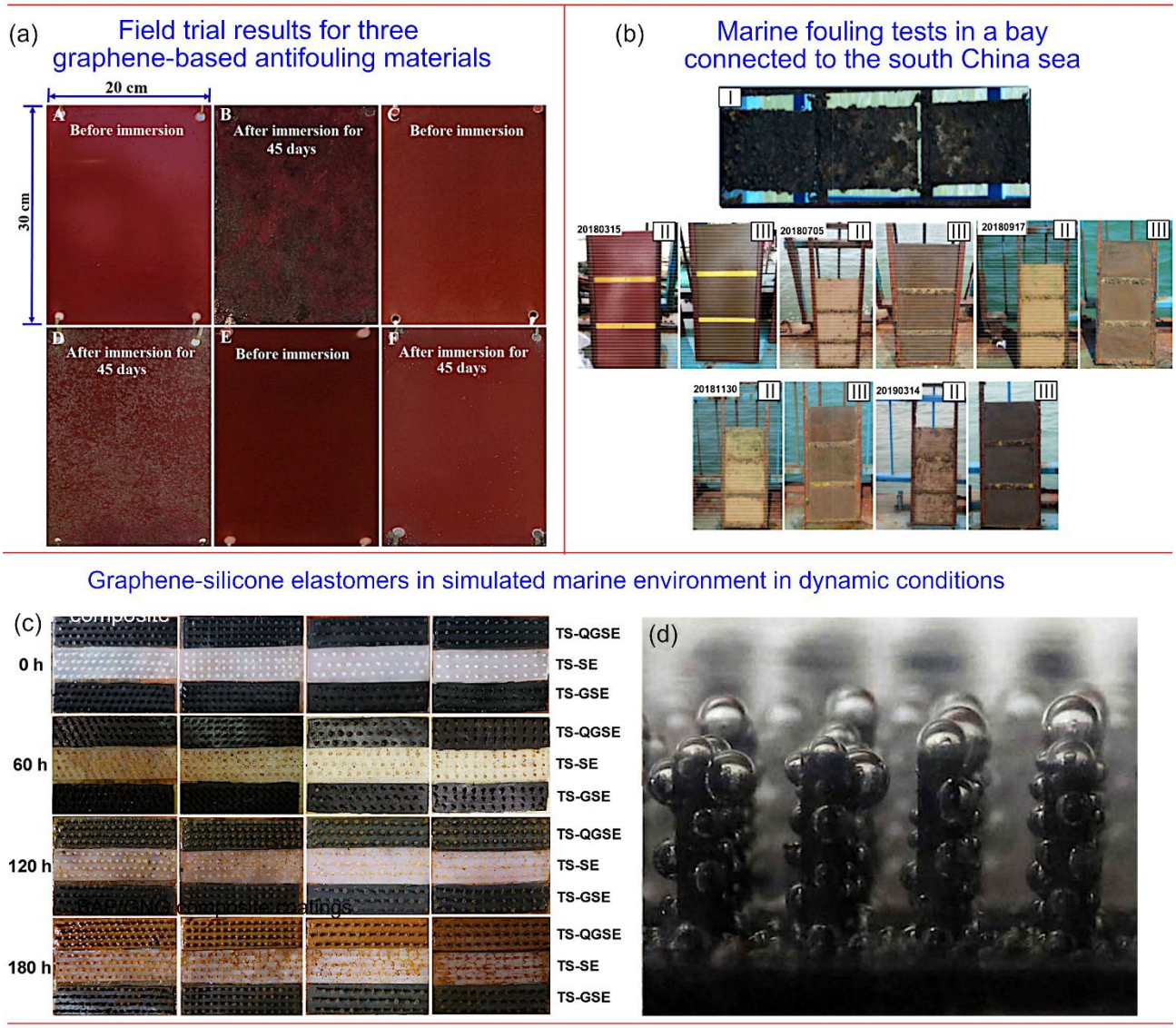

Figure 20. Tests of graphene-based antifouling materials in marine field and simulated marine conditions. (a) The results of field trial of virgin polydimethylsiloxane (A & B), polydimethylsiloxane/reduced graphene oxide (3 wt%, C & D), and polydimethylsiloxane/graphene oxide/boehmite nanorods (3 wt%, E & F) nanocomposites before and after immersion in natural seawater water. Test duration was 45 days. Reproduced with permission **from Selim** *et al.*[123] (b) *In situ* marine fouling tests over a period in a sheltered bay connected to the south China sea: (I) Bared panels (90 days); (II) Cu_2O paint coated surfaces (0-365 days) and (III) rGO@Cu_2O paint coated surfaces (0-365 days). Reproduced under the terms and conditions of the **CC BY 4 license**.[138] (c,d) Bio-inspired graphene-silicone elastomers of various structures in simulated marine environment. (c) Incubated with *P. pantotrophus*, and (d) The formation of gas-filled bubbles by the coating prevented surface attachment of organisms during the test. Reproduced with permission **from Bing *et al.***[121]

Figure 21a shows the results of a field test of the epoxy-polydimethylsiloxane-graphene oxide antifouling nanomaterial at Chennai Port, Bay of Bengal, Southern India. The epoxy-polydimethylsiloxane neat (EPN) nanocomposite was produced by immersing the graphene oxide nanomaterial into a matrix of epoxy-hydroxy-terminated-polydimethylsiloxane by use of conventional in-situ technology.[140] After the seawater tests, the epoxy-polydimethylsiloxane neat exhibited a very large number of fouling structures like barnacles, mussels, polychaetes, oysters, tunicates enveloped by a slime layer. The dominant fouling structure is marked in **Figure 21a** with 'C' label and is identified as a *Balanus amphitrite* Darwin barnacle, for which the Bay of Bengal, India, is the main habitat. Marine sponges and algae, which are consumed by the barnacles, that covered the surfaces after their extraction were also found to have well-developed structures. At the same time, optimized nanocomposite layers exhibited improved anti-fouling behaviour with a thin film of slime linkage, as shown on the panel labelled with 'D' label. This fact can be

explained by the fine dispersion of GNs in the composite matrix and strong chemical bonding in the coating compound thus showing appropriate antifouling characteristics. These field tests provided comprehensive evidence of the antifouling properties under the realistic conditions of the Chennai Port, Bay of Bengal, which is the place of a very heavy vessel traffic.

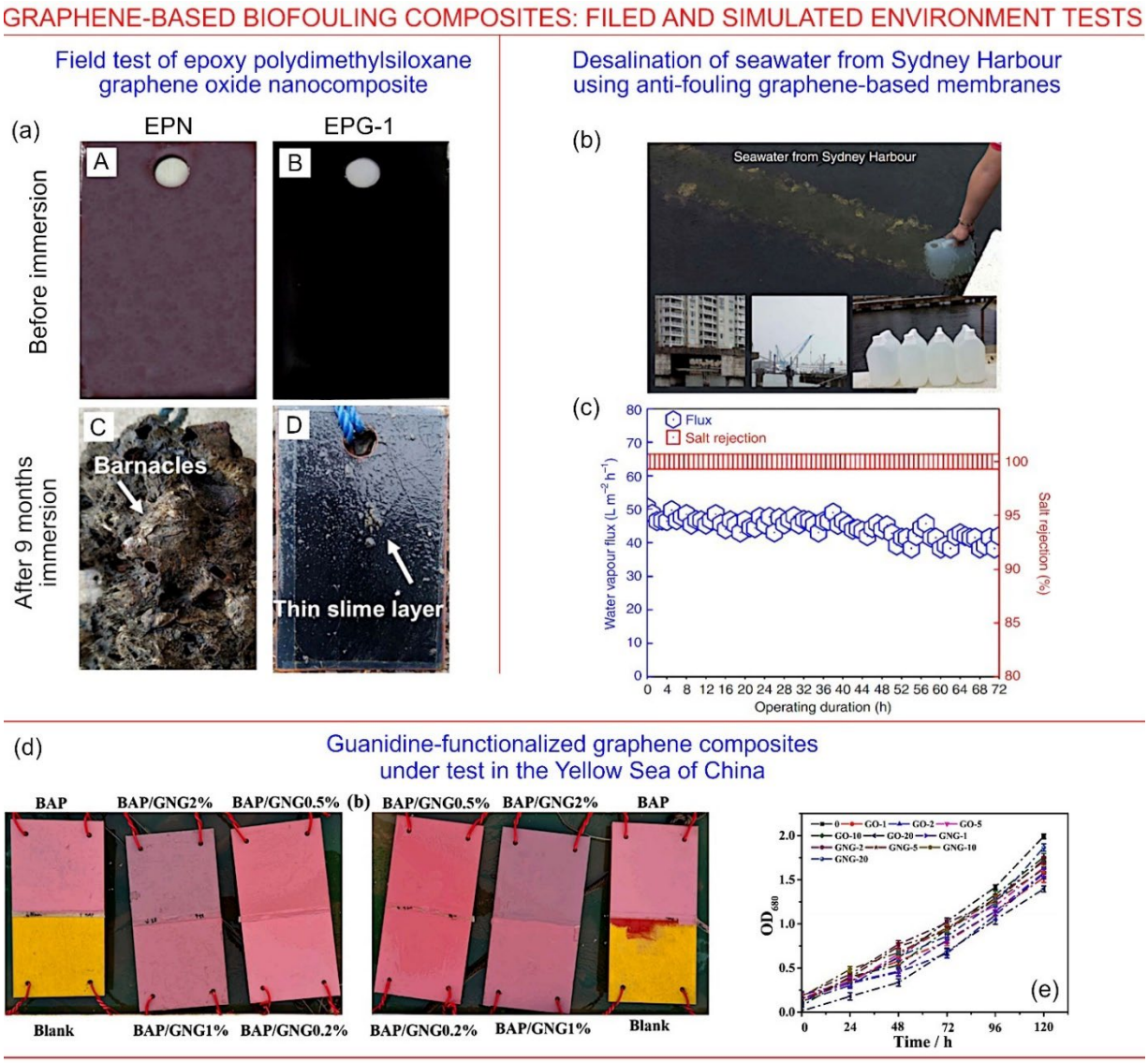

Figure 21. Tests of graphene-based antifouling materials under marine field conditions. (a) Results of the sea field tests of the epoxy-polydimethylsiloxane neat (EPN) and epoxy-polydimethylsiloxane-graphene oxide antifouling nanomaterial (EPG-1): (A, B before immersion and (C, D) after immersion for 9 months in shallow seawater to the depth of 5 feet at Chennai Port, Bay of Bengal, Southern India. Reproduced with permission from **Verma *et al.***[140] (b,c) The field tests (b) and performance results (c) obtained for the water sampled in Sydney Harbor. (b) Photos of the water collection method and view of the collection. (c) Performances of the penetrable graphene-based composite in the membrane desalination treatment for 72 h. Suitable resistance to fouling of penetrable graphene films with an intensive flux of water vapour is confirmed over a long treatment time. Constant, 100% salt rejection rate is achieved. Reproduced with permission from Seo ***et al.***[141] (d,e) Field trials of self-polishing boron acrylate polymer (BAP) and guanidine-functionalized graphene (GNG) antifouling nanocomposites in the Yellow Sea of China. (d) The fronts and backs of the plates of BAP/GNG nanocomposite coatings, along with the blank plates after two months of immersion in the Yellow Sea of China. (e) Optical density of 680 nm (OD_{680}) values for different concentrations of GO and GNG with respect to *N. closterium*. Reproduced with permission from **Zhang *et al.***[125]

Desalination of seawater by membrane technology is also a very important problem, in particular for providing fresh water on sea vessels in emergency. Membrane filters used for seawater desalination also suffer from fouling, and the novel materials for the membranes should be tested directly in seawater, under the realistic conditions to ensure thrustable results. **Figures 21b,c** illustrate the field tests (b) and performance results (c) obtained for graphene-based membranes in the water

sampled in Sydney Harbor. To show practical benefits of the permeable graphene-based membrane for real desalination environment, the authors conducted water desalination experiment using real seawater samples (the number of dissolved solids of 34.2 gL^{-1}) that were obtained from the Sydney Harbour, NSW, Australia. Field trials based on a real unprocessed water collected from the industrial area ensured the most realistic results.

Another direct field trial has been conducted in the Yellow Sea of China. The self-polishing boron acrylate polymer (BAP) and guanidine-functionalized graphene (GNG) antifouling nanocomposites were fabricated based on the GNG nanosheets embedded in BAP. For field treatment in real marine conditions for two months, the BAP/GNG compound stayed free of slime and fouling structures.[125] **Figure 21d** presents the fronts and backs of the plates of BAP/GNG nanocomposite coatings, along with the blank plates after two months long immersion in the Yellow Sea of China. **Figure 21e** shows the optical density of 680 nm (OD_{680}) values for different concentrations of GO and GNG with respect to N. *closterium*.

6. Future Outlook and Challenges

Next steps. Presently available technologies for combating marine fouling are quite different and often expensive, but they still do not guarantee the required antifouling efficiency and durability, as it was outlined in our review. Apparently, further progress is required to ensure the necessary level of antifouling efficiency and vessel protection for many years, resulting in the significant decrease of operating expenses and hence, lowering the cost and environmental footprint of cargo transportation.

Here we will briefly outline several directions that could, in our opinion, contribute to the further development of the marine antifouling technology. First, the majority of the above discussed coatings were based on some specific functions yet marine foulants are extremely diverse (see **Figures 1, 2**) and hence, multifunctional materials and nanomaterials should be better explored as a multi-modal protection against the heterogeneous flora and fauna present in different ecosystems.

Next, the world of nanostructures is also quite diverse, with a large number of nanostructures already identified as having properties that renders them suitable for antifouling applications. Here, it is worth noting that the antifouling requirements over the surface structure and topology are multi-dimensional; e.g. the surface irregularities could prevent the formation of fouling and on the other hand, could serve as attachment points for marine organisms, depending on the shape, density, height and other parameters of the textured surface.[81,142] This in turn means that more types and shapes of carbonous nanostructures need to be tested. On the other hand, a large number of nanostructures has been currently tested for antifouling (see **Table 2**) yet other types of nanostructures still need to be explored for marine antifouling technologies.

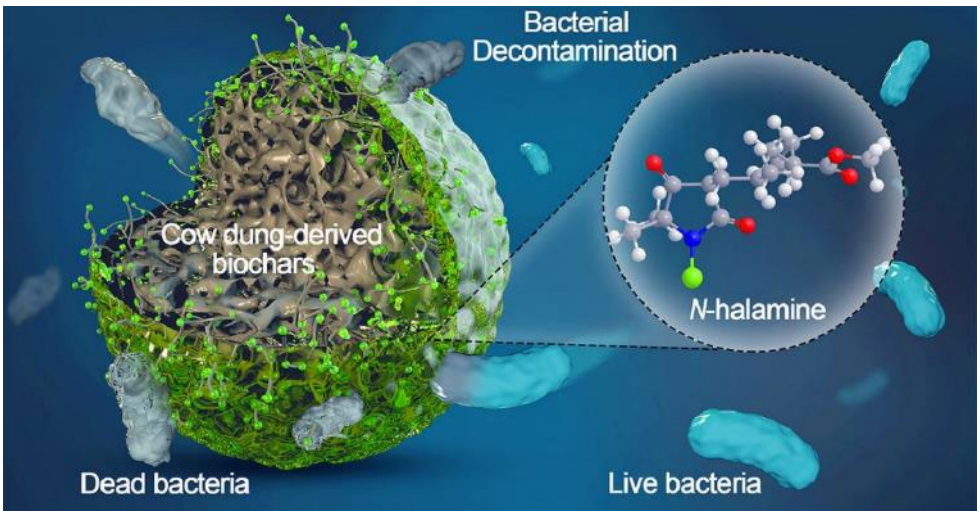

Figure 22. Antibacterial carbonous agents from natural wastes. Cow dung-derived biochars as antibacterial agents for water decontamination is a promising technology that may ensure cheap fabrication of antibacterial pains and coatings. The biochars were coated by *N*-halamine polymer, then loaded with chlorine such as Cl^+. Reprinted with permission from Yao *et al.*, 2021.[149]

Table 2. Examples of various nanostructures and materials tested for marine antifouling action.

Composite	Material	Action	Ref.
Graphene oxide/silicone rubber composite	Graphene oxide	Harmonic motion effect	88
Graphene oxide/epoxy coatings	Graphene oxide/ZnO	Anti-corrosion and anti-fouling	143
Polydimethylsiloxane and metal-organic framework / graphene oxide	Graphene oxide	Corrosion and fouling protection	144
Nanocomposite polymer	Various	Antifouling	145
Membranes, GO, RGO	Graphene oxide	Antibacterial activity	146
RGO / Epoxy nanocomposite	Graphene oxide	Antibacterial activity	147
Epoxy coatings / graphene oxide	Graphene oxide	Antibacterial activity	148
Graphene-silicone elastomer	Graphene	Removing the fouls	121
Elastic graphene – silicone rubber composite	Graphene	Micron-size deformations on surface	122
Reduced GO and GO-γ-AlOOH	Reduced graphene oxide	Superhydrophobic	123
Graphene oxide in chitosan	Graphene oxide	Cracking free sturdy films	124
Boron acrylate polymer/guanidine-functionalized graphene	Graphene	Self-polishing	125
GNP composite	Graphene	deferring formation of biofilms	126
Acrylic acid modified graphene oxide	Graphene oxide	Self-polishing	127
Polydimethylsiloxane / graphene nanoplatelets	Graphene	Membrane deterioration	128
Polyaniline/p-phenylenediamine-functionalized graphene oxide	Graphene oxide	Limiting the passage of water	130
Graphene oxide-nano-SiO2/polydimethylsiloxane composite	Graphene oxide	Enhanced surface stiffness	131
Graphene oxide/silver nanocomposites	Graphene oxide	Dispersibility of Ag nanoparticles	
Graphene oxide/Ag nanocomposite	Graphene oxide	Synergistic effect	135
Few-layer graphene flakes/Ag	Graphene	Maximizing the active surface area	136
Polydimethysiloxane/ZnO–Graphene oxide	Graphene oxide	High Ra and hydrophobicity	137
Cow dung-derived biochars	Biochars	Surface chemistry of biochar-graphene composites	149
TiO_2@MXene composite	MXene	Synergistic effect	151
Laser-induced graphene coatings	Graphene	Chemical and electrical effects	152
Zinc oxide	Nanorods	Fouling release	36
Copper oxide	Nanoparticles	Retardation of proliferation	37
Flexible zinc oxide arrays	Nanopillars	Damage to cells	38
Cobalt	Vertical dendrites	Reducing bacteria attachment	39
Silicon	Lotus leaf-like	Kills cells by membrane rupturing	40

Natural wastes for the future antifouling agents. Then, the natural product and waste–derived antifouling agents would be very beneficial, since the demand of antifouling coatings is huge and on the other hand, some natural wastes also represent a large stock of cheap precursors. As an example, the fabrication of antibacterial agents from cow dung was recently demonstrated.[149] (**Figure 22**). It is found that graphene deposited on a biochar surface acts as an active site of very high potential, thus increasing the stability of the composite. Both the geometry, via its porous structure, and the surface chemistry of biochar-graphene composites regulate the adsorption rate of pollutant molecules, yielding improved adsorption performance.[150] This promising technology allows for the fabrication of antimicrobial agents using practically non-expendable source of raw material.

MXenes as a possible antifouling platform. The fabrication of highly-performant 2D membranes represents a conspicuous challenge, even despite the considerable attention devoted to the development of composite membranes endowed with 2D lamellar materials such as graphene. In this respect, two dimensional MXene materials have attracted a great deal of interest as a novel fabrication method, possessing in addition unique chemical properties[151] (**Figure 23**). In the latter, the authors show how to fabricate PES-TiO2@MXene composite membrane by starting from a 2D based material of TiO2@MXene hybrid. The thus obtained composite membrane shows a large separation performance and excellent antifouling ability.

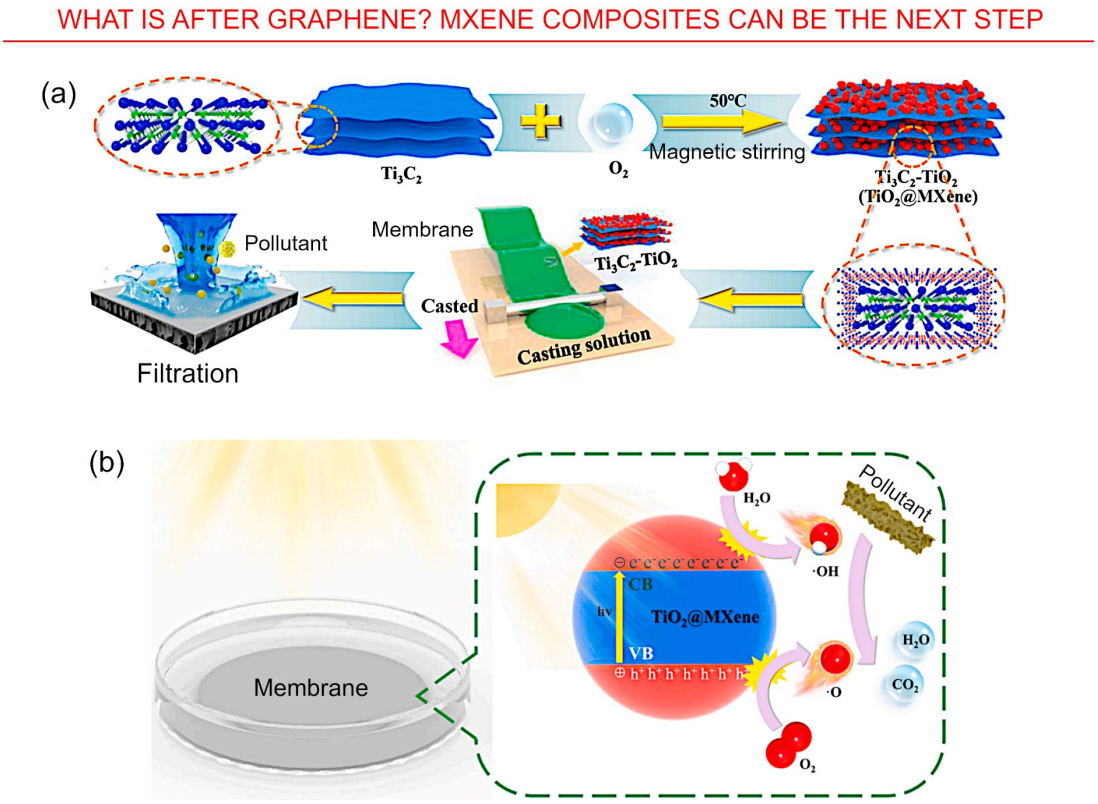

Figure 23. (a) Preparation processes of TiO_2@MXene materials and composite membranes. (b) Photocatalytic mechanism diagram of the TiO_2@MXene composite membrane. Reprinted with permission from Huang at al. **2021**.[151]

Laser-induced graphene coatings for antifouling. Manderfield *at al*. has recently discussed the laser-induced graphene (LIG) coatings, which are found to inhibit fouling by reducing the ability of biofilm growth.[152] A bacteria analysis revealed that initially higher bacteria densities accumulate at the treated surfaces compared to the reference ones. However, this initial attachment could be reduced by applying either a negative or a positive electric potential. The latter was found to reduce bacteria attachment to a larger extent (**Figure 24**). The effect of such positive potentials was explained in terms several causes such as chemical and electrical effects, the formation of H_2O_2 and of chlorine, the latter observed to start at about 1.5 V, and a change in the pH-value. In contrast, for negative potentials, the reduction in bacteria concentration was attributed to the electrical repulsion between the negative surface charge and negative

zeta potential at the bacteria. This study manifests the importance of suppressing bacteria during the early attempted attachments and, as a result, this initial suppression will prevent the biofilm growth over the long run. As a general conclusion, it appears that LIG coatings of polymer surfaces may find important applications for reducing fouling on membrane spacers and possibly other type of materials exposed to the ocean.

Importance of modelling and simulation for designing novel antifouling materials. In the view of a complexity and longevity of marine tests, modelling technology may become an increasingly useful tool for designing and screening novel advanced antifouling systems. The modern theoretical approaches are capable to adequately describe the formation and growth of very complex nanomaterials in various process environments[153,154,155] including plasma,[156] yet modelling of nanostructure interaction with living cells require more advanced theoretical approaches.[157,158] Further development of models for the detailed simulation of nanostructure-cell interaction could help advance the marine antifouling materials.

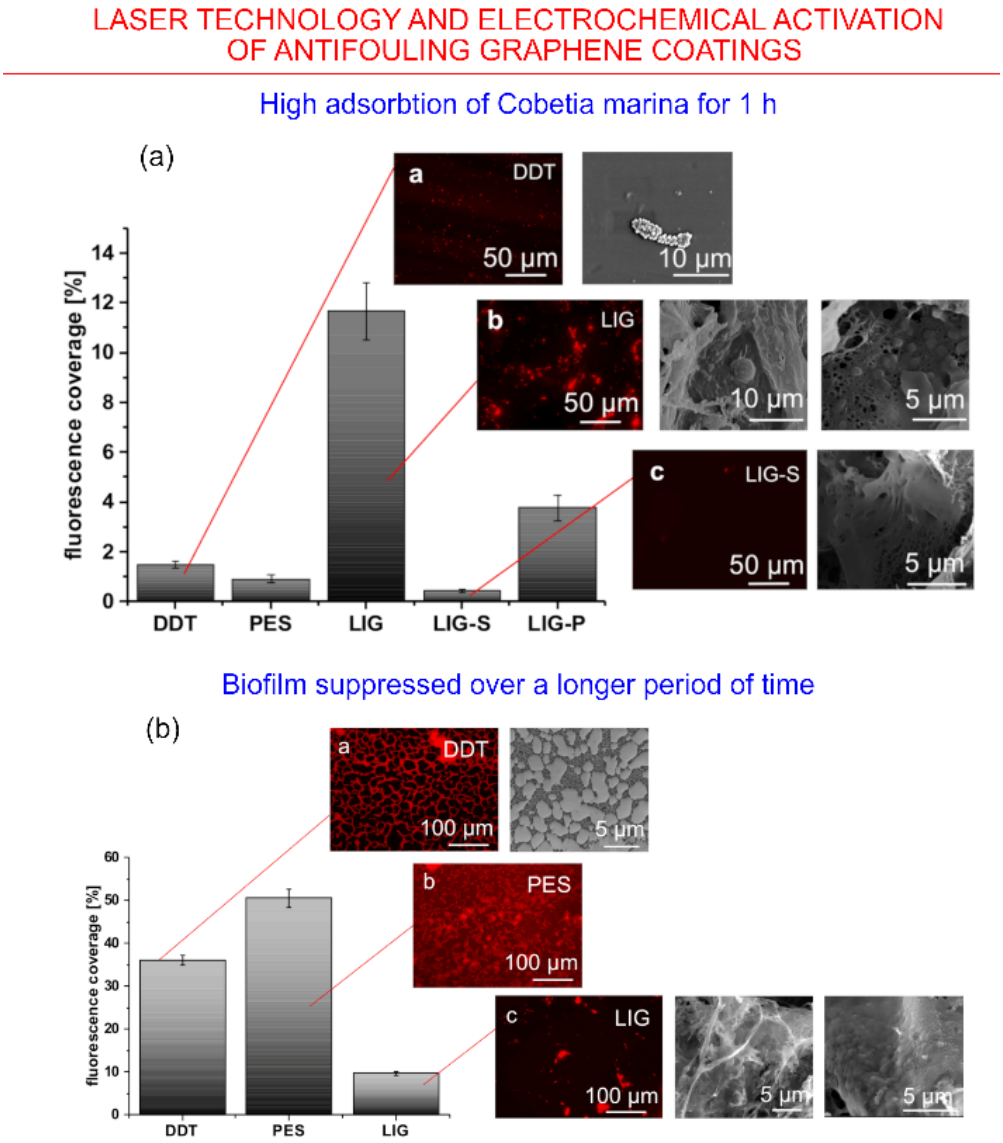

Figure 24. Laser technology and electrochemical activation of antifouling graphene coatings. (I) Fluorescence coverage [%] of the different surfaces after dynamic exposure to a *Cobetia marina* suspension for 1 h. The microscopy (20× objective) and Sem images of *Cobetia marina* show exemplary the location of the bacteria on the different surfaces. a) DDT, b) LIG and c) LIG-S. Error bars are the standard errors (n = 3). The differences between DDT and all LIG modifications was statistically significant at a level of α = 0.05 (ANOVA with post hoc Tukey test). (II) Fluorescence coverage [%] of the marine bacterium *Cobetia marina* on the different surfaces. After allowing bacteria to attach for 1 h under dynamic conditions the biofilm was allowed to grow for further 36 h. Microscopy images (20 × objective) and SEM images of *Cobetia marina* show their distribution on the different surfaces (a) DDT, b) PES and c) LIG. Error bars are the standard error (n = 3). Differences between all surfaces were statistically significant at a level of α = 0.05 (ANOVA with *post hoc* Tukey test). Reprinted with permission from Manderfield *at al*. **2021.**[152]

Open questions – environmental stability, persistence and potential danger to marine ecosystems. Finally, two important issues need to be discussed in view of designing novel graphene-based antifouling materials, namely the stability of antifouling coatings during prolonged exposure to different environmental conditions, and the persistence and potential harmful effects the leached graphene particles may have on marine ecosystem and the food chain. The potentially negative effects that nanoparticles (NPs) may have on the health of the environment and human population are diverse, and need to be studied carefully and thoroughly across the entire spectrum of potential interactions.[159] This presents a considerable challenge, and may require the design of new continuous risk assessment methodologies specifically targeting these new classes of nanomaterial contaminants and newly engineered nanomaterials in order to capture and mitigate all possible deleterious effects on the marine ecosystems. Specifically, the development of improved extraction methods, new detection tools and more accurate characterization technologies would be needed.

Recent attempts to quantify GO toxicity cannot be seen as conclusive and future studies on the effects associated to its release in the marine environment need to be considered.[160] The new assessment should elucidate the way in which physical and molecular aspects of nanoparticle toxicity depend on the production methods and their surface functionalization. Some steps forward have been already made to evaluate graphene toxicity on marine shrimp and fish by varying nanoparticle size and concentration also in the presence of other pollutants.[161,162] As a result of these studies, possible mitigation effects have been suggested.[163–168]

It is known that exposure to small concentrations of GO (in the range 1-100 μg/L) can cause impaired zebrafish development due to several processes, such as critical modification of its DNA, protein carbonylation and excessive generation of superoxide radicals, the latter being a strongly reactive oxygen species (ROS).[163] Poor development of zebrafish embryos and larvae due to the toxicity of GO has been also demonstrated,[164] suggesting that one of the main determinants of toxicity is exposure concentration, in addition to the known lateral size effects. Indeed, three different experiments performed at high GO concentration (100 mg/L), each consisting of predetermined GO sizes, i.e. S=(50–200) nm, S<500 nm, and S>500 nm, clearly revealed the occurrence of morphological, physiological, biochemical, and behavioural changes in zebrafish bodies, which were attributed to oxidative stress and expected to promote apoptosis.

Direct toxicity risks of GO on marine organisms have been studied on *Artemia salina*,[165] while its indirect toxicity, due to its remarkable adsorption capacity, was quantified in the presence of other aquatic pollutants, such as Phe and Cd^{2+}. The study demonstrated that exposure of *A. salina* to GO alone required a significantly high concentration of 500 mg/L to be lethal. In contrast, when combined with Cd^{2+} or Phe, even at lower concentrations, GO facilitated bioaccumulation of toxicants, resulting in stronger toxicological effects on zooplankton.

In another recent study, the authors discussed the potential role that GO may play as a carrier of organic pollutants toward the aquatic organisms.[166] It was found that typical environmental concentrations of GO and reduced graphene oxide/polyvinylpyrrolidone (rGO/PVP) did not produce any significant effect on the development of zebrafish embryo (EC50 > 10 mg/L), even in the presence of polycyclic aromatic hydrocarbons (PAHs). Sub-lethal toxicity effects in adult zebrafish were observed from catalase activity in zebrafish gills, without appearance of histopathological alterations in the gill tissue.

Further studies were focused on side effects arising from the interactions of GO with classical pollutants in aquatic environments.[167] Ecotoxicological effects of GO, cadmium, zinc and their co-exposures, on *Palaemon pandaliformis* shrimp were evaluated by means of acute toxicity and routine metabolism tests, the latter represented by oxygen consumption and ammonia excretion. It was found that after 96 h of exposure, GO did not show any acute eco-toxicity for concentrations up to about 5.0 mg/L. However, the co-exposure to GO/Cd or GO/Zn did increase the toxicity of both Cd and Zn.

The main causes of toxicity relate to the ability of nanomaterials to penetrate cell membranes and not be expelled through conventional defense mechanisms, and include such factors as agglomeration, long-term persistence, and toxic effects that were recently reviewed by Malhotra *et al*.[160] This work describes the types of toxic effects graphene and GO produced on aquatic invertebrates and fish (cell line and organisms), with the goal of pointing out our current understanding, and knowledge gaps, of graphene and GO toxicity. While extensive, the data, however, is limited by several information gaps, and further efforts are needed to develop fully comprehensive toxicity criteria guidelines. An additional difficulty emerges from the vast diversity in size, shape, surface modification, synthesis techniques used to fabricate nanomaterials, and an equally diversity of model organisms and their combinations that could be considered, which do not allow to compare toxicological effects of graphene and GO among different studies. Therefore, it is important to understand the toxicity caused by graphene nanomaterials on aquatic organisms before one can move on to the possible practical applications of these new promising graphene-based nanomaterials.

As a counterbalance, some mitigation effects have been also reported. In one example, the authors consider Humic Acid to mitigate GO toxicity, by preparing the mix in a range of concentrations, [GO] = (0-100) mg/L, [HA] = (0-100) mg/L.[168] They demonstrate that HA is able to diminish the damage to both mitochondria and cell morphology, and reduce oxidative stress on embryos, produced by GO.

It should be stressed here that the potential impact of graphene and its derivatives on the marine environment is closely linked to the degradation and release of this material from the surface. Unlike other nanoparticles, the strong adherence to surfaces and durability of graphene may to some extent mitigate its negative effects as it is less likely to leach out and disperse in the environment. Yet, the durability of the material also means that it may persist for extended periods, unless a clear biodegradation pathway is suggested.

On the other hand it should be noted that while graphene based antifouling materials may represent a possible danger to marine ecosystems, there are no ideal solutions, and while potential negative features of novel material platforms should be actively studied and mitigated, they should not hinder the progress and interest in this promising family of materials. Further studies are necessary to enhance the antifouling action together with improving material stability, adhesion of the graphene-based agents in the matrix, and possibly searching for some self-destroying mechanisms and other ways to mitigate the adverse effects of graphene on living ecosystem. At this stage, the studies on graphene-based antifouling materials are in progress as follows from the recent publications cited in this review. The following further specific steps could be suggested:

1. *Design and test novel techniques to significantly decrease the rate of nanomaterials release to the water by enhancing their stability and adhesion in the matrix;*
2. *Enhance the general stability of the graphene-based antifouling materials;*
3. *Study in greater detail the effects of graphene-based nanomaterials on various types of living marine environments, and*
4. *Design efficient, environmentally benign methods for timely removal and restoration of graphene-based antifouling materials on vessels.*

Also, further studies on the long-term effect of graphene-based nanomaterials should be conducted.

Table 3 summarizes some recent (from 2020 onwards) studies focused on graphene-based antifouling coatings in marine environments.

Table 3. Recent (from 2020 onwards) studies focused on graphene-based antifouling coatings in marine environments. Adapted from F. Sousa-Cardoso *et al*. **2022**[107] under the terms and conditions of CC BY license.

Coating	Material Matrix	Organism	Experimental Setup	Main Conclusions	Ref.
Guanidine-functionalized graphene	Boron acrylate polymer	*Escherichia coli* *Staphylococcus aureus* *Phaeodactylum tricornutum* *Nitzschia Closterium f. minutíssima* *Halamphora sp.* Marine micro- and macrofoulers	*In vitro* study: Luria–Bertani medium 37 °C, 12 h *In vitro* study: F/2 medium 21 °C, 14 days *In situ* study: Natural seawater (Yellow Sea, China), 2 months	The coatings showed excellent antibacterial properties (up to 95% reduction) and diatom antiadhesion rates (up to 99%). The field trial revealed no fouling adhesion or surface deterioration	125
Laser-induced graphene	Poly(ether)sulfone	Cobetia marina	In vitro study: Dynamic assay (65 rpm), Artificial seawater, 1 and 36 h	Compared with negative control surfaces, laser-induced graphene coatings showed greater initial bacterial attachment (1 h) but up to 80% less bacterial coverage after 36 h. Initial attachment rates were reduced by the application of negative or positive potential	152
Graphene oxide-silver nanoparticles	PDMS-silica	*Escherichia coli* *Phaeodactylum tricornutum* *Navicula torguatum* *Chlorella sp.*	*In vitro* study: Shaking flask method, Saline solution (0.9 wt%), 37°C, 24 h *In vitro* study: Artificial seawater, 24 h	The coating containing silver nanoparticles showed improved antibacterial (60% greater inactivation rate) and antialgal (up to 17% reduction in surface coverage) properties, in comparison to pristine graphene oxide.	132
Graphene oxide-silver nanoparticles	Polypropylene	*Halomonas pacifica* Marine microalgae	*In vitro* study: Static assay, Marine broth, 26°C, 24 h *In vitro* study: Adam medium *a*, 1 week	GO showed almost no AF properties. GO /silver nanocomposites showed more than 80% of biofilm inhibition, as well as no visible fouling by microalgae.	134
Graphene oxide/silica nanoparticles	PDMS	*Pseudomonas* sp. *Bacillus* sp. Freshwater bacterial culture	*In vitro* study: Nutrient broth72 h	The coated surfaces showed up to a 4-Log reduction in total viable cells. Analysis of biofilm architecture confirmed a significant reduction of biomass and biofilm thickness on coated surfaces.	169
Graphene oxide/cuprous oxide nanoparticles	Acrylic resin	Marine micro and macrofoulers	In situ study (0.2–2.0 m below the surface) Natural seawater (South China Sea) Weak water currents (less than 2 m×s-1 90 and 365 days	Bare panels showed an abundant growth of marine organisms within 90 days, while coated surfaces were hardly fouled by marine organisms after 365 days.	138
Acrylic acid-modified graphene oxide	Acrylic resin	Marine micro and macrofoulers	In situ study: Natural seawater (Zhoushan Sea, China), 6 months	Composite-based paint showed great self-polishing AF performance in natural seawater.	127
Polyaniline/*p*-phenylenediamine-functionalized graphene oxide	Epoxy resin	Organisms in a simulated marine environment (e.g., guppy fish, *spirulina* algae, and dwarf hair grass)	*In vitro* study: Simulated marine environment 25–27 °C, 3 months	The anticorrosion and AF properties of commercialized epoxy coatings were improved by the addition of the functionalized graphene oxide composite.	130

Reduced graphene oxide Graphene oxide/boehmite nanorods	PDMS PDMS	*Staphylococcus aureus* *Kocuria rhizophila* *Pseudomonas fluorescens* *Pseudomonas Aeruginosa* *Candida albicans* *Aspergillus brasiliensis* Marine micro- and macrofoulers	*In vitro* study: Nutrient-infused medium 25°C, 28 days *In situ* study: Natural seawater 23–28 °C, 45 days	In laboratory assays, boehmite nanorod composite coating showed higher antimicrobial activity (endurability percentages for Gram-positive, Gram-negative, and fungi of 86.4%, 97.9%, and 85.9%, respectively) in comparison with bare PDMS and reduced graphene oxide/PDMS. The higher self-cleaning and FR performance of the boehmite nanorod composite coating was confirmed by the field trial.	123

Acknowledgements

I.L. acknowledges the support from the NIE, Nanyang Technological University, and the National Australian University. K.B. acknowledges the support from the National Australian University (Futures Fellowship Scheme), and the Australian Research Council (DP180101254). O. Baranov acknowledges the support from the project funded by the National Research Foundation of Ukraine, under grant agreement No. 2020.02/0119, and NATO Science for Peace and Security Programme under grant id. G5814 project NOOSE.

References

[1] M. P. Schultz, Effects of coating roughness and biofouling on ship resistance and powering. *Biofouling* **2007**, *23*, 331-341. https://doi.org/10.1080/08927010701461974

[2] H. Titah-Benbouzid, M. Benbouzid. Biofouling issue on marine renewable energy converters: A state of the art review on impacts and prevention. *Int. J. Energy Convers*. **2017**, *5*, 67–78. https://doi.org/10.15866/irecon.v5i3.12749

[3] F. Laranjeiro, P. Sánchez-Marín, I. B. Oliveira, S. Galante-Oliveira, C. Barroso. Fifteen years of imposex and tributyltin pollution monitoring along the Portuguese coast. *Environ. Pollut*. **2018**, 232, 411-421. http://doi.org/10.1016/j.envpol.2017.09.056

[4] J. Bannister, M. Sievers, F. Bush, N. Nina Bloecher. Biofouling in marine aquaculture: A review of recent research and developments. *Biofouling* **2019**, 35, 631–648. https://doi.org/10.1080/08927014.2019.1640214

[5] X. Li, J. Gou, H. Feng, X. Sun, X. Qin, W. Wang, W. Li, S. Chen. improved antifouling ability for double-network hydrogel coatings with excellent elastic and toughness under marine tidal environment. *Adv. Eng. Mater.* **2023**, *25*, 2201801, https://doi.org/10.1002/adem.202201801

[6] R. A. Fenati, M. S. Quinn, H. C. Bilinsky, C. Neto. Antifouling properties of liquid-infused riblets fabricated by direct contactless microfabrication. *Adv. Eng. Mater*. **2021**, *23*, 2000905. https://doi.org/10.1002/adem.202000905

[7] X. Ren, M. Guo, L. Xue, Q. Zeng, X. Gao, Y. Xin, L. Xu, L. Li. A self-cleaning mucus-like and hierarchical ciliary bionic surface for marine antifouling. *Adv. Eng. Mater*. **2020**, *22*, 1901198. https://doi.org/10.1002/adem.201901198

[8] T. Simovich, A. Rosenhahn, R. N. Lamb. Thermoregeneration of plastrons on superhydrophobic coatings for sustained antifouling properties. *Adv. Eng. Mater*. **2020**, *22*, 1900806. https://doi.org/10.1002/adem.201900806

[9] L. Chen, J.C.W. Lam. SeaNine 211 as antifouling biocide: a coastal pollutant of emerging concern. *J. Environ. Sci*. **2017**, *61*, 68 –79 https://doi.org/10.1016/j.jes.2017.03.040

[10] N. H. Lam, H. Jeong, S. Kang, D.-J. Kim, M.-J. Ju, T. Horiguchi, H.-S. Cho. Organotins and new antifouling biocides in water and sediments from three Korean Special Management Sea Areas following ten years of tributyltin regulation: Contamination pro files and risk assessment. *Marine Poll. Bull.* **2017**, *121*, 302–312. http://dx.doi.org/10.1016/j.marpolbul.2017.06.026

[11] W. J. Langston, N. D. Pope, K. M. Langston, S. C. M O'Hara, P. E. Gibbs, P. L. Pascoe. Recovery from TBT pollution in English Channel environments: A problem solved? *Mar. Pollut. Bull*. **2015**, *95*, 551–564. https://doi.org/10.1016/j.marpolbul.2014.12.011

[12] L. Gipperth. The legal design of the international and European Union ban on tributyltin antifouling paint: Direct and indirect effects. *J. Environ. Manag.* **2009,** *90*, S86-S95. https://doi.org/10.1016/j.jenvman.2008.08.013

[13] Min, B.H., Ravikumar, Y., Lee, D.-H., Choi, K.S., Kim, B.-M., Rhee, J.-S., Age-dependent antioxidant responses to the bioconcentration of microcystin-LR in the mysid crustacean, Neomysis awatschensis. *Environ. Pollut*. **2018**, *232*, 284–292, https://doi.org/10.1016/j.envpol.2017.09.050

[14] Md. N. Haque, D.-H. Lee, B.-M. Kim, S.-E. Nam, J.-S. Rhee. Dose- and age-specific antioxidant responses of the mysid crustacean Neomysis awatschensis to metal exposure. *Aquat. Toxicol*. **2018**, *201*, 21–30 https://doi.org/10.1016/j.aquatox.2018.05.023

[15] B.-M. Kim, M. Saravanan, D.-H. Lee, J.-H. Kang, M. Kim, J.-H. Jung, J.-S. Rhee. Exposure to sublethal concentrations of tributyltin reduced survival, growth, and 20-hydroxyecdysone levels in a marine mysid. *Mar*. *Environ*. *Res*. **2018**, *140*, 96 –103, https://doi.org/10.1016/j.marenvres.2018.06.006

[16] I. Levchenko, K. Bazaka, M. Keidar, S. Xu, J. Fang. Hierarchical multicomponent inorganic metamaterials: intrinsically driven self-assembly at the nanoscale. *Adv. Mater*. **2018**, *30*, 1702226, https://doi.org/10.1002/adma.201702226

[17] X. Wen, S. Sun, P. Wu. Dynamic wrinkling of a hydrogel–elastomer hybrid microtube enables blood vessel-like hydraulic pressure sensing and flow regulation. *Mater. Horizons* **2020**, *7*, 2150-2157. https://doi.org/10.1039/D0MH00089B

[18] J. Broek, I. C. Weber, A. T. Güntner, S. E. Pratsinis. Highly selective gas sensing enabled by filters. *Mater*. *Horizons* **2021**, *8*, 661-684. https://doi.org/10.1039/D0MH01453B

[19] J. F. Olorunyomi, S. T. Geh, R. A. Caruso, C. M. Doherty. Metal–organic frameworks for chemical sensing devices. *Mater. Horiz.* **2021***, 8, 2387-2419*. https://doi.org/10.1039/D1MH00609F

[20] S. M. Berger, T. B. Marder. Applications of triarylborane materials in cell imaging and sensing of bio-relevant molecules such as DNA, RNA, and proteins. *Mater. Horiz.* **2022**, *9*, 112-120. https://doi.org/10.1039/D1MH00696G

[21] C. Wang, Y. V. Kaneti, Y. Bando, J. Lin, C. Liu, J. Li, Y. Yamauchi. Metal–organic framework-derived one-dimensional porous or hollow carbon-based nanofibers for energy storage and conversion. *Mater. Horizons* **2018**, 5, 394-407. https://doi.org/10.1039/C8MH00133B

[22] Y. Wu, X. Huang, L. Huang, J. Chen. Strategies for rational design of high-power lithium-ion batteries. *Energy Environ. Mater*. **2021**, *4*, 19-45. https://doi.org/10.1002/eem2.12088

[23] J. Yang, L.-S. Tang, L. Bai, R.-Y. Bao, Z.-Y. Liu, B.-H. Xie, M.-B. Yang, W. Yang. High-performance composite phase change materials for energy conversion based on macroscopically three-dimensional structural materials. *Mater. Horizons* **2019**, *6*, 250-273. https://doi.org/10.1039/C8MH01219A

[24] O. Baranov, I. Levchenko, J. M. Bell, J. W. M. Lim, S. Huang, L. Xu, B. Wang, D. U. B. Aussems, S. Xu, K. Bazaka. From nanometre to millimetre: a range of capabilities for plasma-enabled surface functionalization and nanostructuring. *Mater. Horizons* **2018,** *5*, 765-798. https://doi.org/10.1039/C8MH00326B

[25] I. Levchenko, O. Baranov, C. Riccardi, H. E. Roman, U. Cvelbar, E. Ivanova, M. Mandhakini, P. Ščajev, T. Malinauskas, S. Xu, K. Bazaka. Nanoengineered carbon-based interfaces for advanced energy and photonics applications: A recent progress and innovations. *Adv. Mater. Interfaces* **2023**, *10*, 2201739. https://doi.org/10.1002/admi.202201739

[26] O. Baranov, K. Bazaka, T. Belmonte, C. Riccardi, E. Roman, M. Mandhakini, S. Xu, U. Cvelbar, I. Levchenko. Recent innovations in the technology and applications of low-dimensional CuO nanostructures for sensing, energy and catalysis. *Nanoscale Horiz.* **2023**, *8*, 568-602. https://doi.org/10.1039/D2NH00546H

[27] I. Levchenko, M. Mandhakini, K. Prasad, O. Bazaka, E. P. Ivanova, M. V. Jacob, O. Baranov, C. Riccardi, H. E. Roman, S. Xu, K. Bazaka. Functional nanomaterials from waste and low-value natural products: A technological approach level. *Adv. Mater. Technol.* **2022**, *7*, 2101471. https://doi.org/10.1002/admt.202101471

[28] J. Weerasinghe, K. Prasad, J. Mathew, E. Trifoni, O. Baranov, I. Levchenko, K. Bazaka. Carbon nanocomposites in aerospace technology: A way to protect low-orbit satellites. *Nanomaterials* **2023**, *13*, 1763. https://doi.org/10.3390/nano13111763

[29] I. Levchenko, S. Xu, G. Teel, D. Mariotti, M. L. R. Walker, M. Keidar, Recent progress and perspectives of space electric propulsion systems based on smart nanomaterials, *Nat. Commun*. **2018,** *9*, 879. https://doi.org/10.1038/s41467-017-02269-7

[30] I. Levchenko, S. Xu, S. Mazouffre, M. Keidar, K. Bazaka. Mars colonization: Beyond getting there. *Glob. Chall.* **2018**, *2*, 1800062. https://doi.org/10.1002/gch2.201800062

[31] I. Levchenko, K. Bazaka, T. Belmonte, M. Keidar, S. Xu. Advanced materials for next generation spacecraft. *Adv. Mater.* **2018**, *30*, 1802201. https://doi.org/10.1002/adma.201802201

[32] a) I. Levchenko, M. Keidar, J. Cantrell, Y.-L. Wu, H. Kuninaka, K. Bazaka, S. Xu. Explore space using swarms of tiny satellites. *Nature* **2018**, *562*, 185-187. https://doi.org/10.1038/d41586-018-06957-2; b) I. Levchenko, O. Baranov, D. Pedrini, C. Riccardi, H. E. Roman, S. Xu, D. Lev, K. Bazaka. Diversity of Physical Processes: Challenges and Opportunities for Space Electric Propulsion. Appl. Sci. **2022**, *12*, 11143. https://doi.org/10.3390/app122111143; c) I. Levchenko, D. M. Goebel, K. Bazaka. Electric propulsion of spacecraft. *Phys. Today* **2022**, *75*, 38, https://doi.org/10.1063/PT.3.5081; d) I. Levchenko, K. Bazaka. Iodine powers low-cost engines for satellites. *Nature* **2021**, *599*, 373-374. https://doi.org/10.1038/d41586-021-03384-8

[33] Z. Wang, L. Scheres, H. Xia, H. Zuilhof. Developments and challenges in self-healing antifouling materials. *Adv. Functional Mater.* **2020**, *30*, 1908098. https://doi.org/10.1002/adfm.201908098

[34] R. Chen, Y. Zhang, Q. Xie, Z. Chen, C. Ma, G. Zhang. Transparent polymer-ceramic hybrid antifouling coating with superior mechanical properties. *Adv. Functional Mater.* **2021**, *31*, 2011145. https://doi.org/10.1002/adfm.202011145

[35] A. M. C. Maan, A. H. Hofman, W. M. de Vos, M. Kamperman. Recent developments and practical feasibility of polymer-based antifouling coatings. *Adv. Functional Mater.* **2020**, *30*, 2000936. https://doi.org/10.1002/adfm.202000936

[36] M. S. Selim, H. Yang, F. Q. Wang, N. A. Fatthallah, Y. Huang and S. Kuga, Silicone/ZnO nanorod composite coating as a marine antifouling surface, *Appl. Surf. Sci.*, **2019**, *466*, 40–50. https://doi.org/10.1016/j.apsusc.2018.10.004

[37] A. S. Adeleye, E. A. Oranu, M. Tao and A. A. Keller, Release and detection of nanosized copper from a commercial antifouling paint, *Water Res.* **2016**, *102*, 374–382. https://doi.org/10.1016/j.watres.2016.06.056

[38] K. Lee, C. Kim, S. Jeong, Y. Song, N. Bae, S. Lee and K. Lee, Ultrasonic fabrication of flexible antibacterial ZnO nanopillar array film, *Colloids Surf. B* **2018**, *170*, 172–178. https://doi.org/10.1016/j.colsurfb.2018.06.007

[39] Y. Ouyang, J. Zhao, R. Qiu, S. Hu, H. Niu, M. Chen and P. Wang, Biomimetics leading to liquid-infused surface based on vertical dendritic Co matrix: A barrier to inhibit bioadhesion and microbiologically induced corrosion, *Colloids Surf. A* **2019**, *583*, 124006. https://doi.org/10.1016/j.colsurfa.2019.124006

[40] R. Jiang, L. Hao, L. Song, L. Tian, Y. Fan, J. Zhao, C. Liu, W. Ming and L. Ren, Lotus-leaf-inspired hierarchical structured surface with non-fouling and mechanical bactericidal performances, *Chem. Eng. J.* **2020**, *398*, 125609. https://doi.org/10.1016/j.cej.2020.125609

[41] T. Gu, R. Jia, T. Unsal, D. Xu, Toward a better understanding of microbiologically influenced corrosion caused by sulfate reducing bacteria, *J. Mater. Sci. Technol.* **2019**, *35,* 631–636. https://doi.org/10.1016/j.jmst.2018.10.026

[42] Y.-S. Moon, M. Kim, C. P. Hong, J.-H. Kang, J.-H. Jung. Overlapping and unique toxic effects of three alternative antifouling biocides (Diuron, Irgarol 1051, Sea-Nine 211) on non-target marine fish. *Ecotoxicol. Environment. Safety* **2019,** *180*, 23–32. https://doi.org/10.1016/j.ecoenv.2019.04.070

[43] L. Chen, P. Y. Qian. Review on molecular mechanisms of antifouling compounds: an update since 2012. *Mar. Drugs* **2017**, *15*, 1 –20. https://doi.org/10.3390/md15090264

[44] A. Mukherjee, M. Joshi, S.C. Misra, U.S. Ramesh. Antifouling paint schemes for green SHIPS. *Ocean Engineering* **2019,** *173*, 227–234. https://doi.org/10.1016/j.oceaneng.2018.12.057

[45] J. A. Batista-Andrade, S. S. Caldas, R. M. Batista, I. B. Castro, G. Fillmann, E. G. Primel. From TBT to booster biocides: Levels and impacts of antifouling along coastal areas of Panama. *Environment. Pollution* **2018**, *234,* 243-252. https://doi.org/10.1016/j.envpol.2017.11.063

[46] L. Chen, Y. Duan, M. Cui, R. Huang, R. Su, W. Qi, Z. He. Biomimetic surface coatings for marine antifouling: Natural antifoulants, synthetic polymers and surface microtopography. *Sci. Total Environment* **2021**, *766,* 144469. https://doi.org/10.1016/j.scitotenv.2020.144469

[47] P. A. Vinagre, T. Simas, E. Cruz, E. Pinori, J. Svenson. Marine biofouling: A European database for the marine renewable energy sector. *J. Mar. Sci. Eng*. **2020**, *8*, 495; https://doi.org/10.3390/jmse8070495

[48] W. M. Dunne. Bacterial adhesion: Seen any good biofilms lately? *Clin. Microbiol. Rev*. **2002**, *15*, 155-166. https://doi.org/10.1128/CMR.15.2.155-166.2002

[49] Palmer, J., S. Flint, and J. Brooks, Bacterial cell attachment, the beginning of a biofilm. *J. Industr. Microbiol. Biotechnol*. **2007**, *34*, 577-588. https://doi.org/10.1007/s10295-007-0234-4

[50] D. M. Yebra, S. Kiil, K. Dam-Johansen, C. Weinell. Reaction rate estimation of controlled-release antifouling paint binders: Rosin-based systems. *Prog. Org. Coat*. **2005**, *53*, 256-275. https://doi.org/10.1016/j.porgcoat.2005.03.008

[51] H.-C. Flemming, T. Griebe, G. Schaule. Antifouling strategies in technical systems. *Water Sci. Technol*. **1996**, *34*, 517-524. https://doi.org/10.1007/978-3-642-19940-0_5

[52] F. T. Arce, R.Avci, I. B. Beech, K. E. Cooksey, B. Wigglesworth-Cooksey. A live bioprobe for studying diatom-surface interactions. *Biophys. J.* **2004**, *87*, 4284-4297. https://doi.org/10.1529/biophysj.104.043307

[53] I. Amara, W. Mileda, R. B. Slama, N. Ladhari. Antifouling processes and toxicity effects of antifouling paints on marine environment. A review. *Environmental Toxicol. Pharmacol*. **2018**, *57*, 115-130. https://doi.org/10.1016/j.etap.2017.12.001

[54] P. Almeida, J. W. P. Coolena. Modelling thickness variations of macrofouling communities on offshore platforms in the Dutch North Sea. *J. Sea Res*. **2020**, *156*, 101836. https://doi.org/10.1016/j.seares.2019.101836

[55] C. Hellio, D. Yebra. Advances in marine antifouling coatings and technologies. 1st Edition, Elsevier **2009**. ISBN 978-1-84569-386-2

[56] M. E. Callow, J. A. Callow, L. K. Ista, S. E. Coleman, A. C. Nolasco, G. P. Lopez. Use of self-assembled monolayers of different wettabilities to study surface selection and primary adhesion processes of green algal (Enteromorpha) zoospores. *Appl. Environ. Microbiol***. 2000**, *66*, 3249-3254. https://doi.org/10.1128/AEM.66.8.3249-3254.2000

[57] N. Aldred, A. S. Clare. Mechanisms and principles underlying temporary adhesion, surface exploration and settlement site selection by Barnacle Cyprids: A short review. In: Gorb S.N. (eds) Functional Surfaces in Biology. Springer, Dordrecht **2009**. https://doi.org/10.1007/978-1-4020-6695-5_3

[58] D. Howell, B. Behrends. A review of surface roughness in antifouling coatings illustrating the importance of cutoff length. *Biofouling* **2006**, *22*, 401-410. https://doi.org/10.1080/08927010601035738

[59] A. Kumar, A. Aljumaili, O. Bazaka,; E. P. Ivanova, I. Levchenko, K. Bazaka, M. Jacob. Functional nanomaterials, synergism and biomimicry for environmentally benign marine antifouling technology. *Mater. Horiz*. **2021**, *8*, 3201-3238. https://doi.org/10.1039/D1MH01103K

[60] V. O. Agostini, E. Muxagata, G. L. Pinho, I. S. Pessi, A. J. Macedo. Bacteria-invertebrate interactions as an asset in developing new antifouling coatings for man-made aquatic surfaces. *Environ. Pollut*. **2021**, *271*, 116284. https://doi.org/10.1016/j.envpol.2020.116284

[61] T. Onduka, K. Kono, M. Ito, N. Ohkubo, T. Hano, K. Ito, K. Mochida. Ecological risk assessment of an antifouling biocide triphenyl (octadecylamine) boron in the Seto Inland Sea, Japan. *Mar. Pollut. Bull*. **2020**, *157,* 111320. https://doi.org/10.1016/j.marpolbul.2020.111320

[62] J. L. M. Viana, M. S. Diniz, S. R. V. Santos, R. T. Verbinnen, M. A. P. Almeida, T. C. R. S. Franco. Antifouling biocides as a continuous threat to the aquatic environment: Sources, temporal trends and ecological risk assessment in an impacted region of Brazil. *Sci. Total Environ*. **2020**, *730*, 139026. https://doi.org/10.1016/j.scitotenv.2020.139026

[63] J. T. Koning, U. E. Bollmann, K. Bester. The occurrence of modern organic antifouling biocides in Danish marinas. *Mar. Pollut. Bull*. **2020**, *158,* 111402. https://doi.org/10.1016/j.marpolbul.2020.111402

[64] F. E. L. Abreu, R. M. Batista, I. B. Castro, G. Fillmann. Legacy and emerging antifouling biocide residues in a tropical estuarine system (Vitoria state, SE, Brazil). *Mar. Pollut. Bull*. **2021**, *166*, 112255. https://doi.org/10.1016/j.marpolbul.2021.112255

[65] K. A Dafforn, J. A. Lewis, E. L. Johnston. Antifouling strategies: History and regulation, ecological impacts and mitigation. *Mar. Pollut. Bull*. **2011**, *62*, 453-65. https://doi.org/10.1016/j.marpolbul.2011.01.012

[66] D. J. Blackwood, C. S. Lim, S. L. Teo, X. Hu, J. Pang. Macrofouling induced localized corrosion of stainless steel in Singapore seawater. *Corros. Sci*. **2017**, *129*, 152–160. https://doi.org/10.1016/j.corsci.2017.10.008

[67] L. Chen, C. Xia, P. Y. Qian, Optimization of antifouling coatings incorporating butenolide, a potent antifouling agent via field and laboratory tests. *Prog. Org. Coat*. **2017**, *109*, 22–29. https://doi.org/10.1016/j.porgcoat.2017.04.014

[68] B.-M. Kim, K. Kim, I.-Y. Choi, J.-S. Rhee. Transcriptome response of the Pacific oyster, Crassostrea gigas susceptible to thermal stress: a comparison with the re-sponse of tolerant oyster. *Mol. Cell. Toxicol*. **2017,** *13*, 105–113 https://doi.org/10.1007/s13273-017-0011-z

[69] T. Onduka, D. Ojima, Mana Ito, K. Ito, K. Mochida, K. Fujii. Toxicity of the antifouling biocide Sea-Nine 211 to marine algae, crustacea, and a polychaete. *Fisheries Sci*. **2013**, *79*, 999-1006. https://doi.org/10.1007/s12562-013-0678-6

[70] J. R. Kucklick, M. D.Ellisor. A review of organotin contamination in arctic and subarctic regions. *Emerging Contaminants* **2019**, *5,* 150-156. https://doi.org/10.1016/j.emcon.2019.04.003

[71] L. Shtykova, C. Fant, P. Handa, A. Larsson, K. Berntsson, H. Blanck, R. Simonsson, M. Nyd, H. I. Helinda. Adsorption of antifouling booster biocides on metal oxide nanoparticles: Effect of different metal oxides and solvents. *Prog. Org. Coat.* **2009**, *64*, 20-26. https://doi.org/10.1016/j.porgcoat.2008.07.005

[72] K. Thomas, S. Brooks. The environmental fate and effects of antifouling paint biocides. *Biofouling* **2010**, *26*, 73-88. https://doi.org/10.1080/08927010903216564

[73] Chambers, K. R. Stokes, F. C. Walsh, R. J. K. Wood. Modern approaches to marine antifouling coatings. *Surf. Coat. Technol*. **2006**, *201*, 3642-3652. https://doi.org/10.1016/j.surfcoat.2006.08.129

[74] L. Tian, Y. Yin, W. Bing, E. Jin. Antifouling technology trends in marine environmental protection. *Bionic Eng*. **2021**, *18*, 239–263. https://doi.org/10.1007/s42235-021-0017-z

[75] S. E. Martins, G. Fillmann, A. Lillicrap, K. V. Thomas, Ecotoxicity of organic and organo-metallic antifouling co-biocides and implications for environmental hazard and risk assessments in aquatic ecosystems, *Biofouling* **2018**, *34*, 34-52. https://doi.org/10.1080/08927014.2017.1404036

[76] Abioye, O.P., C. Loto, and O. Fayomi, Evaluation of anti-biofouling progresses in marine application, *J. Bio-and Tribo-Corrosion* **2019**, *5*, 22. https://doi.org/10.1007/s40735-018-0213-5

[77] J. Zhou, C. Yang, J. Wang, P. Sun, P. Fan, K. Tian, S. Liu, C. Xia, Toxic effects of environment-friendly antifoulant nonivamide on Phaeodactylum tricornutum, *Environ. Toxicol. Chem.* **2013**, *32*, 802-809. https://doi.org/10.1002/etc.2132

[78] I. B. Gomes, M. Sims, L. C. Sims. Copper surfaces in biofilm control. *Nanomaterials* **2020**, *10*, 2491. https://doi.org/10.3390/nano10122491

[79] B. Antizar-Ladislao, Environmental levels, toxicity and human exposure to tributyltin (TBT)-contaminated marine environment. A review. *Environ. Int*. **2008**, *34*, 292-308. https://doi.org/10.1016/j.envint.2007.09.005

[80] M. S. Selim, M. Shenashen, S. A. El-Safty, S. Higazy, M.M. Selim, H. Isago, A. Elmarakbi. Recent progress in marine foul-release polymeric nanocomposite coatings. *Prog. Mater. Sci*. **2017**, *87,* 32. https://doi.org/10.1016/j.pmatsci.2017.02.001

[81] X. Han, J. Wu, X. Zhang, J. Shi, J. Wei, Y. Yang, B. Wu, Y. Feng. The progress on antifouling organic coating: From biocide to biomimetic surface. *J. Mater. Sci. Technol*. **2021**, *61*, 46–62. https://doi.org/10.1016/j.jmst.2020.07.002

[82] E. Aykin, B.u Omuzbuken, A. Kacar. Microfouling bacteria and the use of enzymes in eco-friendly antifouling technology. *J. Coat. Technol. Res*. **2019,** *16*, 847–856, https://doi.org/10.1007/s11998-018-00161-7

[83] E. Almeida, T. C. Diamantino, O. de Sousa. Marine paints: the particular case of antifouling paints. *Prog. Org. Coat*. **2007**, *59*, 2-20. https://doi.org/10.1016/j.porgcoat.2007.01.017

[84] I. Banerjee, Pangule R. C., Kane R. S. Antifouling coatings: recent developments in the design of surfaces that prevent fouling by proteins, bacteria, and marine organisms. *Adv. Mater*. **2011**, *23*, 690-718. https://doi.org/10.1002/adma.201001215

[85] S. M. Olsen, L. T. Pedersen, M. H. Laursen, S. Kiil, K. Dam-Johansen. Enzyme-based antifouling coatings: A review. *Biofouling* **2007**, *23*, 369-383. https://doi.org/10.1080/08927010701566384

[86] A. M. Brzozowska, S. Maassen, R. G. Z. Rong, P. I. Benke, C.-S. Lim, E. M. Marzinelli, D. Jańczewski, S. L.-M. Teo, G. J. Vancso. Effect of variations in micropatterns and surface modulus on marine fouling of engineering polymers. *ACS Appl. Mater. Interf*. **2017**, *9*, 17508-17516. https://doi.org/10.1021/acsami.6b14262

[87] J. Kim, B. J. Chisholm, J. Bahr. Adhesion study of silicone coatings: the interaction of thickness, modulus and shear rate on adhesion force. *Biofouling* **2007**, *23*, 113-120. https://doi.org/10.1080/08927010701189708

[88] H. Jin, W. Bing, L. Tian, P. Wang, J. Zhao. Combined effects of color and elastic modulus on antifouling performance: A study of graphene oxide/silicone rubber composite membranes. *Materials* **2019**, *12*, 2608. https://dx.doi.org/10.3390%2Fma12162608

[89] A. K. Halvey, B. Macdonald, A. Dhyani, A. Tuteja. Design of surfaces for controlling hard and soft fouling. *Philos. Trans. A Math. Phys. Eng. Sci*. **2019**, *377*, 20180266. https://dx.doi.org/10.1098%2Frsta.2018.0266

[90] J. R. Griffith, J. D. Bultman. Fluorinated naval coatings. *Ind. Eng. Chem. Prod. Res. Dev*. **1978**, *17*, 8–9. https://doi.org/10.1021/i360065a003

[91] Y. Gu, L. Yu, J. Mou, D. Wu, M. Xu, P. Zhou, Y. Ren. Research strategies to develop environmentally friendly marine antifouling coatings. *Mar. Drugs* **2020,** *18*, 371. https://doi.org/10.3390/MD18070371

[92] P. Hu, Q. Xie, C. Ma, G. Zhang. Silicone-Based Fouling-Release Coatings for Marine Antifouling. *Langmuir* **2020** *36*, 9, 2170–2183. https://doi.org/10.1021/acs.langmuir.9b03926

[93] S. Holberg, R. Losada, F. H. Blaikie, H. H. W. B. Hansen, S. Soreau, R. C. A. Onderwater. Hydrophilic silicone coatings as fouling release: Simple synthesis, comparison to commercial, marine coatings and application on fresh water-cooled heat exchangers. *Mater. Today Commun*. **2020**, *22*, 100750. https://doi.org/10.1016/j.mtcomm.2019.100750

[94] M. S. Selim, S. A. El-Safty, M. A. El-Sockary, A. I. Hashem, O. M. A. Elenien, A. M. EL-Saeed, N. A. Fatthallah. Smart photo-induced silicone/TiO2 nanocomposites with dominant [110] exposed surfaces for self-cleaning foul-release coatings of ship hulls. *Materials and Design* **2016,** *101,* 218-225. http://dx.doi.org/10.1016/j.matdes.2016.03.124

[95] A. Derbalah, S. A. El-Safty, M. A. Shenashen, N. A. A. Ghany. Mesoporous alumina nanoparticles as host tunnel-like pores for removal and recovery of insecticides from environmental samples. *ChemPlusChem* **2015**, *80*, 1119-1126. https://doi.org/10.1002/cplu.201500098

[96] M. C. Parrott, J. M. DeSimon., Relieving PEGylation. *Nat. Chem.* **2012**, *4*, 13-14. https://doi.org/10.1038/nchem.1230

[97] E. Wassel, M. Es-Sounia, A. Laghrissi, A. Roth, M. Dietze, M. Es-Souni. Scratch resistant non-fouling surfaces via grafting non-fouling polymers on the pore walls of supported porous oxide structures. *Mater. Design* **2019**, *163,* 107542. https://doi.org/10.1016/j.matdes.2018.107542

[98] W. Taylor, R. A. Jones. Protein adsorption on well-characterized polyethylene oxide brushes on gold: Dependence on molecular weight and grafting density. *Langmuir* **2013**, *29*, 6116-6122. https://doi.org/10.1021/la40054833

[99] W. Yandi, S. Mieszkin, P. Martin-Tanchereau, M. E. Callow, J. A. Callow, L. Tyson, B. Liedberg, T. Ederth. Hydration and chain entanglement determines the optimum thickness of Poly (HEMA-co-PEG10MA) brushes for effective resistance to settlement and adhesion of marine fouling organisms. *ACS Appl. Mater. Interfaces* **2014**, *6*, 11448-11458. https://doi.org/10.1021/am502084x

[100] C. Ventura, A. J. Guerin, O. El-Zubir, A. J. Ruiz-Sanchez, L. I. Dixon, K. J. Reynolds, M. L. Dale, J. Ferguson, A. Houlton, B. R. Horrocks, A. S. Clare, D. A. Fulton. Marine antifouling performance of polymer coatings incorporating zwitterions. *Biofouling* **2017**, *33*, 892-903. https://doi.org/10.1080/08927014.2017.1383983

[101] N. Punitha, P. Saravanan, R. Mohan, P. S. Ramesh. Antifouling activities of b-cyclodextrin stabilized peg based silver nanocomposites. *Appl. Surf. Sci.* **2017**, *392,* 126–134. http://dx.doi.org/10.1016/j.apsusc.2016.07.114

[102] L. Xue, X. Lu, H. Wei, P. Long, J. Xu, Y. Zheng. Bio-inspired self-cleaning PAAS hydrogel released coating for marine antifouling. *J. Colloid Interf. Sci*. **2014**, *421*, 178-183. https://doi.org/10.1016/j.jcis.2013.12.063

[103] M. Winfield, A. Downer, J. Longyear, M. Dale, G. Barker. Comparative study of biofilm formation on biocidal antifouling and fouling-release coatings using next-generation DNA sequencing. *Biofouling* **2018,** *34*, 464-477. https://doi.org/10.1080/08927014.2018.1464152

[104] A. L. Patterson, B. Wenning, G. Rizis, D. R. Calabrese, J. A. Finlay, S. C. Franco, R. N. Zuckermann, A. S. Clare, E. J. Kramer, C. K. Ober, R. A. Segalman. Role of backbone chemistry and monomer sequence in amphiphilic oligopeptide- and oligopeptoid-functionalized PDMS- and PEO-based block copolymers for marine antifouling and fouling release coatings. *Macromolecules* **2017**, *50*, 2656–2667. https://doi.org/10.1021/acs.macromol.6b02505

[105] A. D. Staneva, D. K. Dimitrov, D. N. Gospodinova, T. G. Vladkova. Antibiofouling activity of graphene materials and graphene-based antimicrobial coatings. *Microorganisms* **2021**, *9*, 1839. https://doi.org/10.3390/microorganisms9091839

[106] H. Jin, L. Tian, W. Bing, J. Zhao, L. Ren. Toward the application of graphene for combating marine biofouling. *Adv. Sustainable Syst.* **2020**, *5*, 2000076. https://doi.org/10.1002/adsu.202000076

[107] F. Sousa-Cardoso, R. Teixeira-Santos, F. J. M. Mergulhão. Antifouling performance of carbon-based coatings for marine applications: A systematic review. *Antibiotics* **2022**, *11*, 1102. https://doi.org/10.3390/antibiotics11081102

[108] N. M. Das, A. K. Singh, D. Ghosh, D. Bandyopadhyay. Graphene oxide nanohybrids for electron transfer-mediated antimicrobial activity. *Nanoscale Adv*. **2019**, *1*, 3727. https://doi.org/10.1039/C9NA00272C

[109] L. Liu, M. Zhang, Q. Zhang, W. Jiang. Graphene nanosheets damage the lysosomal and mitochondrial membranes and induce the apoptosis of RBL-2H3 Cells. *Sci. Total Environ.* **2020**, *734*, 139229. https://doi.org/10.1016/j.scitotenv.2020.139229

[110] L. Feng, Y. Gao, Y. Xu, H. Dan, Y. Qi, S. Wang, F. Yin, Q. Yue, B. Gao. A dual-functional layer modified GO@SiO2 membrane with excellent anti-fouling performance for continuous separation of oil-in-water emulsion. *J. Hazard. Mater*. **2021**, *420*, 126681. https://doi.org/10.1016/j.jhazmat.2021.126681

[111] L. Ni, Y. Zhu, J. Ma, M. Wu, H. Wang, Z. Jiang, Y. Wang. Improved anti-biofouling performance of CdS/g-C3N4/rGO modified membranes based on in situ visible light photocatalysis in anammox membrane bioreactor. *J. Membrane Sci.* **2021**, *620*, 118861. https://doi.org/10.1016/j.memsci.2020.118861

[112] A. Radhi, D. Mohamad, F. S. A. Rahman, A. Man af Abdullah, H. Hasan. Mechanism and factors influence of graphene-based nanomaterials antimicrobial activities and application in dentistry. *J. Mater. Res. Technol*. **2021**, *11*, 1290-1307. https://doi.org/10.1016/j.jmrt.2021.01.093

[113] C. Piferi, K. Bazaka, D. L. D'Aversa, R. Di Girolamo, C. De Rosa, H. E. Roman, C. Riccardi, I. Levchenko. Hydrophilicity and hydrophobicity control of plasma-treated surfaces via fractal parameters. *Adv. Mater. Interfaces* **2021**, *8*, 2100724. https://doi.org/10.1002/admi.202100724

[114] S. Verma, S. Mohanty, S. Nayak. A review on protective polymeric coatings for marine applications. *J. Coat. Technol*. Res. **2019**, *16*, 307-338. https://doi.org/10.1007/s11998-018-00174-2

[115] J. Fu, H. Zhang, Z. Guo, D. Feng, V. Thiyagarajan, H. Yao. Combat biofouling with microscopic ridge-like surface morphology: a bioinspired study. *J. R. Soc. Interface* **2018**, *15,* 20170823. http://dx.doi.org/10.1098/rsif.2017.0823

[116] L. Xiao, J. A. Finlay, M. Röhrig, S. Mieszkin, M. Worgull, H. Hölscher, J. A. Callow, M. E. Callow, M. Grunze, A. Rosenhahn.Topographic cues guide the attachment of diatom cells and algal zoospores. *Biofouling* **2018,** *34*, 86-97. http://dx.doi.org/10.1080/08927014.2017.1408801

[117] K. Efimenko, J. Finlay, M. Callow, J. Callow, J. Genzer. Development and testing of hierarchically wrinkled coatings for marine antifouling. *ACS App. Mater. Interfaces* **2009**, *1*, 1031–1040. https://doi.org/10.1021/am9000562

[118] M. S. Selim, M. A. Shenashen, A. Elmarakbi, N. A. Fatthallah, S. Hasegawa, S. A. El- Safty. Synthesis of ultrahydrophobic and thermally stable inorganic-organic nanocomposites for self-cleaning foul release coatings. *Chem. Eng. J.* **2017**, *320*, 653-666. https://doi.org/10.1016/j.cej.2017.03.067

[119] M. Carve, A. Scardino, J. Shimeta. Effects of surface texture and interrelated properties on marine biofouling: a systematic review. *Biofouling* **2019**, *35*, 597-617. https://doi.org/10.1080/08927014.2019.1636036

[120] S. K. Kyei, G. Darko, O. Akaranta. Chemistry and application of emerging ecofriendly antifouling paints: a review. *J. Coat. Technol. Res*. **2020**, *17*, 315-332. https://doi.org/10.1007/s11998-019-00294-3

[121] W. Bing, L. Tian, Y. Wang, H. Jin, L. Ren, S, Dong. Bio-Inspired non-bactericidal coating used for antibiofouling. *Adv. Mater. Technol*. **2019**, *4*, 1800480. https://doi.org/10.1002/admt.201800480

[122] H. Jin, T. Zhang, W. Bing, S. Dong, L, Tian, Antifouling performance and mechanism of elastic graphene–silicone rubber composite membranes. J. *Mater. Chem. B* **2019**, *7*, 488–497. https://doi.org/10.1039/C8TB02648C

[123] M. S. Selim, N. A. Fatthallah, S. A. Higazy, Z. Hao, P. J. Mo. A comparative study between two novel silicone/graphene-based nanostructured surfaces for maritime antifouling. *J. Colloid Interf. Sci*. **2022**, *606*, 367–383. https://doi.org/10.1016/j.jcis.2021.08.026

[124] G. Jena, B. Anandkumar, S. C. Vanithakumari, R. P. George, J. Philip, G. Amarendra. Graphene oxide-chitosan-silver composite coating on Cu-Ni alloy with enhanced anticorrosive and antibacterial properties suitable for marine applications. *Prog. Org. Coat.* **2020**, *139,* 105444. https://doi.org/10.1016/j.porgcoat.2019.105444

[125] Z. Zhang, R. Chen, D. Song, Jing Yu, G. Sun, Qi Liu, S. Han, J. Liu, H. Zhang, J. Wang. Guanidine-functionalized graphene to improve the antifouling performance of boron acrylate polymer. *Prog*. Org. *Coat*. **2021**, *159*, 106396. https://doi.org/10.1016/j.porgcoat.2021.106396

[126] M. J. Romeu, L. C. Gomes, F. Sousa-Cardoso, J. Morais, V. Vasconcelos, K. A. Whitehead, M. F. R. Pereira, O. S. G. P. Soares, F. J. Mergulhão. How do graphene composite surfaces affect the develo and structure of marine cyanobacterial biofilms? *Coatings* **2022**, *12*, 1775. https://doi.org/10.3390/coatings12111775

[127] Y. Li, Y. Huang, F. Wang, W. Liang, H. Yang, D. Wu. Fabrication of acrylic acid modified graphene oxide (AGO)/acrylate composites and their synergistic mechanisms of anticorrosion and antifouling properties. *Prog. Org. Coat*. **2022**, *168,* 106910. https://doi.org/10.1016/j.porgcoat.2022.106910

[128] F. Sousa-Cardoso, R. Teixeira-Santos, A. F. Campos, M. Lima, L. C. Gomes, O. S. G. P. Soares, F. J. Mergulhão. Graphene-based coating to mitigate biofilm development in marine environments. *Nanomaterials* **2023**, *13*, 381. https://doi.org/10.3390/nano13030381

[129] S. Fazli-Shokouhi, F. Nasirpouri, M. Khatamian. Polyaniline-modified graphene oxide nanocomposites in epoxy coatings for enhancing the anticorrosion and antifouling properties. *J. Coat. Technol. Res*. **2019**, *16*, 983–997. https://doi.org/10.1007/s11998-018-00173-3

[130] S. Fazli-Shokouhi, F. Nasirpouri, M. Khatamian. Epoxy-matrix polyaniline/p-phenylenediamine-functionalised graphene oxide coatings with dual anti-corrosion and anti-fouling performance. *RSC Adv.* **2021**, *11*, 11627. https://doi.org/10.1039/d0ra10665h

[131] G. Jena, R. P. George, J. Philip. Fabrication of a robust graphene oxide-nano SiO2-polydimethylsiloxane composite coating on carbon steel for marine applications. *Prog. Org. Coat*. **2021**, *161,* 106462. https://doi.org/10.1016/j.porgcoat.2021.106462

[132] Z. Liu, S. Tian, Q. Li, J. Wang, J. Pu, G. Wang, W. Zhao, F. Feng, J. Qin, L. Ren. Integrated dual-functional ORMOSIL coatings with AgNPs@rGO nanocomposite for corrosion resistance and antifouling applications. *ACS Sustain. Chem. Eng*. **2020**, *8*, 6786–6797. https://doi.org/10.1021/acssuschemeng.0c01294

[133] K. D. Efird. Inter-relation of corrosion and fouling for metals in sea water. Vol. 15, Materials Performance, 1976. p. 16–25.

[134] X. Zhang, Ø. Mikkelsen. Graphene oxide/silver nanocomposites as antifouling coating on sensor housing materials. *J. Clust. Sci.* **2022**, *33*, 627–635. https://doi.org/10.1007/s10876-020-01953-x

[135] S. Soleimani, A. Jannesari, M. Yousefzadi, A. Ghaderi, A. Shahdadi. Eco-friendly foul release coatings based on a novel reduced graphene oxide/Ag nanocomposite prepared by a green synthesis approach. *Prog. Org. Coat*. **2021**, *151,* 106107. https://doi.org/10.1016/j.porgcoat.2020.106107

[136] M. S.-L. Yee, P.-S. Khiew, W. S. Chiu, Y. F. Tan, Y.-Y. Kok, C.-O. Leong. Green synthesis of graphene-silver nanocomposites and its application as a potent marine antifouling agent. *Colloids and Surfaces B: Biointerfaces* **2016**, *148,* 392–401. http://dx.doi.org/10.1016/j.colsurfb.2016.09.011

[137] X. Zhang, E. Årstøl, M. Nymark, M. Fages-Lartaud, Ø. Mikkelsen. The development of polydimethysiloxane/ZnO–GO antifouling coatings. *J. Clust. Sci*. **2022**, *33*, 2407–2417. https://doi.org/10.1007/s10876-021-02165-7

[138] J. Gu, L. Li, D. Huang, L. Jiang, L. Liu, F. Li, A. Pang, X. Guo, B. Tao. *In Situ* synthesis of graphene@cuprous oxide nano composite incorporated marine antifouling coating with elevated antifouling performance. *Open J. Org. Polymer Mater.* **2019**, *9*, 47-62. https://doi.org/10.4236/ojopm.2019.93003

[139] O. Ferreira, P. Rijo, J. Gomes, R. Santos, S. Monteiro, R. Guedes, M. L. Serralheiro, M. Gomes, L. C. Gomes, F. J. Mergulhão, E. R. Silva. Antimicrobial ceramic filters for water bio-decontamination. *Coatings* **2021**, *11*, 323. https://doi.org/10.3390/coatings11030323

[140] S. Verma, S. Mohanty, S. K. Nayak. Preparation of hydrophobic epoxy polydimethylsiloxane graphene oxide nanocomposite coatings for antifouling application. *Soft Matter* **2020**, *16*, 1211-1226. https://doi.org/10.1039/C9SM01952A

[141] D. H. Seo, S. Pineda, Y. C. Woo, M. Xie, A. T. Murdock, E. Y. M. Ang, Y. Jiao, M. J. Park, S. I. Lim, M. Lawn *et al.* Anti-fouling graphene-based membranes for effective water desalination. *Nat. Commun.* **2018**, *9*, 683. https://doi.org/10.1038/s41467-018-02871-3

[142] Z. Lu, Z. Chen, Y. Guo, Y. Ju, Y. Liu, R. Feng, C. Xiong, C. K. Ober, L. Dong. Flexible hydrophobic antifouling coating with oriented nanotopography and nonleaking capsaicin. *ACS Appl. Mater. Interf*. **2018**, *10*, 9718-9726. https://doi.org/10.1021/acsami.7b19436

[143] Z. Zhou, S. Pourhashem, Z. Wang, J. Duan, R. Zhang, B. Hou. Distinctive roles of graphene oxide, ZnO quantum dots, and their nanohybrids in anti-corrosion and anti-fouling performance of waterborne epoxy coatings. *Chem. Eng. J*. **2022**, *439*, 135765. https://doi.org/10.1016/j.cej.2022.135765

[144] Z. Zhou, A. Seif, S. Pourhashem, J. Duan, A Rashidi, P. L. Silvestrelli, X. Ji., M. Mirzaee, B. Hou. Multi-treatments based on polydimethylsiloxane and metal-organic framework wrapped with graphene oxide for achieving long-term corrosion and fouling protection: experimental and density functional theory aspects. *Construct. Building Mater*. **2023**, *384*, 131229. https://doi.org/10.1016/j.conbuildmat.2023.131229

[145] S. Pourhashem, A. Seif, F. Saba, E. G. Nezhad, X. Ji, Z. Zhou, X. Zhai, M. Mirzaee, J. Duan, A. Rashidi, B. Hou. Antifouling nanocomposite polymer coatings for marine applications: A review on experiments, mechanisms, and theoretical studies. *J. Mater. Sci. Technol*. **2022**, *118*, 73-113. https://doi.org/10.1016/j.jmst.2021.11.061

[146] S. Liu, T. H. Zeng, M. Hofmann, E. Burcombe, J. Wei, R. Jiang, J. Kong, Y. Chen. Antibacterial activity of graphite, graphite oxide, graphene oxide, and reduced graphene oxide: Membrane and oxidative stress. *ACS Nano* **2011**, *5*, 6971–6980. https://doi.org/10.1021/nn202451x

[147] X. Luo, J. Zhong, Q. Zhou, S. Du, S. Yuan, Y. Liu. Cationic reduced graphene oxide as self-aligned nanofiller in the epoxy nanocomposite coating with excellent anticorrosive performance and its high antibacterial activity. *ACS Appl. Mater. Interfaces* **2018**, *10*, 18400–18415. https://doi.org/10.1021/acsami.8b01982

[148] R. Xu, J. Li, Z. Xiong, H. Qiu, Y. Xue, J. Yang. Antibacterial waterborne epoxy coatings containing poly m-aminophenol-deposited graphene oxide. *Prog. Org. Coat.* **2020**, *147*, 105802. https://doi.org/10.1016/j.porgcoat.2020.105802

[149] Q. Yao, Q. Borjihan, H. Qu, Y. Guo, Z. Zhao, L. Qiao, T. Li, A. Dong, Y. Liu. Cow dung-derived biochars engineered as antibacterial agents for bacterial decontamination. *J. Environ. Sci.* **2021**, *105,* 33–43. https://doi.org/10.1016/j.jes.2020.12.022

[150] Z. Yu, W. Wang, H. Gao, D. Liang. Properties analysis and preparation of biochar–graphene composites under a one-step dip coating method in water treatment. *Appl. Sci.* **2020**, *10*, 3689. https://doi.org/10.3390/app10113689

[151] Z. Huang, Q. Zeng, Y. Liu, Y. Xu, R. Li, H. Hong, L. Shen. Facile synthesis of 2D TiO2@MXene composite membrane with enhanced separation and antifouling performance. *J. Membrane Sci*. **2021**, *640,* 119854. https://doi.org/10.1016/j.memsci.2021.119854

[152] E. Manderfeld, M. N. Kleinberg, C. Thamaraiselvan, F. Koschitzki, P. Gnutt, N. Plumere, C. J. Arnusch, A. Rosenhahn. Electrochemically activated laser-induced graphene coatings against marine biofouling. *Appl*. *Surf. Sci*. **2021**, *569*, 150853. https://doi.org/10.1016/j.apsusc.2021.150853

[153] O. Baranov, I. Levchenko, S. Xu, J. W. M Lim, U. Cvelbar, K. Bazaka. Formation of vertically oriented graphenes: what are the key drivers of growth? *2D Mater*. **2018**, *5*, 044002. https://doi.org/10.1088/2053-1583/aad2bc

[154] O. Baranov, T. Belmonte, I. Levchenko, K. Bazaka, M. Košiček, U. Cvelbar. Hierarchical nanomaterials by selective deposition of noble metal nanoparticles: Insight into control and growth processes. *Adv. Theor. Simulations* **2023**, *6*, 2300288. https://doi.org/10.1002/adts.202300288

[155] O. Baranov, M. Košiček, G. Filipič, U. Cvelbar, A deterministic approach to the thermal synthesis and growth of 1D metal oxide nanostructures, *Appl. Surf. Sci.* **2021**, *566*, 150619. https://doi.org/10.1016/j.apsusc.2021.150619

[156] G. Filipič, O. Baranov, M. Mozetic, U. Cvelbar, Growth dynamics of copper oxide nanowires in plasma at low pressures, *J. Appl. Phys*. **2015**, *117*, 043304, https://doi.org/10.1063/1.4906501

[157] I. Levchenko, S. Xu, O. Baranov, O. Bazaka, E. P. Ivanova, K. Bazaka. Plasma and polymers: Recent progress and trends. *Molecules* **2021**, *26*, 4091. https://doi.org/10.3390/molecules26134091

[158] S. Sasi, K. Prasad, J. Weerasinghe, O. Bazaka, E. P. Ivanova, I. Levchenko, K. Bazaka. Plasma for Aquaponics. *Trends Biotechnol*. **2023**, *41*, 46-62. https://doi.org/10.1016/j.tibtech.2022.08.001

[159] A. S. El-Kalliny, M. S. Abdel-Wahed, A. A. El-Zahhar, I. A. Hamza, T. A. Gad-Allah. Nanomaterials: A review of emerging contaminants with potential health or environmental impact. *Discover Nano* **2023**, *18,* 68. https://doi.org/10.1186/s11671-023-03787-8

[160] N. Malhotra, O. B. Villaflores, G. Audira, P. Siregar, J.-S. Lee, T.-R. Ger, C.-D. Hsiao. Toxicity studies on graphene-based nanomaterials in aquatic organisms: Current understanding. *Molecules* **2020**, *25*, 3618. https://doi.org/10.3390/molecules25163618

[161] A. L. Fernandes, M. E. Josende, J. P. Nascimento, A. P. Santos, S. K. Sahoo, F. M. Rodrigues da Silva, Júnior, L. A. Romano, C. A. Furtado, W. W., J. M. Monserrat, J. Ventura-Lima. Exposure to few-layer graphene through diet induces oxidative stress and histological changes in the marine shrimp *Litopenaeus vannamei*. *Toxic. Res.* **2017**, *6*, 205–214. https://doi.org/10.1039/c6tx00380j

[162] A. K. Dasmahapatra, T. P. S. Dasari, P. B. Tchounwou. Graphene-based nanomaterials toxicity in fish. In: de Voogt, P. (eds) *Rev. Environment. Contamin. Toxicology*, vol. 247. Springer, Cham **2018**. https://doi.org/10.1007/398_2018_15

[163] X. Zhang, Q. Zhou, W. Zou, X. Hu. Molecular Mechanisms of developmental toxicity induced by graphene oxide at predicted environmental concentrations. *Environ. Sci. Technol.* **2017**, *51*, 7861–7871. https://doi.org/10.1021/acs.est.7b01922

[164] Z. Chen, C. Yu, I. A. Khan, Y. Tang, S. Liu, M. Yang. Toxic effects of different-sized graphene oxide particles on zebrafish embryonic development. *Ecotoxicol. Environment. Safety* **2020**, *197*, 110608. https://doi.org/10.1016/j.ecoenv.2020.110608

[165] J. Lu, X. Zhu, S. Tian, X. Lv, Z. Chen, Y. Jiang, X. Liao, Z. Cai, B. Chen. Graphene oxide in the marine environment: Toxicity to *Artemia salina* with and without the presence of Phe and Cd2+. *Chemosphere* **2018**, *211*, 390-396. https://doi.org/10.1016/j.chemosphere.2018.07.140

[166] I. Martínez-Álvarez, K. Le Menach, M.-H. Devier, I. Barbarin, R. Tomovska, M. P. Cajaraville, H. Budzinski, A. Orbea. Uptake and effects of graphene oxide nanomaterials alone and in combination with polycyclic aromatic hydrocarbons in zebrafish. *Sci. Total Environment* **2021**, *775*, 145669. https://doi.org/10.1016/j.scitotenv.2021.145669

[167] C. Batista de Melo, F. Côa, O. L. Alves, D. S. T. Martinez, E. Barbieri. Co-exposure of graphene oxide with trace elements: Effects on acute ecotoxicity and routine metabolism in Palaemon pandaliformis (shrimp). *Chemosphere* **2019**, *223*, 157-164. https://doi.org/10.1016/j.chemosphere.2019.02.017

[168] Y. Chen, C. Ren, S. Ouyang, X. Hu, Q. Zhou. Mitigation in multiple effects of graphene oxide toxicity in zebrafish embryogenesis driven by humic acid. *Environ. Sci. Technol.* **2015**, *49*, 16, 10147–10154. https://doi.org/10.1021/acs.est.5b02220

[169] A. Balakrishnan, G. Jena, R. Pongachira George, J. Philip. Polydimethylsiloxane-graphene oxide nanocomposite coatings with improved anti-corrosion and anti-biofouling properties. *Environ. Sci. Pollut. Res*. **2021**, *28*, 7404–7422. https://doi.org/10.1007/s11356-020-11068-5